

Final Technical Report

Reporting Period: September 1, 2010 to February 15, 2012

Date of Report: May 15, 2012

Award Number: DE-EE0003483

Project Title: Production of Energy Efficient Preform Structures (PEEPS)

Project Period: 9/1/2010 through 02/15/2012

Recipient Organization: The Boeing Company
5301 Bolsa Avenue
Huntington Beach, CA 92647-2099

Partners: TWI Technology Center, Advanced Manufacturing Park,
Wallis Way, Catcliffe, Rotherham S60 5TZ, UK

Principal Investigator: John A. Baumann, 314-232-3764,
john.a.baumann@boeing.com

Business Contact: Luke A. Mowry, 314-233-5475, luke.a.mowry@boeing.com

DOE Project Officer: Debo Aichbhaumik, 720-356-1423,
debo.aichbhaumik@go.doe.gov

DOE Project Monitor: Chad T. Sapp, 720 356-1302, chad.sapp@go.doe.gov

DOE HQ Contact: Steve Sikirica, 202 586-5041, Stephen.sikirica@hq.doe.gov

DOE Contract Specialist: Christina Kouch, 720-356-1674, christina.kouch@go.doe.gov

Acknowledgment: This report is based upon work supported by the U. S.
Department of Energy under Award No. DE-EE0003483.

Disclaimer: Any findings, opinions, and conclusions or recommendations expressed in this report are those of the author(s) and do not necessarily reflect the views of the Department of Energy.

Document Availability: Reports are available free via the U.S. Department of Energy (DOE) Information Bridge Website: <http://www.osti.gov/bridge>

Reports are available to DOE employees, DOE contractors, Energy Technology Data Exchange (ETDE) representatives, and Informational Nuclear Information System (INIS) representatives from the following source:

Office of Scientific and Technical Information
P.O. Box 62
Oak Ridge, TN 37831
Tel: (865) 576-8401
FAX: (865) 576-5728
E-mail: reports@osti.gov
Website: <http://www.osti.gov/contract.html>

Table of Contents

Section	PAGE
Table of Contents	iii
List of Acronyms	iv
Lists of Figures	v
List of Tables	vii
1. Executive Summary	1
2. Introduction	4
3. Background	6
4. Results and Discussion	10
4.0 Overview of Planned / Executed Project Tasks	10
4.1.1 Task 1.1 – Capture / Refine Baseline Energy Usage	10
4.1.2.0 Task 2.0 - Energy Efficient Aluminum Preforms	12
4.1.2.1 Task 2.1 - Identify Energy Input Streams for Use in SMF model	13
4.1.2.2 Task 2.2 - Produce Case Study for Net-Shape Preforming	14
4.1.2.3 Task 2.3 - Compare Energy Consumption of FSW Preform to Baseline	15
4.1.3.0 Complex Aluminum Intersection Development	15
4.1.3.1 Task 3.1 – Evaluate Combinations of SSJ techniques for Optimum Energy Efficient Preforms	16
4.1.3.2 Task 3.2 - Development of Corner Angle Welding for Vertical Stiffener Joining	16
4.2.0 Specific Details of Work Performed and Results, by Project Task	17
4.2.1 Task 1.1 – Capture / Refine Baseline Energy Usage	17
4.2.2.1 Task 2.1 - Identify Energy Input Streams for Use in SMF model: State of Energy Consumption Model	37
4.2.2.2 Task 2.2 - Produce Case Study for Net-Shape Preforming	48
4.2.2.2.1 Predictive Model Applied to Case Study #1	48
4.2.2.2.2 Surveys of High BTF Aircraft Components.1	51
4.2.2.2.3 Produce Case Study for Net-Shape Preforming, Case Study 2	51
4.2.2.3 Task 2.3 - Compare Energy Consumption of FSW Preform to Baseline	58
4.2.3.1 Task 3.1 – Evaluate Combinations of SSJ techniques for Optimum Energy Efficient Preforms	60
4.2.3.2 Task 3.2 - Development of Corner Angle Welding for Vertical Stiffener Joining	66
4.3 Project Milestones	70
4.4 Computer Modeling: The Boeing Energy Consumption Model	71
4.4.1 Model Description:	71
4.4.2 Key Assumptions:	71
4.4.3 Version:	71
4.4.4 Intended Use:	71
4.4.5 Goals of Model:	72
4.4.6 Performance criteria for the model related to the intended use:	72
4.4.7 Theory behind the model, expressed in non-mathematical terms:	72
4.4.7.1 Determination of Energy Consumed in Bar Stock Aluminum Production	72
4.4.7.2 Reason for Life-Cycle Analysis Method Selection	73
4.4.7.3 The Determination of a Carbon Dioxide Emission Per Pound of Primary Aluminum Production	75

4.4.8 Mathematics to be used, including formulas and calculation methods:	75
4.4.9 Whether or not the theory and mathematical algorithms were peer reviewed:	76
4.4.10 Hardware requirements:	76
4.4.11 Documentation:	76
5. Benefits Assessment	76
6. Commercialization	77
7. Accomplishments	78
8. Conclusions	80
9. Recommendations	81
10. References	82

List of Acronyms

BR&T	Boeing Research & Technology
BTF	Buy-to-fly ratio (ratio of volume of starting material to volume of material of fly-away component)
CO ₂	Carbon Dioxide
COTS	Commercial-Off-The-Shelf
CS	Composite Skinned
DOE	Department of Energy
ECM	Energy Consumption Model
EP	engineering parts
FB	Forged Block
FS	Friction Stir
FSCW	Friction Stir Corner Welding
FSW	Friction Stir Welding
LCA	Life-Cycle Analysis
LFW	Linear Friction Welding
MS	Metal Skinned
MTCE	Metric Tons of Carbon Equivalent
NACFAM	NAtional Council For Advanced Manufacturing
NC	Numerical Controller
NEPM	Network Enable Power Monitoring System
NG	Next Generation (737)
PEEPS	Production of Energy Efficient Preform Structures
RFW	Rotary Friction Welding
SMF	Sustainable Manufacturing Framework model
SSCA	Stationary Shoulder Corner Angle (FSW)
SSJ	Solid State Joining
TRL	Technology Readiness Level
3-D	Three Dimensional

Lists of Figures

Figure 2.1.	Conversion of an assembly of many pieces formed from thin sheet materials into complex, one-piece component machined from thick stock, for transport aircraft nose crown assembly.	5
Figure 2.2.	Emerging aluminum fabrication technologies for low buy-to-fly stock: 1) Rotary Friction Welding (RFW), 2) Friction Stir Welding (FSW), and 3) Linear Friction Welding (LFW).	5
Figure 3.1.	Mill processing energy consumption relative to overall aluminum production.	7
Figure 3.2.	North American aluminum consumption by industrial sector.	8
Figure 3.3.	Space shuttle external tank that exhibits Boeing's Solid State Joining expertise.	10
Figure 4.1.2.2-1.	Bulkhead Example, final component on left, FSW-produced preform on right.	15
Figure 4.2.1-1.	New Fleet Builds by year, 90-175 Seat Single Aisle Aircraft.	19
Figure 4.2.1-2.	New Fleet Builds by year, >175 Seat Single Aisle Aircraft.	19
Figure 4.2.1-3.	New Fleet Builds by year, Small Twin Aisle Aircraft.	20
Figure 4.2.1-4.	New Fleet Builds by year, Medium Twin Aisle Aircraft.	20
Figure 4.2.1-5.	New Fleet Builds by year, Large Twin Aisle Aircraft.	21
Figure 4.2.1-6.	Material Usage on 777 Platform and Associated Pie Chart.	23
Figure 4.2.1-7.	Material Usage on 787 platform and associated pie chart.	24
Figure 4.2.1-8.	Projected Aluminum Savings in Single Aisle Aircraft Fleet.	27
Figure 4.2.1-9.	Projected Aluminum Savings for each aircraft type and Total New Build Fleet.	28
Figure 4.2.1-10.	Distribution of number of individual aluminum parts of a 777 aircraft, by starting product form / application area.	29
Figure 4.2.1-11.	Distribution of fly weight of aluminum parts, by starting product form / application area.	30
Figure 4.2.1-12.	Distribution of buy weight of aluminum parts, by starting product form / application area.	31
Figure 4.2.1-13.	Forged Block initial stock and engineering part ****514-3 paired in Catia V5.	33
Figure 4.2.1-14.	SSJ initial stock and engineering part ****514-3 paired in Catia V5.	33
Figure 4.2.1-15.	Block initial stock and engineering part *****515-3 paired in Catia V5.	34
Figure 4.2.1-16.	SSJ initial stock and engineering part *****515-3 paired in Catia V5.	35
Figure 4.2.2.1-1.	A. Acuvim Unit mounted on Brötje power panel. B. Close up of the front panel display of the unit.	38
Figure 4.2.2.1-2.	Energy Visibility Architecture.	38
Figure 4.2.2.1-3.	a) The PEEPS Pseudo Bulkhead Clamping Approach; b) a Cross-section of a dual-pass FSW Weld.	39
Figure 4.2.2.1-4.	Schematic of the Locations of the Welds on the 1 st Layer of the Top Surface.	40
Figure 4.2.2.1-5.	Photographs at Two Different Stages of Weld T11.	40
Figure 4.2.2.1-6.	Various Stages of Welding of the 1st Layer of the Pseudo Bulkhead.	41
Figure 4.2.2.1-7.	The Completed FSW Bulkhead Preform Ready for Final Machining.	41
Figure 4.2.2.1-8.	Progression of the Machining Operations Reducing a Thick Plate into the Pseudo Bulkhead.	42
Figure 4.2.2.1-9.	Web Interface of Energy Visibility Data from the Brötje FSW Platform during Welding of the Preform.	42
Figure 4.2.2.1-10.	Web Interface of Energy Visibility from the Cincinnati 20V Milling Platform during Machining of the Preform to Final Part.	43
Figure 4.2.2.1-11.	Current or Future Fabrication Techniques To Be Incorporated into the PEEPS Energy Consumption Model	45

Figure 4.2.2.1-1.	Conventional hog-out process.	49
Figure 4.2.2.1-2.	FSW....Face Milling....FSW/Face Milling Repeating.....Final Part.	49
Figure 4.2.2.2-1.	Part machined from 2124 block.	51
Figure 4.2.2.2-2.	Part machined from 2124 block.	51
Figure 4.2.2.2.3-1.	777 Floor Component: a) Top Surface and b) Bottom Surface.	52
Figure 4.2.2.2.3-2.	The Top (left) and Bottom (right) Surfaces of the Subtended Version of the 777 Floor Component.	52
Figure 4.2.2.2.3-3	a) Cross-Section of the 777 Floor Article Showing Pertinent Dimensions and b) A Top View Showing the Plates that will be Welded onto the Top Surface.	53
Figure 4.2.2.2.3-4.	Schematic of Bottom Plate Attachment Welds.	54
Figure 4.2.2.2.3-5.	The Approach for Welding the Subtended Article.	54
Figure 4.2.2.2.3-6.	Cross-section of a Double Pass Weld.	55
Figure 4.2.2.2.3-7.	The Subtended Article After Tack Welding and in Position for Welding Weld 1 of Layer 1.	55
Figure 4.2.2.2.3-8.	A Schematic Showing the Location of Weld #1 of Layer 1.	55
Figure 4.2.2.2.3-9.	A Schematic Showing the Location of Weld #2 of Layer 1.	56
Figure 4.2.2.2.3-10.	A Photograph Showing Weld 2 of Layer 1.	56
Figure 4.2.2.2.3-11.	A Photograph Showing Weld 2 of Layer 1 After Removal of the Welding Flash.	56
Figure 4.2.2.2.3-12.	Representation of Layer 2 and Layer 3 Welds.	57
Figure 4.2.2.2.3-13.	Photograph of the Completely Welded Subtended Article Showing the Clamping Approach for the Layer 2 and Layer 3 Welds	57
Figure 4.2.2.2.3-14.	The Subtended Article During and After Machining.	58
Figure 4.2.3.1-1.	The Third Welding Approach for the Subtended Article, Based on Welding through the Cap.	61
Figure 4.2.3.1-2.	The FSW/LFW Welding Approach for the Subtended Article.	61
Figure 4.2.3.1-3.	The FSCW/LFW Approach for the Subtended Article.	62
Figure 4.2.3.1-4.	Cross-Sections of the Full-sized Article Depicting the Amount of Procured Material.	62
Figure 4.2.3.1-5.	Energy Consumption Model Input Data for the Five Approaches to Fabricate the 777 Floor.	63
Figure 4.2.3.1-6.	Total Energy Predictions for Fabricating the 777 Floor Article by each of the Six Scenarios.	64
Figure 4.2.3.1-7.	Carbon Dioxide Emission Predictions for Fabricating the 777 Floor Article by each of the Six Scenarios.	64
Figure 4.2.3.1-8.	Total Scrap Predictions for Fabricating the 777 Floor Article by each of the Six Scenarios.	65
Figure 4.2.3.1-9.	Buy-to-Fly Calculations for Fabricating the 777 Floor Article by each of the Six Scenarios.	65
Figure 4.2.3.1-10.	Total Machine Processing Time for Fabricating the 777 Floor Article by each of the Six Scenarios.	66
Figure 4.2.3.2-1.	Two Corner Welds to create a Tee.	67
Figure 4.2.3.2-2.	Corner Welded Tee.	67
Figure 4.2.3.2-3.	Cross Sections of welds obtained in 2024 T4 with original (left) and revised tool design (right.).	68
Figure 4.2.3.2-4.	Stronger Tool and Shoulder, as designed by TWI under this CRAD.	68
Figure 4.2.3.2-5.	Force, Torque, and other Data Collected from the TWI FSW System during a Weld Operation.	69
Figure 4.2.3.2-6.	TWI Stationary Shoulder Corner Angle Friction Stir Weld Tool.	70
Figure 4.2.3.2-7.	Boeing Preliminary Design of SSCA FSW tool for use on the Brotje FSW System.	70

Figure 4.4.7-1.	Inputs and outputs of production for 1000 kg of primary rolled aluminum, utilizing the Life-Cycle Analysis (LCA) method.	73
Figure 4.4.7-2.	Bauxite mining constituent of the primary aluminum life-cycle analysis.	74
Figure 4.4.7-3.	Alumina refining constituent of the primary aluminum life-cycle analysis.	74
Figure 4.4.7-4.	Anode production constituent of the primary aluminum life-cycle analysis.	74
Figure 4.4.7-5.	Aluminum smelting constituent of the primary aluminum life-cycle analysis.	74
Figure 4.4.7-6.	Primary ingot casting constituent of the primary aluminum life-cycle analysis.	74
Figure 4.4.7-7.	Secondary ingot casting constituent of the secondary aluminum life-cycle analysis.	74
Figure 4.4.7-8.	Primary and secondary ingot energy inputs broken down into, process non-electric; process electric, transportation and feedstock categories.	75

List of Tables

Table 3.1.	Project team roster and areas of expertise.	10
Table 4.2.1-1.	World Aircraft Fleet Composition by Type, With 20-Year Projections.	18
Table 4.2.1-2.	World Aircraft Fleet Utilization of Aluminum, by Type.	22
Table 4.2.1-3.	Projected Impact on BTF and Utilization of Aluminum, by Type.	26
Table 4.2.1-4.	Buy to fly values of Aluminum product forms for 777 aircraft components.	31
Table 4.2.1-5.	Results of Forged Block SSJ Preform Studies.	36
Table 4.2.2.1-1.	Weld Energy and Power data provided by TWI for Corner Angle Welding.	45
Table 4.2.2.1-2.	Measured process data from case studies fed into calculation table to increase predictive model's capabilities and accuracy.	46
Table 4.2.2.1-3.	Calculated Process Variable from case studies fed into calculation table to increase predictive model's capabilities and accuracy.	46
Table 4.2.2.1-4.	The predictive model input section accepts parameters from the calculation tables shown in Table 4.2.2.1-3, user-defined part-specific variables, and processing variables cited from literature.	47
Table 4.2.2.1-5.	The predictive model output section displays energy, emissions, and fabrication data for each of the manufacturing techniques; and will have the ability to calculate the optimum construction method.	48
Table 4.2.2.2.1-1.	Input Table of current version of the model, for Hog-Out Machining.	49
Table 4.2.2.2.1-2.	Input Table of current version of the model, for FSW preform process.	49
Table 4.2.2.2.1-3.	Model Outputs for Hog-Out Machining Process.	50
Table 4.2.2.2.1-4.	Model Outputs for FSW preform - Machining Process.	50
Table 4.2.2.2.1-5.	Comparison of Processes, Case Study 1.	50
Table 4.2.2.3-1.	Measured Power Usage Collected During Fabrication of the Subtended Article.	58
Table 4.2.2.3-2.	Predictive model inputs for the Subtended Article.	59
Table 4.2.2.3-3.	Energy Consumption Model Output Results for the Subtended Article.	59
Table 4.2.2.3-4.	Comparison of the Predicted and Actual Power Usages for fabrication of the Subtended Article.	59

1.0 Executive Summary

The current preferred method of making unitized aluminum aircraft structure is to machine it from a solid plate of material. This approach can be very wasteful in terms of material and energy, as much of the starting material is usually removed to create the final required part geometry. Nearer-net starting product forms, such as die forgings, require special dies, which have high costs, long lead times, and limited lifetimes. The forging process generally results in significant residual stresses in forgings, which can lead to production issues related to distortion when material is removed via machining to final part geometries. What is needed are ways to make tailored, near-net shape machining blanks, without expensive dies, and low residual stresses.

A major objective of this project was to identify the energy benefits of combining a variety of solid state joining techniques, which are geometry independent, in order to produce high performance aluminum structures, while enabling the achievement of manufacturing benefits of lower-cost, faster cycle-time, and highly efficient joined structural assemblies. A further objective was to produce an energy consumption prediction model, which was capable of calculating the total energy consumption, solid waste burden, acidification potential, and CO₂ burden in producing a starting product form, and then calculating the further energy consumption and environmental impacts of fabricating a final part configuration from the starting configuration. Yet another objective was to be able to utilize the model to compute and compare, on an individual part/geometry basis, multiple possible manufacturing pathways, to identify the best balance of energy consumption, environmental impact, and costs. Finally, another project goal was to help enable Solid State Joining (SSJ) technologies become better characterized, better utilized, and considered as mainstream processes, especially replacing/supplanting the energy intensive arc-welding / fusion processes of joining such as gas-tungsten arc welding.

The original scope of the project was based on refining and expanding the Sustainable Manufacturing Framework model (SMF), which had been created by personnel at the National Council For Advanced Manufacturing (NACFAM), and applying it to the SSJ processes, obtaining explicit energy consumption data from energy monitoring equipment installed on process equipment available to Boeing Research and Technology, to populate the model with process-specific information. These processes included both machining and conventional friction stir welding performed inside Boeing. An additional effort was undertaken with the TWI Technology Centre in the United Kingdom, to obtain energy consumption data on Corner Angle Welding, a specialized Friction Stir Welding (FSW) methodology useful for fabricating three dimensional shapes, such as vertical ribs on plate structures.

The first major result of this project was the completion of the evaluation of the potential impact of implementing solid state joining technologies to reduce the buy-to-fly (BTF) ratio of aluminum product forms required to produce components for the next twenty years of production of the world's commercial airline fleet. This quantity of "avoided" aluminum production has been equated with the energy consumption required to produce the aluminum starting product, and the CO₂ emissions level associated with producing that energy.

Widespread and aggressive implementation of SSJ technologies over the next 20 years has been shown to have the potential to avoid the consumption of 4 to 5 billion pounds of high-strength aluminum, in starting product forms (plate, sheet, extrusions, and forgings). With each pound of aluminum in such product forms requiring 16.71 kWh of energy to produce, resulting in 12.476 pounds of CO₂ emissions for each pound of aluminum, the potential energy savings for implementing these technologies could range from 66.9 to 83.6 billion kWh, resulting in reduced CO₂ emissions ranging from 49.9 to 62.4 billion pounds.

The NACFAM SMF model was found to be inadequate / inappropriate in meeting the program objects, and, as a result of this project, it has been replaced by a Boeing-derived Energy Consumption Model (ECM), which was based on a “bottom-up” approach which could be applied to specific processes used to produce starting product forms, and specific manufacturing processes used to turn those starting forms to final products. The model has sufficient flexibility to accommodate different geometries, volumes, part features, material alloys and tempers, and revisions in process-related information, such as platform-specific energy consumption rates. The ECM was also constructed so that users could populate the model with user-determined energy consumption values for specific platforms and specific processes. These user-defined inputs include values for machining processes, which are needed to produce final component geometries, whether from current starting product forms, or from existing or to be developed SSJ processes. The ECM has been demonstrated in this project to be able to compare multiple pathways to obtain a final component, enabling its use as a pathway selector tool based on energy consumption and environmental impact. In building this model, revised, more defensible energy / CO₂ emission values for the production of a pound of aluminum were identified, and used in the baseline energy usage impact calculation above.

A survey of aluminum components used in the 777 aircraft was completed within this project. This effort yielded a revision of the current total aluminum usage (fly weight), the total buy weight, and a resultant average BTF value for this modern design aircraft, but otherwise confirmed many of the other assumptions used in calculating the baseline energy usage impact of implementing SSJ technologies.

To provide valuable baseline process information for the model, and, in turn, validate the model, Boeing completed several case studies. These included machining components from thick plate starting stock, and welding of tailored preforms using Friction Stir Welding, and then machining these preforms to the same final component configurations. While the fabrication of the Case Study 1 pseudo bulkhead was not expected to be found to bolster the energy case for using a preform, given the minor reduction in BTF value over a thick plate, it was instrumental in both guiding the development of the ECM and populating it with actual energy consumption process data for both the FSW process and the machining processes. The completion of the fabrication of the Case Study 2 preform and final component yielded a clear demonstration of the practical state of FSW as a preform building process. It highlighted the shortfalls of this particular welding platform with respect to process and energy efficiency and points to the need to utilize a purpose-built platform for FS welding of preforms.

Finally, some significant advancement of Stationary Shoulder Corner Angle (SSCA) Friction Stir Welding was accomplished under this project. TWI developed improved tools for welding 2024 and 7075 Al alloys, obtaining energy consumption data which Boeing incorporated into the ECM. These values were used in a comparison of multiple pathways to produce a preform for the 777 floor component, demonstrating the value of the ECM in predicting the most energy efficient pathway for this component, given current SSJ process capabilities.

The results of the project are as follows. First, Solid State Joining processes, such as Rotary Friction Welding, Linear Friction Welding, Friction Stir Welding, and Stationary Shoulder Corner Angle welding, could have a significant impact on energy consumption and greenhouse gas emission by the aircraft fabrication industry, if they become widely and aggressively implemented. Using the SSJ processes allows the fabrication of tailored preforms which retain the ability of obtaining the large, complex structural form but with starting from a lower buy-to-fly product form. Secondly, the successful demonstration articles produced in this project show that these technologies are approaching the practical stage of implementation, but that to achieve this promise of energy savings and environmental impact reduction, some improvements of the joining processes are still required, especially with respect to the energy efficiency of FSW. A properly energy efficient FSW platform would have low energy consumption during idle times, minimal axes and drive motors, to reduce energy of platform motion, and high torque capacity to enable maximum depth and width of welding to produce the necessary volume of added material in single weld passes.

Technical barriers to implementation still exist, which relate principally with the accumulation of sufficient performance data and analytical modeling capability to enable facile certification of performance, especially in flight-critical applications where fitness for application includes consideration of durability and damage tolerance performance. Commercialization of these processes will depend upon a complex relationship and risk/benefits sharing between members of the aircraft component supply chain, including the systems integrators, component fabricators, and the material suppliers. The system integrators will lead this commercialization through pathfinder projects such as this and internally-funded ones, but it is unclear how these initiatives will eventually flow down into the supply chain. Today, there seems little incentive for the material suppliers to move from their baseline business model.

Possible follow-up R&D work should first focus on gathering of energy consumption data from a purpose-built FSW machine, one optimized for platform energy efficiency, and instrumented to gather processes consumption data. The impact of scaling the width and depth of welding needs to be confirmed, and charted for several high strength aluminum alloys. A second subject area would be to undertake additional case studies, with added focus on acquisition of performance characteristics, including pathfinder data in such areas as crack initiation, crack growth, stress corrosion cracking, in some key high strength alloys, such as 7050 and 7055 aluminum. Another area which has not been explicitly addressed in this project is the need for additional 3-D joining capabilities. The SSCA welding can only be used to add a standing rib in one direction. If another rib is added at an angle to this rib,

the junction between the two cannot be accommodated today by a friction stir process. It can be achieved with a linear friction welding process. There is another emerging technique, known as friction hydro pillar processing (see www.twi.co.uk) which may prove to be a better method of creating intersecting ribs.

Finally, all of the assessments in this project on the impact of the implementation of SSJ technology have been made at the technical level, with respect to BTF reduction and the energy savings and environmental impact associated with the avoided consumption of starting aluminum product form. The overwhelming driver for implementation, however, will be a business case argument, and any follow-on work funded by the Department of Energy would be well served if the development of a business case model for SSJ would be a major component of that work. All of the factors associated with the ECM have costs associated with them, and this would be a good starting point for a model, with provisions for users to add/modify cost data and computational formulations specific to their organizations and supply chain.

2.0 Introduction

The transportation industry continues to be the largest consumer of aluminum products, with aerospace as a principal driver for this use. The extensive use of aluminum to build aircraft and launch vehicles has been sustained, despite the growing reliance on more structurally efficient carbon fiber reinforced plastic composite materials. An often overlooked trend in the aerospace industry over the past two decades has been the trend toward the use of less material efficient aluminum product forms when manufacturing aluminum airframe structure. The aerospace industry now relies extensively on large, complex, thin-walled, monolithic machined structural components that are high speed machined from heavy billets and thick plate, where part count reduction translates into major cost efficiency benefits. See Figure 2.1 for an example of the replacement of a riveted assembly of many pieces of components, formed from thin sheets of aluminum alloy, with a unitized, complex structure produced by machining from a thick plate of high-strength aluminum alloy.

The ever-increasing usage of such unitized, machined structures has been facilitated by the stability of price of aluminum product forms, due to generally stable energy prices and DOE-sponsored initiatives related to smelter technology and establishment of the recycling infrastructure. It is ironic that these initiatives further facilitated the aerospace manufacturing trend toward producing very low-yield finished components (with weights often 10% or less of the machining blank weight), selling the chip waste to recyclers, and achieving a net cost reduction compared to the assemblies being replaced. With an increasing emphasis on consideration of the costs of energy consumption (both in terms of financial impact and environmental impact), and as pricing pressures of aluminum supply increase (as usage rates climb and costs to produce it increase), a new approach to fabricating complex aluminum structural components will be required in order to reduce cost escalation risk to aerospace companies.

Transport Aircraft Nose Crown Assembly

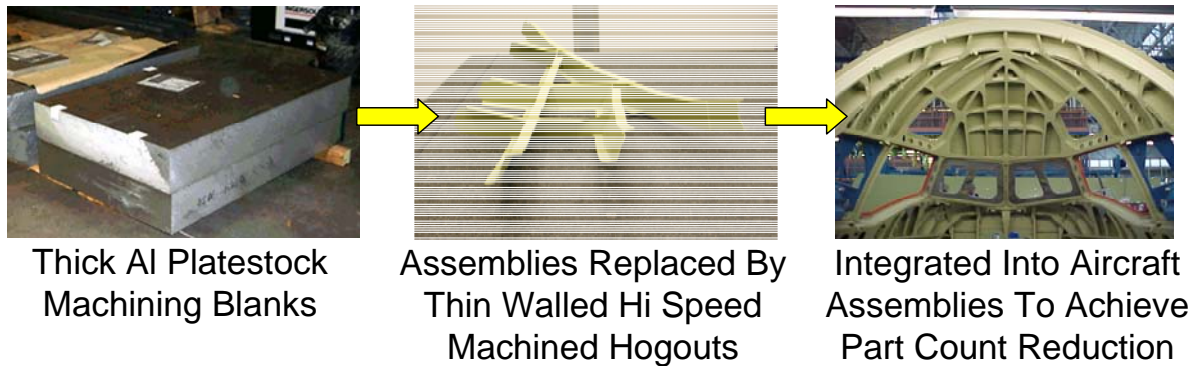


Figure 2.1. Conversion of an assembly of many pieces formed from thin sheet materials into complex, one-piece component machined from thick stock, for transport aircraft nose crown assembly.

Emerging advanced aluminum forming and joining technologies will enable aerospace companies to drive a fundamental shift in manufacturing technology away from the reliance on high buy-to-fly machined hogouts of aluminum billet and thick plate. These technologies should not only resolve current cost barriers associated with using net shape assembly details to producing aluminum structures, but more importantly, they offer breakthrough energy consumption benefits. Primary examples of these solid state joining fabrication technologies, which are being matured to a Technology Readiness Level (TRL) of 4 and beyond, include: 1) Rotary Friction Welding (RFW) (also known as inertia welding), 2) Friction Stir Welding (FSW), and 3) Linear Friction Welding (LFW). (See Figure 2.2.) All offer potential utility in the production of ultra net-shaped tailored geometry machining blanks. All offer potential energy savings and a reduction in environmental impact of production of aerospace aluminum components, principally through the reduction in the initial amount of material that needs to be produced and the percentage of that supply rendered into waste chips (albeit chips that can be recycled).

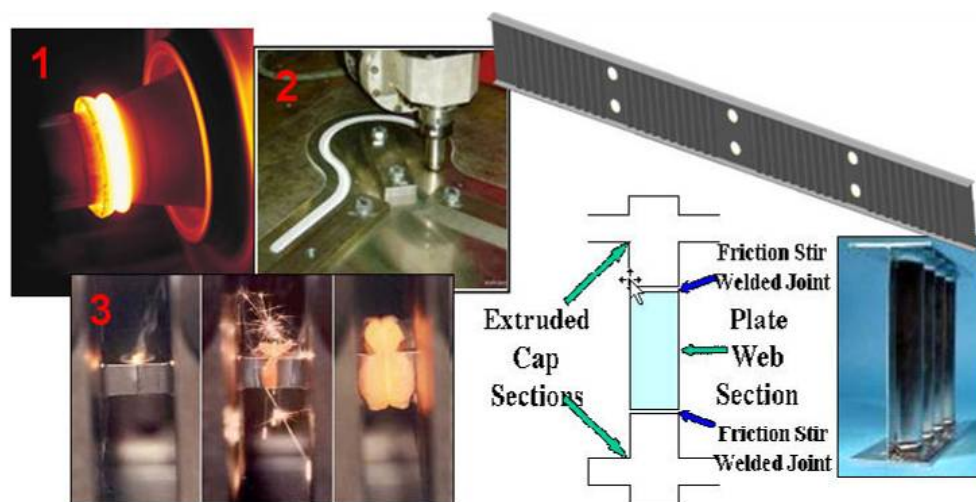


Figure 2.2. Emerging aluminum fabrication technologies for low buy-to-fly stock: 1) Rotary Friction Welding, 2) Friction Stir Welding, and 3) Linear Friction Welding.

Thus, the potential benefits of widespread adaptation of the SSJ techniques have been evaluated in this project by analyzing the projections of future aircraft deliveries, the resultant volume of aluminum production required to meet those delivery projects with current values of buy-to-fly ratios for aluminum product forms used in production, and the reduction in that volume of material by the utilization of aluminum product forms with lower buy-to-fly values, achieved through application of the SSJ technologies. This analysis resulted in an estimated reduction in required new aluminum of nearly 5 billion pounds over the next twenty years of new aircraft production, with a resultant avoidance of production of **some 60 billion pounds of CO₂**. These projections are based on several underlying assumptions, such as an eventual impact figure of 60% of high BTF parts being able to be reduced in BTF using preforms produced by SSJ processes (PEEPS preforms), a three year period of process development and property data characterization prior to first introduction, and an additional three-year period of incremental implementation. The other two assumptions were that the average BTF for the components which can be converted to the use of preforms has a value of 20:1, and that this BTF value will be reduced to an average of 6:1 in SSJ-produced preforms. See Section 5 for in-depth details of this benefits assessment.

Boeing and other aerospace companies have on-going efforts to implement various SSF processes on a variety of alloy material systems, for a variety of applications. Little information on these efforts may be found in the public domain. Nevertheless, it is clear that barriers to implementation remain. With respect to Friction Stir Welding, some remaining barriers are: a) accepted structural design practices, accounting for reduction in properties, especially ones which can minimize any weight penalties due to process-induced reduction in properties; b) sufficient durability and damage tolerance performance data on the heterogeneous thermal and mechanically altered materials associated with the weld nugget and adjacent heat affected zones, for use of the components in critical structural applications; c) up-take of the FSW process by mill-level fabricators of product forms (i.e., a mature supply chain, capable of FSW processes); and d) specifications and standards that would allow component-level fabricators to utilize the resultant tailored blanks in producing final components. Similar barriers exist for all of the SSJ processes.

3.0 Background

Due to its low density, corrosion resistance, good structural characteristics, excellent fabrication properties, and attractive appearance, aluminum metal and its alloys continue to be widely utilized in applications throughout the transportation, packaging, and construction industries. Other than iron, aluminum is the most widely used metal worldwide, with annual production exceeding 32 million tonnes.^[1] Even with the emergence of China as a new exporter of aluminum products, Western aluminum production facilities and downstream mill product producers control a large share of the global market. The U.S. is recognized as a 10+ million tonne market that is growing at a very high rate. Projections indicate that the global market for aluminum products will eclipse 51 million tonnes by 2012.^[2]

The physical nature of aluminum, in its natural oxide (bauxite) form, requires a highly energy intensive electrolytic process to extract pure aluminum for use in making aluminum products.

Over \$2B annually in energy is spent on producing aluminum; so in other terms, one-third the average cost of aluminum is for the energy required to produce it. A more detailed assessment of the aluminum production processes reveals that the intensive energy consumption related to aluminum is concentrated in the electrolytic cells used for aluminum reduction. As depicted in Figure 3.1, the smelting operation should be, and has been the focus of the Department of Energy and the aluminum industry in making aluminum production more energy-efficient. As shown, only 7% of the total energy expended for aluminum product production is related to downstream steps for conversion of ingot to mill products.

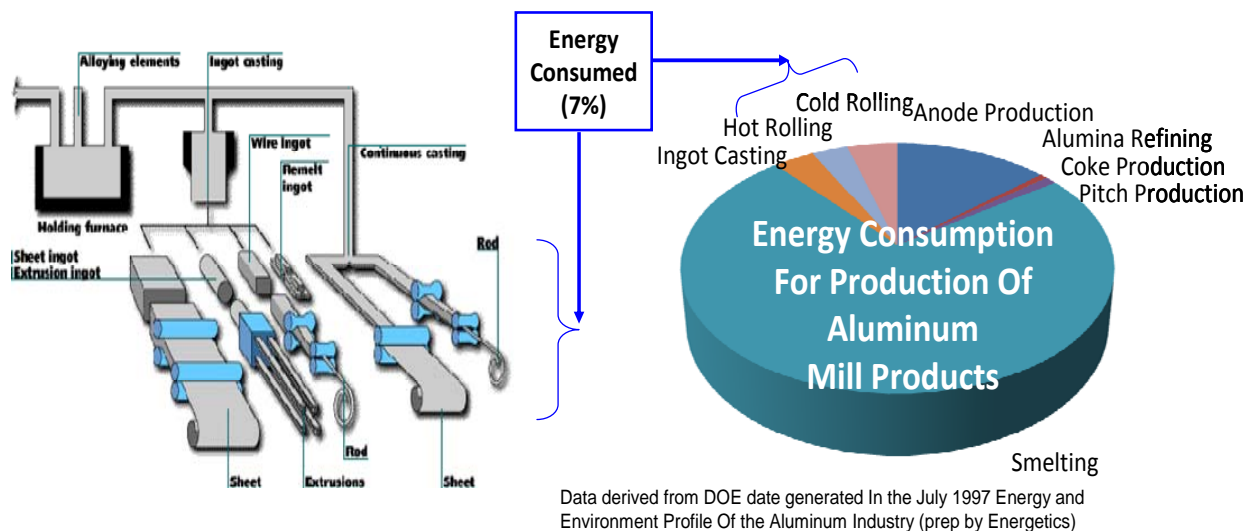


Figure 3.1. Mill processing energy consumption relative to overall aluminum production

In addition to investments in more efficient smelters, the past two decades have seen the emergence of aluminum product recycling as the primary approach to reducing the heavy energy consumption related to aluminum production. The electrolytic cell is by-passed when introducing recycled aluminum into the processing stream. Utilization during the secondary melting / ingot casting steps, results in an astounding 92 to 95% reduction in energy consumption requirements compared to aluminum produced from the full reduction cycle. Although the aluminum waste requires processing prior to re-melting, the net benefits, including consumers' growing awareness of sustainability needs, are so positive that an expansive sub-industry of successful recyclers has been spawned. The enduring benefits of aluminum recycling have intensified this critical step in aluminum production, to the point that the Aluminum Association is proactively challenging U.S. consumers and industries to achieve a 75% recycling rate by 2015.

As stated in the Introduction, the transportation industry continues to be the largest consumer of aluminum products, with over a third of the total domestic market (See Figure 3.2). Aerospace is the principal driver for this use, and Boeing has long remained as the largest single company consumer of heat-treated aluminum in the U.S. This demand is continuously driven to higher volumes, in part because of the ever-increasing utilization of large, complex, thin-walled, monolithic machined structural components that are high speed machined from heavy billets and thick plate. This trend has been accelerated by major advancements in aluminum mill product rolling technology, and breakthrough advancements in physics-based

high speed machining technology and the associated machine tool capability provided by equipment builders. Thick high strength aluminum plate, up to 8 inches thick, is being produced without integrity issues previously caused by center-band porosity and warpage during machining due to residual stresses. The culmination of institutionalizing this trend for the entire industry, including long life military and commercial transport aircraft, were advancements in structural analysis software tools that could accurately predict the structural performance of large, complex, monolithic primary structure. Throughout the 90's, it was common to see structural aluminum mechanical assemblies comprised of formed sheet metal, barstock, and extrusions, converted to one piece high speed machined thick plate hogouts during many program cost reduction initiatives.

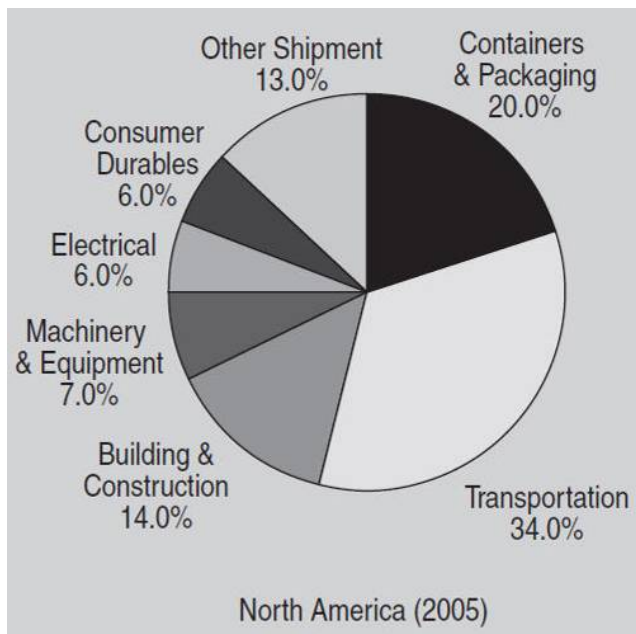


Figure 3.2. North American aluminum consumption by industrial sector.^[1]

Traditional heavy section near-net shape aluminum machining blanks are produced by hot die forging. But the series of matching dies needed, furnaces used for soaking forging billets, and powerful forging presses are all counterintuitive to energy conservation. Aerospace companies have made major investments in near net shape casting technology to produce near net shape aluminum structural components. Although major success have been achieved with titanium structural castings, success with aluminum have been minimal due to inferior structural properties of the “castable” series of aluminum alloys compared to wrought alloys. Therefore, the ultra net-shape preform capability offers the only solution for low waste (including material, energy, and cost) preforms of high mechanical performance materials.

LFW cyclically accelerates two pieces of material in direct contact which generates heat that lowers the yield strength and achieves the joining temperature. The same is true for RFW with the exception that one preform is rotated and the other is stationary. These two processes are very similar in nature and generate similar mechanical results. The processes can be used to add simple shape such as stiffeners for LFW and bosses for RFW. When the

geometry becomes more complex or the requirement is to bridge two intersecting, yet geometrically independent features (such as blade stiffeners intersecting from orthogonal directions) FSW is required.

FSW uses a spinning pin tool that is plunged into aluminum at room temperature. Friction between the tool and base material locally heat the material, lowering the yield strength of the material. The motion of the tool plasticizes the material in the joint and then mechanically stirs or mixes two adjacent pieces of material together forming a solid state weld with no electrical arcing required. The use of FSW to join common mill produced product forms (plates, strips, extrusions, sheets, etc.) into geometry specific near net shape preforms offers a substantial opportunity to reduce the amount of waste material that is produced by inefficient hogout techniques. The other attractive aspect is that the technique utilizes traditional aerospace alloys so that the existing domestic infrastructure for aluminum mill products is invigorated. Specifically, jobs will be created producing high value equipment, product forms, and finished products for domestic and international consumption due to the cost competitive nature of the processes implemented. The equipment required for the process is Numerical Controller (NC) - based and capable of controlling multiple advanced aspects of the process to produce consistent mechanical properties. Boeing has a significant investment into understanding the mechanics of the stir welding process and as a result has developed and installed in St. Louis, MO, a purpose-built, large-frame FSW platform, manufactured by Brotje Automation. This machine is capable of producing 33' x 13' x 5' contoured structural components. It has the required force, torque, and horse power capabilities to weld high strength Al alloys up to 0.5 inches in thickness.

Currently the individual technologies have been advanced to a TRL of 4 or higher; however implementation has been hampered by the ability to validate the process and resulting properties of a large scale preform that encompasses the different intersection geometries and thick raw product forms. This project is specifically scoped to identify and overcome some of the barriers to implementation. On a broader basis, however, this project seeks to enable the justification for further development of the technologies by providing tools to evaluate and substantiate the economic and environmental benefits of utilizing the SSJ technologies to produce near net shape starting product forms with low BTF ratios.

Boeing is regarded as a world leader in the usage of aluminum products based of years of experience and breadth of implementation. Boeing has led the application of flight-worthy Solid State Joining processes. An example is the space shuttle's external fuel tank, where Boeing replaced arc welding with FSW (see Figure 3.3).



Figure 3.3. Space shuttle external tank that exhibits Boeing's Solid State Joining expertise.

The laboratories that support process development for Boeing Research & Technology (BR&T) have immense capability ranging from process simulation, to mechanical testing and destructive and non destructive examination, to advanced high-speed machining, and friction stir welding. The latter is embodied in the Brotje multi axis Friction Stir Welding machine, which is unparalleled in process capability and data collection. The data collection aspect has been utilized to verify energy consumption during the process trials and used to improve the accuracy of the simulation's results. The internal personnel resources which supported this effort are top class, and technical leaders in their respective fields (see Table 3.1)

Table 3.1. Project team roster and areas of expertise.

Name	Title	Areas of Expertise
Dr. John Baumann	Technical Fellow	SSJ, FSW, Program Mgmt.
Richard Lederich	Associate Technical Fellow	Aluminum Alloys, FSW
Dr. David Dietrich	Senior M&P Engineer	Additive Manufacturing
Mike Matlack	Senior Design Engineer	Tool and Fixture Design, FSW
Herb Bommer	Principal Specialist	SSJ programming/Controls
Brent Goodlet	Intern	Process Modeling

4.0 Results and Discussion

4.1 Overview of planned / executed project tasks.

4.1.1 Task 1.1 – Capture / Refine Baseline Energy Usage:

This initial scope of this task was to study the current process streams to identify a baseline of the energy consumption required to produce starting aluminum product forms for aircraft

production, the average buy-to-fly ratios for all such starting product forms, and thereby compute the total scrap material that is produced for recycling, by subtracting the total fly-away weight of aircraft produced. This would yield a starting point for computing the potential positive impact on reduction of CO₂ generation enabled by the widespread implementation of Solid State Joining processes to reduce the average buy-to-fly for the aggregate aluminum starting stock. The energy and environmental impact would be dominated by the reduction in total aluminum product form required by the aerospace industry. In principle, this was a fairly straight-forward proposition.

Estimates of total aluminum utilized in commercial aircraft in any given year would be obtained from a combination of published values of weights of aluminum in individual models multiplied by total number of delivered aircraft. (All of this work is focused on the commercial fleets of aircraft, where some measure of publicly available data is expected, and ignoring the military fleets, where public data sources are much scarcer.) Next, a picture of the average buy-to-fly of all fleet aircraft components would be needed to be able to compute the total weight of produced aluminum product forms used to create the fly-away components. The difference is the amount of aluminum currently turned into chips / recycled waste. Assumptions could then be made on how quickly and to what extent the adaptation of the implementation of SSJ technologies – or any technologies – would reduce the average buy-to-fly values. The reduction in buy-to-fly would reduce the total aluminum required to produce the same parts, and hence reduce the total amount wasted. There would also be a contribution in the reduction in energy required for machining the initial total aluminum obtained down to the final, fly away aluminum produced. [That is assuming, of course, that the energy savings does not get consumed in the processes of producing the net shaped product form.]

This was indeed the initial, basic approach used in executing Task 1.1. Public sources of information were used to identify average fly weights of aluminum on commercial aircraft, broken down by sizing class (a function of both aircraft and passenger-capacity sizing), as well as general values of buy-to-fly ratios for each class. Current 20-year projections of replacement aircraft were coupled with current delivery rates and projected growth rates to obtain year to year projections of aluminum requirements for usage in production processes and total fly-away weights. Simple assumptions were made on both the time to initiate and fully implement the SSJ technologies. Another set of assumptions were required to estimate the potential impact of SSJ technologies on the average buy-to-fly values for any given aircraft class. This initial Baseline Energy Savings projection yielded a calculated avoidance of consumption of nearly 5 billion pounds of new aluminum and a projected aversion of 22.9 billion pounds of CO₂, and 30.7 Billion kilowatt-hours of power.

As the project continued, the refinement of the Baseline Energy Savings changes advanced on three fronts: refinement in the characterization of the fleet opportunities for reduction in buy-to-fly, re-consideration of the energy costs of producing aerospace quality aluminum product forms, and capturing process data to evaluate the net energy change required to implement the preparation and utilization of tailored blanks. The latter was needed to complete the “big picture” of savings potential of changing from a “hog-out” approach to aggressive utilization of prepared, tailored preforms.

A round of engineering effort was expended to obtain and evaluate aluminum procurement and utilization data for the 777 family of aircraft, the Boeing entry in the “medium twin aisle” sizing category. These data - and the parts they represented - were evaluated and analyzed to bring fidelity to the values of total fly weight of aluminum on an average aircraft, the average buy-to-fly for all parts, the percentage of aluminum parts which fit the category of high BTF, the percentage of these might actually be candidates for building and using a preformed blank, and, finally, the change in average buy-to-fly achievable such additive preforms. The results of this assessment on the 777 aircraft family have been considered in making any adjustments the calculations done for the entire fleet, and is reported in section 4.2.1, below.

The substantial work under task 2.1 on developing the Energy Consumption Model (see next section) resulted in the utilization of an updated value for the equivalents of CO₂ required to produce a pound of new aluminum. Thus, our projections of saved aluminum translated to an increased projected aversion of **58.76 billion pounds of CO₂ emissions, or 78.74 billion kWh of energy consumption.**

Finally, the application of the Boeing Energy Consumption Model (see task 2.1) to the case studies 1 and 2 (see Task 2.1, 2.2, and 2.3), led to the conclusion that the trade off of energy required to machine final parts by “hog-out” from full-thickness product forms versus the energy required to first produce a lower buy-to-fly product form and then finish machining it to final part geometry still favors the hog-out approach. (The latter still lead to OVERALL energy savings, due to the reduced material requirements!) This is so, in 2012, because the high speed machining processes are highly mature and efficient, as are the machining platforms, although they, for the most part, have not been fully optimized from an energy consumption perspective. The SSJ processes, in contrast, are all in their relative infancy, and the platforms – certainly as embodied in the Brotje system – are rather energy inefficient.

4.1.2.0 Task 2.0 - Energy Efficient Aluminum Preforms:

This task was intended to focus on developing the accuracy of an energy-consumption and emissions model capable of accurately determining the impact of adaptation of ultra net-shape preform processes on the current and future state of energy consumption and emission. The overall strategy was to begin with an existing model, the Sustainability Framework Model developed by NACFAM, and apply Boeing expertise to refine the model as it could be applied, first, to the various processes that produce existing aluminum product forms, including standard plate material and more-net-shape extrusions and forgings, and, second, to refine the model so that it could account for the specific impact when using new technologies to produce starting forms with shapes even closer to final required geometries (i.e., Solid State Joining). It was even anticipated that the level of detail which would be able to be evaluated with this model would extend to an evaluation of the energy impact of selection of specific alloys and processing tempers which might be “preferred” due to energy impacts. This task certainly required application of proper expertise to identify the details of specific process strategies, to ensure that the model properly accounted for the baseline the energy consumption to produce current product forms, and to be capable of providing user-defined

inputs for the modeling software to account for newly acquired, detailed knowledge of energy consumption associated with specific, targeted processes.

To validate the model, and to use it to completely evaluate the potential impact of applying SSJ technologies on energy footprint of the aerospace industry, two case study subtasks were planned. In the first type of case study, surveys of the portfolio of starting product forms for existing aircraft builds would be reviewed, and evaluated for existing buy-to-fly values, and the potential for adaptation of SSJ techniques to new starting forms for these components, reducing fleet requirements for overall buy-to-fly values. Specific case studies – where SSJ technologies would be used to prepare tailored starting forms and compared to fabrication of final parts using machining from thick plate would be used to validate the energy model and its ability to predict energy consumption for individual components, based on selections of combinations of specific possible manufacturing steps.

The delivered milestone for this task was to be a validated simulation and energy prediction for a test geometry that had been 100% machined from a billet, and additionally validated against a friction joined preform of the same test geometry. A critical, required companion deliverable was the collection of process data from Boeing process platforms, (principally the Brotje FSW machine in St. Louis, MO, along with a milling platform) to provide accurate baseline data for populating the energy model, to ensure an accurate simulation capabilities.

4.1.2.1 Task 2.1 - Identify Energy Input Streams for Use in SMF model:

This subtask was initially intended as the engineering study to determine the optimal approach for utilizing the Sustainable Manufacturing Framework model from NACFAM, and to provide an insight on possible changes in buy-to-fly product forms collected in Task 1.1, to produce simulations via the NACFAM tool for evaluation of the impact of manufacturing alternative new product forms using SSJ technologies. The deliverable was to be a representative simulation of the baselined process, and the resultant energy consumption, solid waste burden, acidification potential, and CO₂ burden, with a further outcome of understanding of how to modify the baseline energy savings projection obtained in Task 1.1, with the added information on the net costs of replacing a process of machining high BTF components with one of producing the tailored blanks with additive processes and then machining these reduced BTF components to final part configurations.

Initial review of the details of the Sustainable Framework Model from NACFAM and subsequent efforts to apply it to the first case study, made it clear that a major edit of the NACFAM model was required. For, instance, the SFM did not account for certain factors related to assess existing inputs needed for produce specific, existing starting product forms of aluminum. It did not have provisions for evaluating the impact of performance lifetime of produced parts or recycling of components, based on product lifetimes. Nor did it have sufficient detail or flexibility to apply it on a part-by-part basis, and compare / compute energy requirements for different combinations of manufacturing / production steps, including the utilization of SSJ technologies.

The NACFAM model was replaced in this project with a Boeing-derived model, using a “bottom-up” approach. The changes, and rational for changes made to this internally

generated model, identified here-in as the Boeing Energy Consumption Model (ECM) were based on reviews of literature sources and then refined based on the in-house experience with the Case Study 1 (see Section 4.2.2.2.1, below). Full details on development and implementation of the ECM are described in Section 4.4 below. It is now capable of providing a meaningful comparison between fabricating an aluminum component from a hog-out approach from plate versus a friction stir welding approach from a tailored blank. It has been constructed so that energy consumption data obtained or generated for other SSJ processes, or any other manufacturing process, can be added to the model. The model has been populated with energy consumption data for Linear Friction Welding, previously obtained by Boeing, and data for Rotary Friction Welding can readily be added in the future. The model can currently differentiate the impact of starting from thick plate, extrusions, or forgings. Finally, energy consumption data collected by TWI during their subcontracted work on developing conditions for corner angle welding, performed as part of Task 3.1, were used to populate the model with information required to use the model to predict energy required for manufacturing components with this particular version of a solid state joining method.

4.1.2.2 Task 2.2 - Produce Case Study for Net-Shape Preforming:

The original scope of this subtask included part reviews and aircraft platform surveys, to identify candidate geometries which could be impacted by SSJ technologies in fashioning reduced buy-to-fly starting product forms, and identifying up to three potential candidates for the process which could be the subject of case studies. These latter case studies were to include at least two physical studies – in which appropriate preforms would be fabricated via SSJ processes and compared head-to-head with fabrication of final components using standard machining practices starting from thick plate stock. FSW would be the preferred SSJ process for these case studies, but others might have been incorporated if both appropriate candidate parts were identified and access to suitable process equipment or a vendor with instrumented process equipment had been located.

As the project progressed, manpower limitations delayed work in performing aircraft part surveys, so a “pseudo-bulkhead” component, depicted in figure 4.1.2-1, was used as Case Study 1. This bulkhead has been designed and produced under another program, and all the processes for producing it by friction stir welding additive methods had already been worked out. It was an excellent candidate for producing it by both the FSW-additive method, and hogging it out of thick plate. With the implementation of web-based capability for capturing and analyzing measurements of actual energy consumption in each approach, Case Study 1 provided detailed considerations for energy consumption elements to be incorporated into the Boeing Energy Consumption Model, under task 2.1.

The preform was assembled on the Brötje FSW system, while energy consumption was monitored both for the overall machine and for the FSW process itself. Machining was done on a power-monitored Cincinnati 20V mill platform to produce the final part from both a thick plate and from the FSW-generated preform. The energy data collected was used to modify and populate the Energy Consumption Model.

As noted for Task 1.1, aircraft components for the 777 aircraft were used in sampling surveys, for identifying potential impact for reducing fleet-wide BTF ratios. They were also used to identify a part to be utilized for the second case study. The second case study, based on a 777 floor component, entailed building another preform using a FSW-based additive process pathway and machining it to final configuration. Once again, energy monitoring equipment on both the Brotje FSW platform used to produce the preform, and the Cincinnati Milling platform used to complete the fabrication of the perform to final part configuration, was used to validate the ECM by comparing predictions of energy consumption, with the actual energy consumption data

Malfunctioning hardware on the Brotje platform long-delayed completion of this work, but the work has been completed and the results are reported in Section 4.2.2.2.

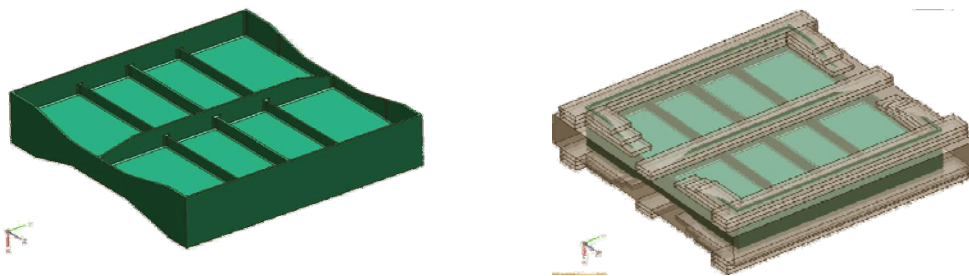


Figure 4.1.2.2-1. Bulkhead Example, final component on left, FSW-produced preform on right.

4.1.2.3 Task 2.3 - Compare Energy Consumption of FSW Preform to Baseline:

This subtask was designed to provide the validation of a model designed to estimate energy consumption, solid waste burden, acidification potential, and CO₂ emission, and the subsequent impact of adopting SSJ technologies which reduce BTF, but need to be checked for relative consumption of energy (and environmental impact) when comparing the baseline approach of hogging out from thick plate with the production of the preform via an SSJ process and machining to final geometry.

As executed, this final step has been achieved in the Case Study 2, which was able to be used to compare predicted energy consumption with measured energy consumption. As discussed in Section 4.2.2.3, the results were excellent, and no modification of the present version of the ECM is recommended based on this case study. It did illustrate the need to populate the model with as-measured consumption values for the precise process being used in the model.

What was not further undertaken was application of the current model to a multitude of potential candidate of parts identified in the 777 fleet surveys. To do so grew beyond the scope of available time and budget.

4.1.3.0 Complex Aluminum Intersection Development

The third task was focused as a risk reduction step that would evaluate concept tooling and fixturing concepts for performing progressive additions of materials using the various SSJ techniques in different orders, for at least two different 3-D structural geometries. Energy

consumption and emission production would be estimated via the NACFAM SFM model for each of these sequences, using process-based data on energy requirements for each technique, gathered from validated sources.

As executed, the focus of the modeling moved away from the NACFAM model, for reasons cited above, and to the Boeing Energy Consumption Model. The scope of this task was also narrowed to looking at using the ECM to assess multiple possible SSJ pathways to produce a preform suitable for the fabrication of the Case Study 2 component.

This task was also scoped to include several activities which would enable the evaluation of the emerging technique of angle Friction Stir Welding and development of a welding head tool design for Boeing's Brotje FSW system, which will enable actual building of demonstration structures in future phase programs. These activities were intended to validate the process as viable, as it should be the most efficient way to add vertical stiffeners to a plate, and therefore would have subsequent value and impact for adding or joining other complex geometries. TWI, which had developed a core capability in this nascent technique, was contracted to perform these demonstration welds on selected representative aluminum alloys, collecting force and energy data, and to provide engineering consultation to Boeing to enable the design of a welding head.

4.1.3.1 Task 3.1 – Evaluate Combinations of SSJ techniques for Optimum Energy Efficient Preforms:

A total of five distinct fabrication pathways, utilizing different combinations of FSW methods, including corner angle welding, and linear friction welding, were identified as possible approaches to building a preform for either the original 777 floor component or the subtended version which was actually produced. In this task, all of these pathways, along with the standard hog-out process, were evaluated using the Energy Consumption Model to ascertain which, in theory, was the most energy efficient pathway. Only one was actually able to be tested against the model, as described in Task 2.3. This exercise illustrated the value achieved with the Boeing model in selecting one manufacturing process over other processes, using the projected energy consumption as part of the decision process.

4.1.3.2 Task 3.2 - Development of Corner Angle Welding for Vertical Stiffener Joining:

A subcontract was established with TWI, with multiple subtasks. The completion of this process development would demonstrate a pathway for minimizing the number of welds required to add perpendicular and canted stiffeners for many applications. This technique will minimize weld count which in turn will help minimize distortion associated with welding.

The tasks to be performed by TWI included: a) Process Development, using their previous experience in Stationary Shoulder FSW welding to design and fabricate two new probes and two new shoulders suitable for welding eight-millimeter thick "T" components, performed in three alloys: AA6082, AA2024, and AA7075; b) production of demonstration examples and collection of process data; c) assistance to Boeing engineers with a design for a Stationary Shoulder FSW weld head suitable for use on the Brotje FSW system to achieve corner angle welding.; produce a final report on their work.

4.2 Specific Details of Work Performed and Results, by Project Task

4.2.1 Task 1.1 – Capture / Refine Baseline Energy Usage:

This task began with a projection of the potential savings in consumption of aluminum required to build the next 20 years of aircraft needed to fulfill the world's projected airline traffic needs, if SSJ technologies could be widely implemented. This first required a projection of aluminum required based on current process streams and production practices, followed by a modification of this projection by the potential savings in the consumption due to the adoption of the SSJ additive processes which could reduce the required buy-to-fly (BTF) for some percentage of the total components currently fabricated from bulk aluminum forms. The results of these fleet impact projections, performed in the first two quarters of this project, coupled with a refinement in the "accepted" baseline value used for the equivalents of CO₂ required to produce a pound of new aluminum (12.476 pounds of CO₂), yielded a projection of an avoidance of 58.76 billion pounds of CO₂ via widespread adaptation of SSJ processes.

Over the last half of this project, efforts were undertaken to refine and validate the fleet impact assessment by obtaining and evaluating aluminum procurement and utilization data for the 777 family of aircraft, the Boeing entry in the medium twin aisle category. These data - and the parts they represent - have been evaluated and analyzed to bring some further fidelity to the values of total fly weight of aluminum on an average aircraft, the average buy-to-fly for all parts, the percentage of aluminum parts which fit the category of high BTF, the percentage of these might actually be candidates for building and using a preformed blank, and, finally, the change in average buy-to-fly achievable using such additive preforms.

Global Fleet Description

The commercial aircraft fleet is divided into six distinct categories. Boeing produces and sells aircraft in five of these, as detailed in below. Because Boeing only competes in these five categories, the energy impact of implementing the additive processes which are the subject of the project has been evaluated based on these five categories only. The five categories are: 1) Single Aisle aircraft, with seats ranging from 95 to 175; 2) Large Single Aisle, with seating greater than 175; 3) Small Twin Aisle; 4) Medium Twin Aisle; and 5) Large Twin Aisle.

Table 4.2.1-1 shows the Boeing aircraft that fall in each category, along with other world fleet aircraft included in each category. Three of the Boeing platforms are no longer in production, but are included in the determination of total fleet sizes. These are the 757, 727, and 717 platforms.

This table also contains data on the size of the Global fleet in 2009, along with twenty-year projections of the fleet size and composition in the year 2029. This data includes projections of new builds required between 2009 and 2029, accounting for expected retirements from service of aged aircraft. These figures are available from Boeing's public web site (www.Boeing.com).

Table 4.2.1-1. World Aircraft Fleet Composition by Type, With 20-Year Projections.

Type of Aircraft	Boeing Platforms	World Fleet Platforms	New Builds 2009-2029	2009 Fleet size	2029 fleet size
Large Twin Aisle	747	A380	720	800	960
Medium Twin Aisle	777	A330-300 A340-300, 500, 600 A350-900, 1000	2420	1620	3830
Small Twin Aisle	787 767	A330-200 A350-800	3680	1880	4430
Large Single Aisle	757 737-900ER	A321	3070	8920*	3920
Single Aisle	737 727 717	A318, A319, A320 BAE 146-300 Avil ARJ-900 AVRO RJ-100 Bomb CS300 CS100, YAK 42 CRJ-1000 Embraer 190, 195	18080	9920	21080

* This entry may be in error. The original Boeing document from which it was taken is no longer available on the web site. It does not enter into subsequent calculations / discussions.

Global Fleet Projection, by Year, by Type

To project the impact of the acceptance and adoption of additive processes, it is necessary to have a picture of the projections of new-build quantity by year, as it will take some period of time before relevant performance data are available to fully qualify the application of the SSJ processes, and all possible applications are fully implemented. The author has been unable to locate sufficient, publicly-available data to accurately know what the planned future production rates are by all commercial aircraft vendors. For the projections made here, a simple model of compounded linear growth rates was applied to new builds, beginning with estimates of current production rates, to compute evolving production rates which result in matches to the Boeing-supplied projections of total new builds over 20 years time. These models are depicted in Figures 4.2.1-1, through 4.2.1-5, graphs mapping builds by year, and accumulated total new aircraft. Again, the model for each aircraft type begins with an estimated total for the number of aircraft produced in 2009. [Data on Boeing's production numbers have been easily found. Public information for totals from other manufacturers has not been uncovered. Estimates of 2009 builds were taken from coupling Boeing rates with estimated market share of new deliveries.] The linear growth rate for each model was then adjusted until the total number of new production aircraft matched the published new-aircraft projections.

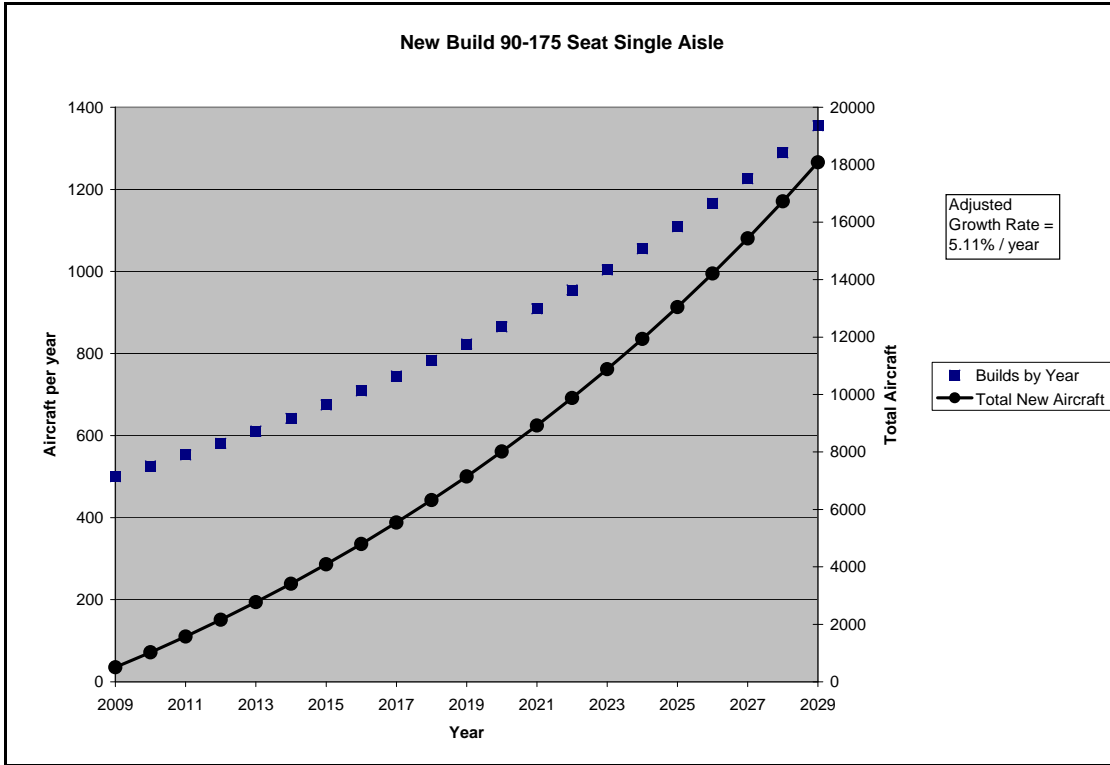


Figure 4.2.1-1. New Fleet Builds by year, 90-175 Seat Single Aisle Aircraft.

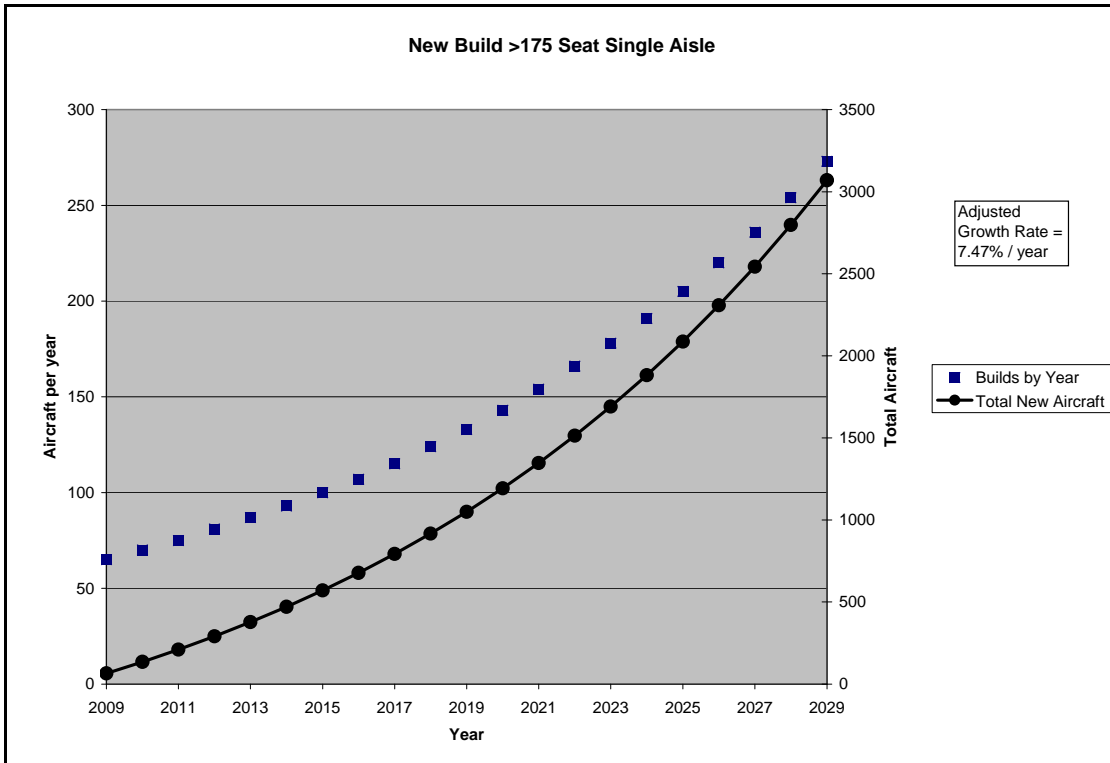


Figure 4.2.1-2. New Fleet Builds by year, >175 Seat Single Aisle Aircraft.

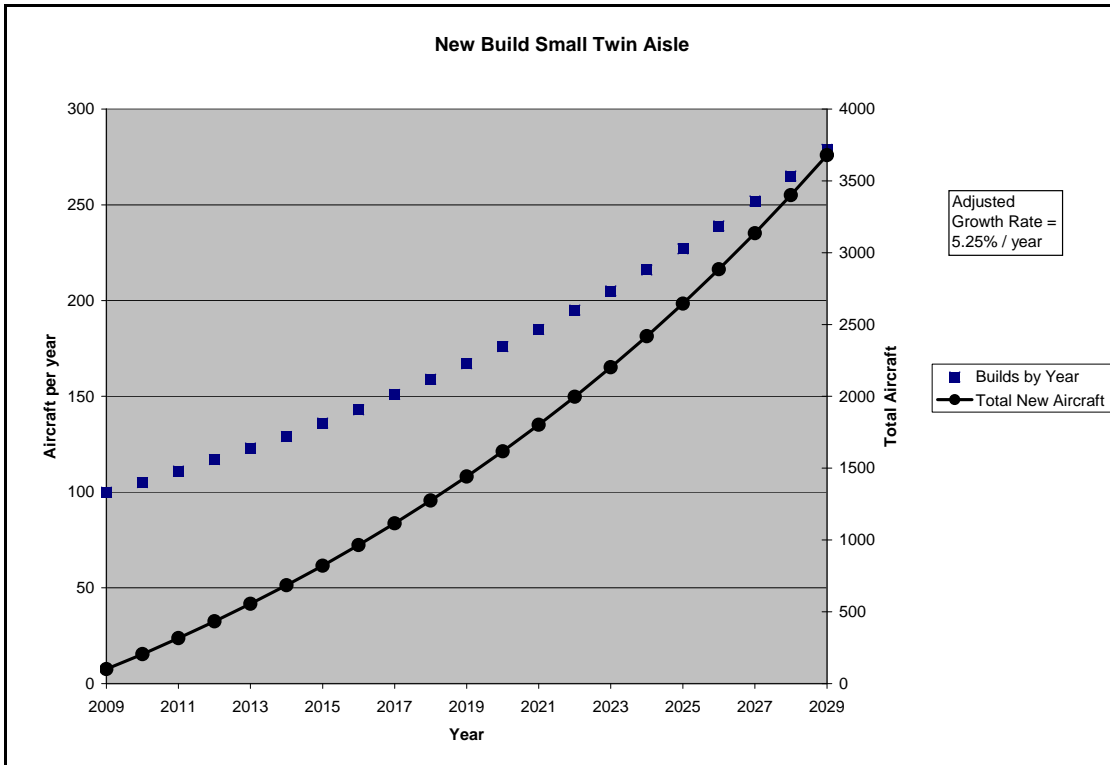


Figure 4.2.1-3. New Fleet Builds by year, Small Twin Aisle Aircraft.

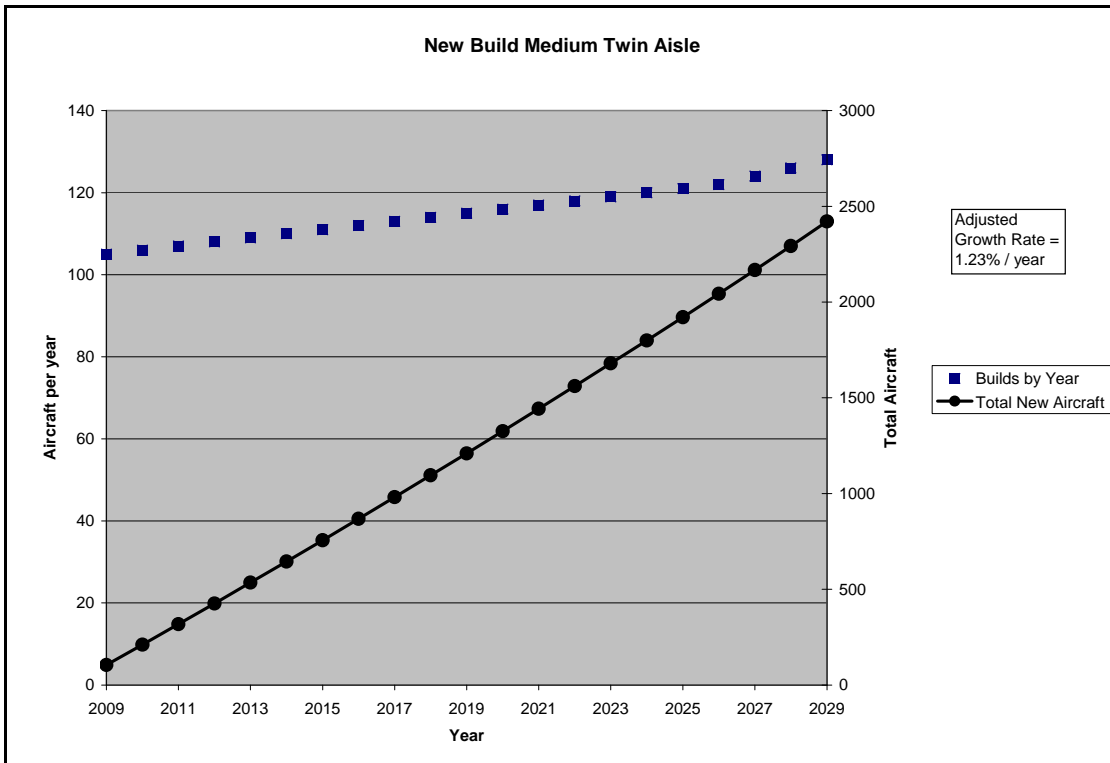


Figure 4.2.1-4. New Fleet Builds by year, Medium Twin Aisle Aircraft.

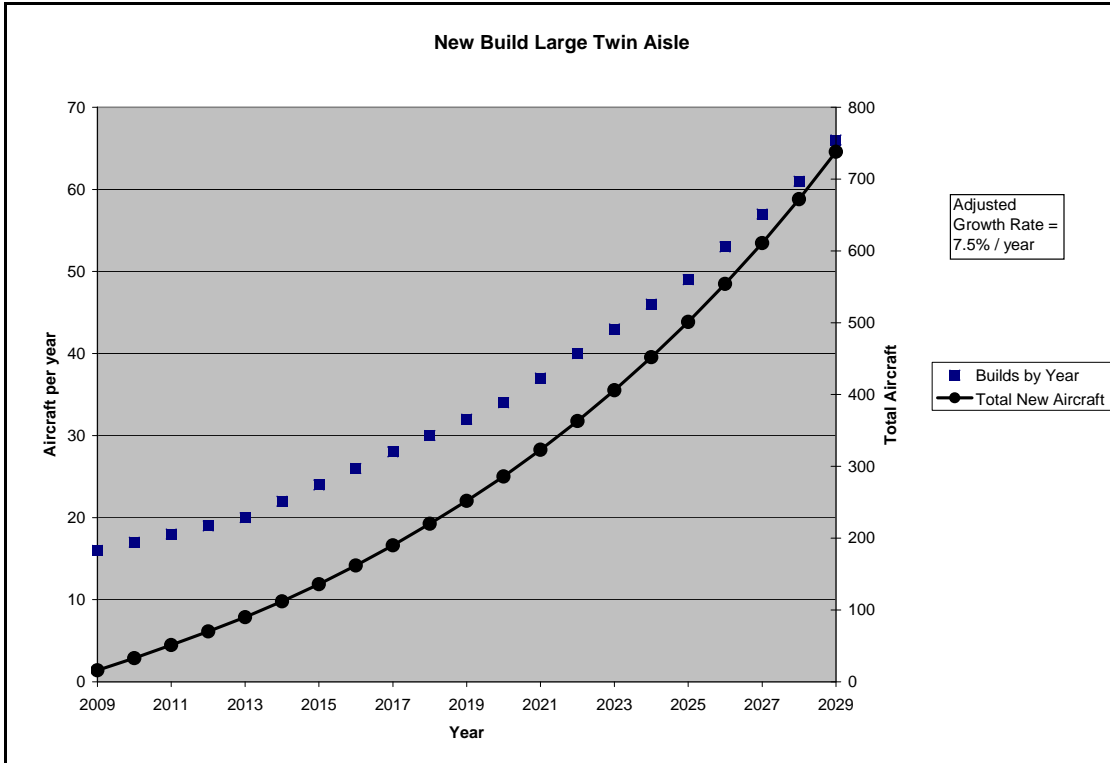


Figure 4.2.1-5. New Fleet Builds by year, Large Twin Aisle Aircraft.

The required growth rates range from a low of 1.25 percent for medium twin aisle aircraft to a high of 7.5 percent for both large single aisle and large twin aisle platforms. For the whole fleet projection of 27980 aircraft, the required growth rate is 4.97%, which parallels the projected growth rate in passenger traffic for the same 20 year period. The variations in growth rate by aircraft type is expected; however, as each aircraft type tends to serve a particular type of traffic routing (transoceanic, transcontinental, hub-to-hub, hub-to-region), the traffic growth rates in each of these routing types vary substantially from the gross rate of 5% for total traffic. These models are a reasonable starting state for the purpose of estimating a baseline projection of energy savings, and the best that can be used without public sources of projected year-by-year production rates.

Global Fleet Aluminum Utilization and Baseline Buy-to-Fly Ratios

The next step in obtaining a baseline projection of the energy impact of implementing the additive build strategies to reduce buy-to-fly requirements of aluminum starting forms is to gather a picture of the existing BTF values and resultant buy volumes of aluminum per aircraft, for each aircraft type. Such data are presented in Table 4.2.1-2.

The information in this table begins with empty weight data for each aircraft, by aircraft type, and a percentage of this weight which are from aluminum alloys. For each aircraft type, data are entered for each of the main platforms which fall into this category (see Table 4.2.1-1 for detailed aircraft designations). These data values are, in turn, averaged over the several models which might fit each category. Then, within each category, the values are again averaged, and the results highlighted (in blue) along the bottom row in each aircraft type category. There is simply not enough public information to breakdown this analysis to

account for the percentage of new builds that each individual platform contributes to the total projected new builds by type.

The Small Twin Aisle category contains both metal skinned (MS) models, such as the Boeing 767 and Airbus A330, and the newly emerging composite skinned (CS) models, such as the Boeing 787 and Airbus A350 aircraft. These two types of aircraft have a significant shift in the percentage of aluminum used in the construction of each aircraft. Ideally, each sub-category of aircraft type should be evaluated separately. But, again, no publicly available breakdown projections of each subtype (MS and CS) to the overall projected fleet growth in this aircraft type was located; so for this analysis, again the average of the table entries were simply averaged (and highlighted in green).

Table 4.2.1-2. World Aircraft Fleet Utilization of Aluminum, by Type.

Type of Aircraft	Platforms	New Builds 2009-2029	Empty Weight (lbs)	Percent Al	Fly Weight Aluminum	BTF	Buy Weight Aluminum (lbs)
Large Twin Aisle	747 Pass	720	387000	81	314000	8	2512000
	747 Freight		448000	80	359000	8	2872000
	A380		395000	61	241000	8	1928000
	avg		410000	74	304667	8	2437333
Medium Twin Aisle	777	2420	333000	70	233000	8	1864000
	A330		171000	68	116280	8	930240
	A340		226000	68	153000	8	1224000
	A350		19400	19	37000	8	296000
avg	187350	56	134820	8	1078560		
Small Twin Aisle	767	3680	206000	80	165000	8	1320000
	A330		171000	68	116280	8	930240
	avg - MS		188500	74	140640	8	1125120
	787		253300	20	50500	16	808000
	A350		173000	19	32870	16	525920
	avg - CS		213150	20	41685	16	666960
avg-both	200825	47	91163	12	1093950		
Large Single Aisle	737	3070	98500	70	69000	8	552000
	A321		61000	68	41480	8	331840
	avg		79750	69	55240	8	441920
Single Aisle	737	18080	92000	70	64000	8	512000
	A318-320		50000	68	34000	8	272000
	avg		71000	69	49000	8	392000

This data compilation was made from public sources of such information. The author of this report has not further verified individual data items, but relied on the providers of these compilations to have given reasonably correct values. Often, the precision of values of such characteristics as empty weight and percent material breakouts that are publicly available are only accurate to one or two significant digits. Technical data sheets, which are not usually made public, would be a better source of the first value, but detailed analysis of the percent

by weight of each constituent material type are not made public, and only the general values, such as those listed in the table, are released.

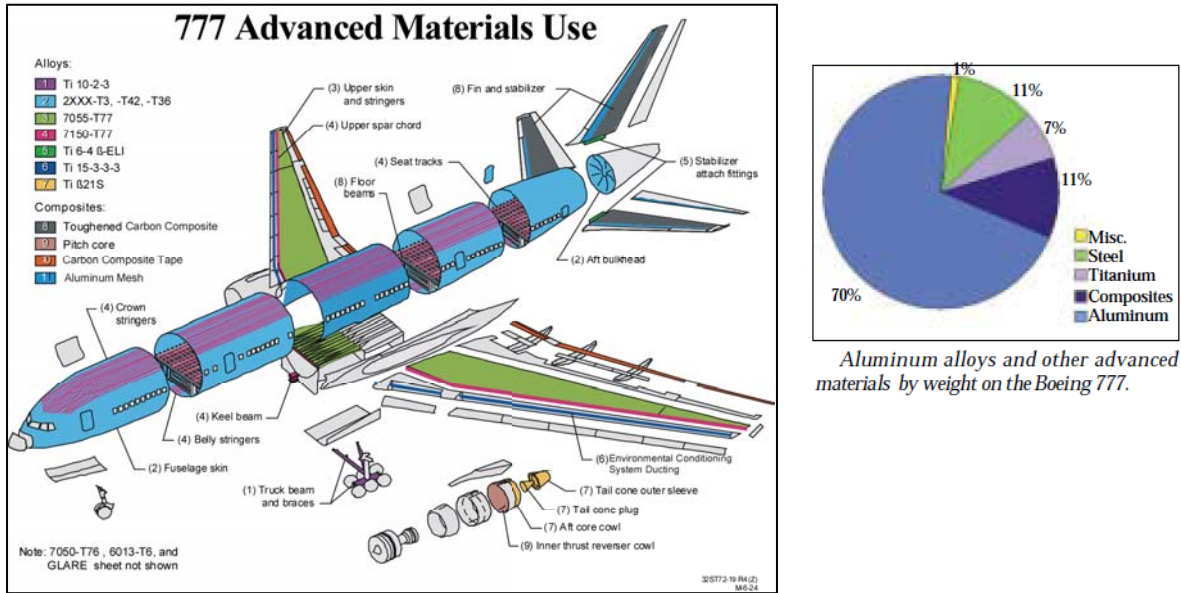


Figure 4.2.1-6. Material Usage on 777 Platform and Associated Pie Chart.

Two such publicly-available examples are shown in Figures 4.2.1-6 and 4.2.1-7, showing the material breakdown for the 777 platform and the 787 platform, respectively. Notice the figures in the pie charts for aluminum of 70 percent and 20 percent, respectively; match the values in table 4.2.1-2.

In a similar manner, the buy-to-fly values (BTF column) in the table are also very generic in nature, and listed as 8 to 1 for all of the metal skinned (MS) aircraft models. The accuracy of these values is a topic discussed in more detail below. For a composite skinned (CS) aircraft, the BTF is considerably higher (16/1). As had been done for the value of empty weight of the aircraft and percentage of aluminum for this aircraft type category, the average value of 12/1 was selected for later usage for this category in projecting total savings of material used and energy impact, as insufficient breakdown of the actual composition of the projected total aircraft in this category is available, based on skin type.

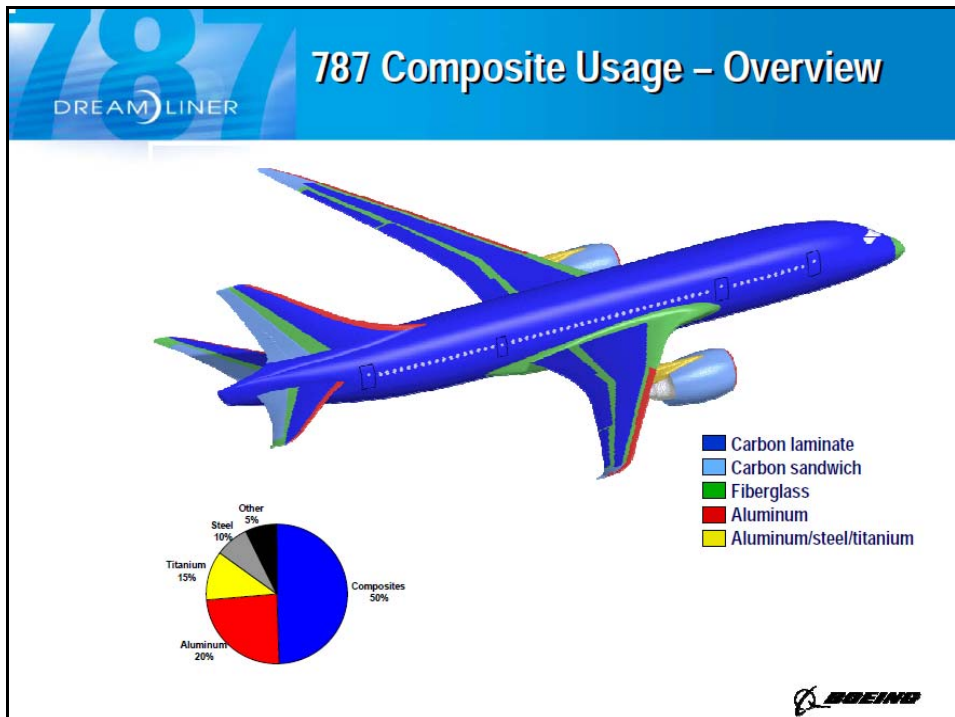


Figure 4.2.1-7. Material Usage on 787 platform and associated pie chart.

Detailed assessments of actual buy-to-fly ratios have been performed by Boeing on several of its own production platforms. These are not available for full release in this report, but general results are provided here. First, aircraft components fall in two general categories, those with a low BTF values and those with high BTF. The latter, with values ranging about a ratio of 2:1, are generally fabricated from thin sheet or plate, have required minimal thinning or shaping requirements, are strongly representative of skin or surface components, formed stiffeners and brackets, and the like. For metal skinned aircraft, these represent 50 percent or more of the total fly-weight of the aluminum components. The remaining components are high BTF items, with the latter ranging from 8 to 1 to over 45 to 1, in some rare cases. In one such detailed assessment of the high BTF components of a specific Boeing aircraft, it was found that 91 % of such components came from bar, forged block, and plate starting forms. The average BTF for these components was 20.7 to 1. To simplify the assessment of the impact of adopting SSJ additive process, the following assumptions have been made. 1) The buy-to-fly ratio for skin-like and other thinned, formed components can be represented by a value of 2-to-1. 2) The remaining aluminum components of an aircraft type can be represented by an average BTF value of 20-to-1. 3) A unique combination of percentages of 2:1 parts and 20:1 parts can be identified which will yield the average BTF values cited in Table 4.2.1-2. For example, at an average BTF value of 8:1, 33.3% of the aluminum parts need to have a BTF of 20:1. At an average BTF value of 12:1, the percentage of high BTF components rises to 55.5%.

Impact of Adopting Additive Processes to Reduce BTF of High BTF components

The necessary groundwork has now all been laid to assess the impact of adopting the solid state joining processes being investigated in this project on reducing the aluminum content in

preforms used to produce complex aluminum components in aircraft assemblies. Certain values associated with implementation have to be made to complete this assessment and these are:

- 1) The percentage of the high BTF components which are likely to be impacted by the implementation of these processes;
- 2) The new BTF values that can be achieved using these processes;
- 3) The time period required to obtain sufficient performance and other engineering data to validate the processes for usage on aircraft, in critically performing structural roles;
- 4) An induction period and induction rate over which these processes can be fully applied.

For purposes of illustrating the potential impact on reduction of energy consumption and reduced of greenhouse gases, by implementation of SSJ processes to lower required BTF values, the following values for the above have been modeled.

- 1) Both a 40% impact on High BTF and a 60% impact of High BTF aluminum starting materials have been assessed. Only a few examples of the former were undertaken, to show the impact of a more conservative value, while the majority of the computations utilized the more aggressive – optimistic? – value of 60% impact.
- 2) An aggressive selection of a new BTF value of 6-to-1 has been selected. This relatively low value is similar to BTF for forgings and extrusions, and if an additive process can't achieve this BTF in preparing a near-net-shape preform, then the conversion of the part starting form from a bar, forged block, or plate to a more aggressive forging should be considered, in order to similarly reduce energy impact.
- 3) Again, being somewhat aggressive / optimistic, a development period of three years has been selected, meaning first applications would not go into effect until 2014, using 2010 as the analysis starting date.
- 4) In addition, a ramp-up period of three years has been used, with ramp rate of 33 % per year. This means that in 2014, only 1/3 of possible applications would transition to the additive processes, 2/3 in 2015, and then in 2016, all applications would be achieved.

Table 4.2.1-3 contains the critical information about the projected impact of adopting the PEEPS-focused processes. The blue highlighted values are the average values for empty weight, percentage of aluminum by weight, the resultant fly weight of aluminum, the average buy-to-fly ratio, and the resultant buy weight per aircraft, for each of the aircraft type, taken from Table 4.2.1-2. In the top portion of the chart, computed values of new average BTF values for each aircraft type, using a 40 percent impact rate, and 60 percent impact rates for each year of a three year implementation total transition timeline.

The second portion of the chart, the projected new average “buy weights” for aircraft by aircraft type is shown for each of the above implementation rates. The last portion of the chart lists the projected savings in avoided purchased aluminum by weight in pounds for each aircraft.

Table 4.2.1-3. Projected Impact on BTF and Utilization of Aluminum, by Type.

Type of Aircraft	Platforms	New Builds 2009-2029	Empty Weight (lbs)	Percent Al	Fly Weight Aluminum	BTF	Buy Weight Aluminum (lbs)	Impact BTF @40%	Impact BTF year 1 @60%	Impact BTF year 2 @60%	Impact BTF @60%
Large Twin	avg	720	410000	74	304667	8	2,437,333	6.13	7.07	6.15	5.20
Medium Twin	avg	2420	187350	56	134820	8	1,078,560	6.13	7.07	6.15	5.20
Small Twin	avg-both	3680	200825	47	91163	12	1,093,950	8.89	10.47	8.93	7.34
Large Single	avg	3070	79750	69	55240	8	441,920	6.13	7.07	6.15	5.20
Single Aisle	avg	18080	71000	69	49000	8	392,000	6.13	7.07	6.15	5.20
Type of Aircraft	Platforms	New Builds 2009-2029	Empty Weight (lbs)	Percent Al	Fly Weight Aluminum	BTF	Buy Weight Aluminum (lbs)	Impact Buy Weight @40%	Impact Buy Weight year 1 @60%	Impact Buy Weight year 2 @60%	Impact Buy Weight @60%
Large Twin	avg	720	410000	74	304667	8	2,437,333	1,867,607	2,153,993	1,873,700	1,584,267
Medium Twin	avg	2420	187350	56	134820	8	1,078,560	826,447	953,177	829,143	701,064
Small Twin	avg-both	3680	200825	47	91163	12	1,093,950	810,435	954,471	814,081	669,133
Large Single	avg	3070	79750	69	55240	8	441,920	338,621	390,547	339,726	287,248
Single Aisle	avg	18080	71000	69	49000	8	392,000	300,370	346,430	301,350	254,800
Type of Aircraft	Platforms	New Builds 2009-2029	Empty Weight (lbs)	Percent Al	Fly Weight Aluminum	BTF	Buy Weight Aluminum (lbs)	Delta Weight @40%	Delta Weight year 1 @60%	Delta Weight year 2 @60%	Delta Weight @60%
Large Twin	avg	720	410000	74	304667	8	2,437,333	(569,727)	(283,340)	(563,633)	(853,067)
Medium Twin	avg	2420	187350	56	134820	8	1,078,560	(252,113)	(125,383)	(249,417)	(377,496)
Small Twin	avg-both	3680	200825	47	91163	12	1,093,950	(283,515)	(139,479)	(279,869)	(424,817)
Large Single	avg	3070	79750	69	55240	8	441,920	(103,299)	(51,373)	(102,194)	(154,672)
Single Aisle	avg	18080	71000	69	49000	8	392,000	(91,630)	(45,570)	(90,650)	(137,200)

The impacted BTF ratio listed in the top portion of the chart can be computed from the selected values cited above, using the following relationship, derived for this analysis.

$$\text{Impacted BTF} = 2 + (\text{ABH} - 2) * (\text{PHBTF}) - ((\text{ABH} - \text{RBTF}) * \text{PHBTF} * \text{PI}) \quad (\text{equation 4.2.1-1})$$

Where

- ABH = Average BTF of high BTF parts = 20
- PHBTF = Percentage of Al parts with high BTF ratio (depends on values from Table 4.2.2-2)
- RBTF = Reduced BTF of high BTF parts, achieved through adapting additive processes) = 6
- PI = Percentage of high BTF parts (weight) impacted by application of additive processes = 40% or 60%

Projected Global Fleet Savings of New Aluminum Requirements

To obtain the projections of fleet savings obtainable by adapting the additive processes to reduce BTF of high BTF components now only requires the application of the per-aircraft projected savings on the projected new aircraft builds by aircraft type. Figure 4.2.1-8, as an example, shows the application of the projected savings for both a 40% impact percentage and a 60% impact percentage on single aisle category, such as the 737 NG aircraft platform.

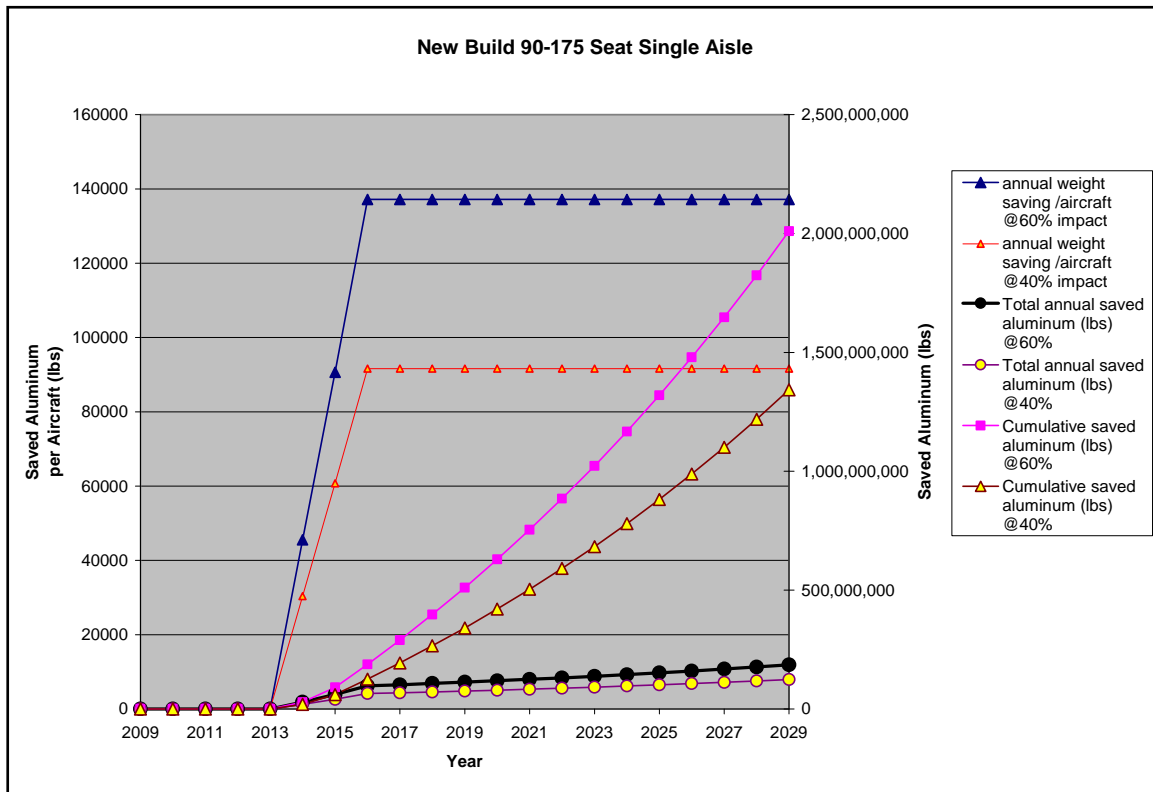


Figure 4.2.1-8. Projected Aluminum Savings in Single Aisle Aircraft Fleet.

The figure illustrates that at a 60% impact rate on high BTF components (that is, reducing 60 percent of the 20-to-1 BTF aluminum components down to a 6-to-1 BTF) would result in a savings of just over 2 Billion pounds of aluminum between 2014 and 2029! If this successful implementation of the additive processes only impacted 40 percent of the high BTF components used on such aircraft, the savings in newly-fabricated aluminum starting materials would still total over 1.3 billion lbs!

Figure 4.2.1-9 illustrates the 60% impact figure applied to the entire fleet of aircraft which include Boeing-build platforms. It shows the accumulated savings for the fleet to approaches nearly 5 Billion pounds of new aluminum production. Clearly the highest contributors to this are the 737-sized single aisle aircraft, followed by the small twin aisle, even though the latter contains both the metal-skinned aircraft and composite-skinned aircraft. There simply are a lot of both of these two types of aircraft which are to be built.

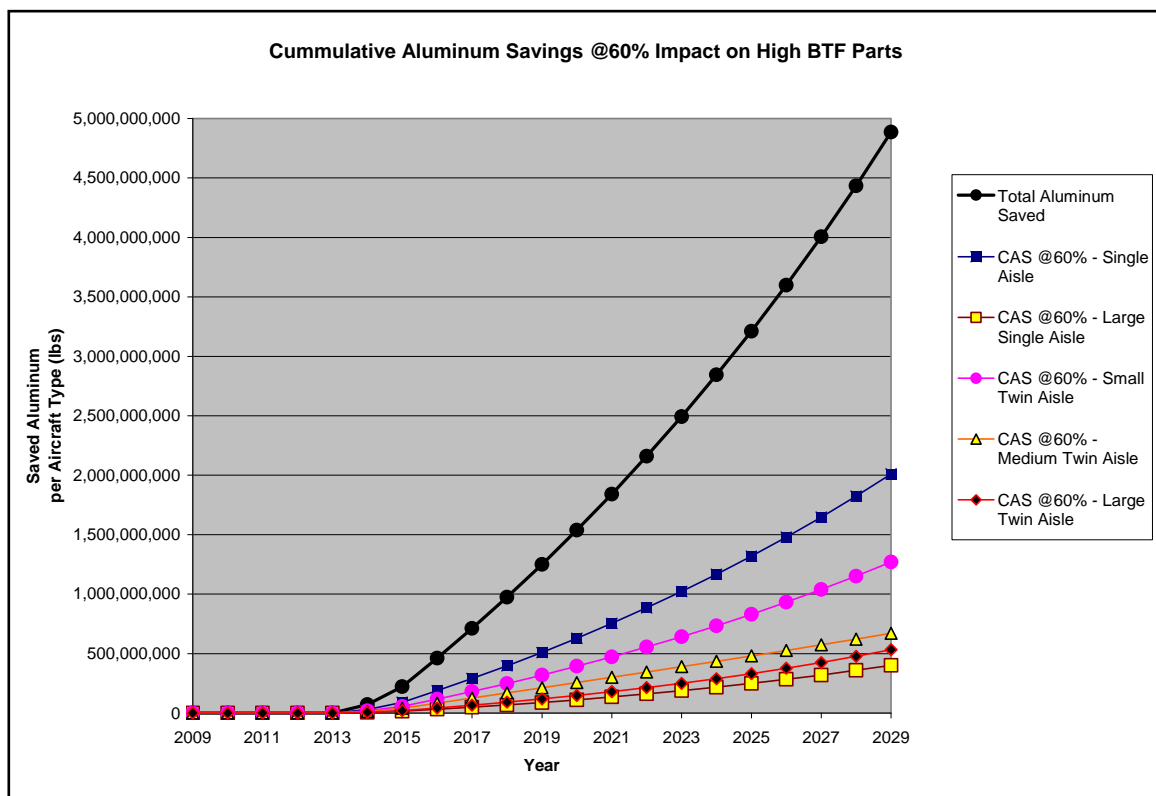


Figure 4.2.1-9. Projected Aluminum Savings for each aircraft type and Total New Build Fleet.

This initial Baseline Energy Savings projection, of 4.71 billion pounds of avoided aluminum being required to build future fleet aircraft, was coupled with the work on the Boeing Energy Consumption Model under Task 2.1, which resulted in a refined value of 12.476 pounds of CO2 being generated for each pound of aluminum produced, yielding a calculated avoidance of 58.8 billion pounds of CO2, and 78.7 Billion kilowatt-hours of power consumed.

Refinement of the Global Fleet Projection of Savings of New Aluminum Requirements, based on 777 Procurement and Utilization

To bring fidelity and validation to the various assumptions used in the calculation of the baseline energy usage model, efforts were expended on evaluating aluminum procurement and utilization data for the 777 family of aircraft, the Boeing entry in the medium twin aisle category. It is a “modern” aircraft, designed in the fully computed-assisted design era, with metallic fuselage and wing structures, and significant composite structure/components in the empennage (horizontal stabilizer and vertical tail).

The overall picture of the utilization of aluminum starting materials on the 777 aircraft is presented in four ways, all as a function of the starting product form and the application area on the aircraft. These four ways look at the a) number of parts fabricated from each type of product form, b) the amount of overall fly weight due to each type of product form, c) the overall buy weight of each product form/application, and d) the average buy-to-fly values for each product type/application.

A 777 aircraft contains over 37,000 individual aluminum components. Figure 4.2.1-10 illustrates the distribution of the number of these individual aircraft components, based on their starting product form with some breakdown by application area. Clearly, components fabricated from sheet starting material dominate the distribution, followed by plate products and then extrusions, forgings, and forged blocks. The plate products have been subdivided into plate for fuselage applications and plate for wing applications. Both of the latter have been further divided into plate for skin applications (both wing and fuselage) and then “other” applications. In the case of both wing skin and fuselage skin applications, these represent components which are very large in area and relatively low in thickness, but too thick to be designated as sheet products. Their very low part counts are a reflection of their large physical size, particularly surface area.

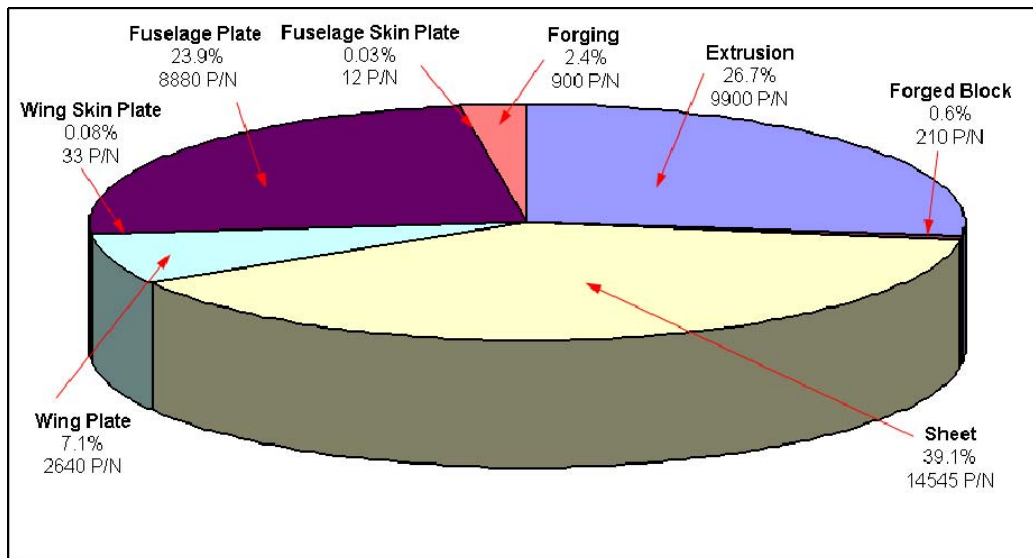


Figure 4.2.1-10. Distribution of number of individual aluminum parts of a 777 aircraft, by starting product form / application area.

A 777 aircraft contains over 200,000 lbs of aluminum. Figure 4.2.1-11 illustrates the distribution of this fly-away weight of aluminum, based on the starting product forms with some breakdown

by application area. Clearly, the fuselage skin and wing components, despite their low part counts, dominate this fly-away weight, followed by forgings, extrusions, plate, forged block and sheet components. The non-skin applications are dominated by substructural components (frames, stringers, bulkheads, floor components, and so on), while the sheet products, which dominate the part count distribution, are generally very small but very numerous items such as brackets, clips, and local stiffeners.

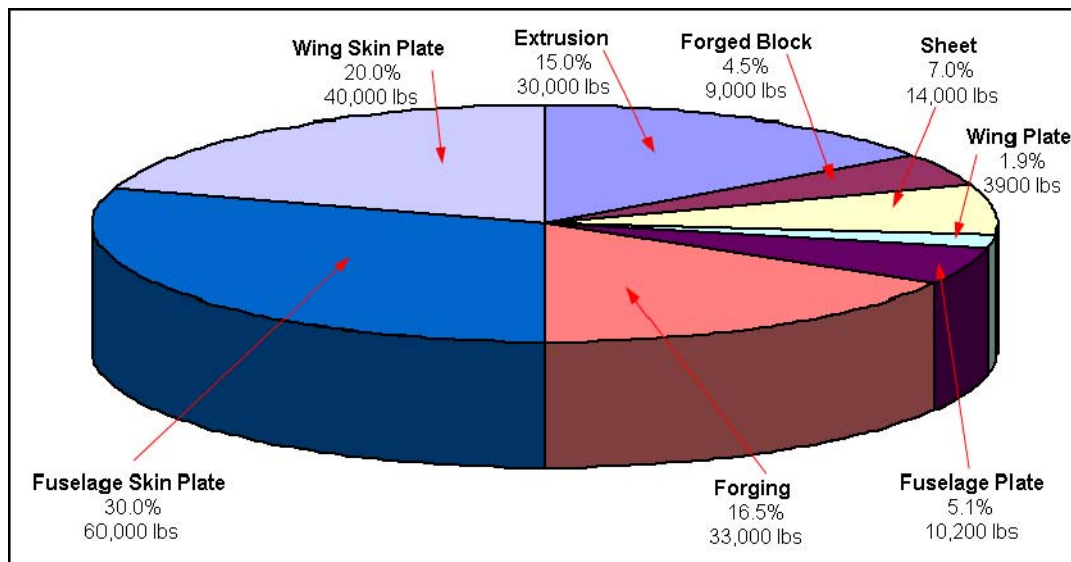


Figure 4.2.1-11. Distribution of fly weight of aluminum parts, by starting product form / application area.

Boeing and its supply chain obtain something in the range of 470 tons of aluminum starting products to produce all of the aluminum components required for a single 777 aircraft. Figure 4.2.1-12 illustrates the distribution of this buy weight of aluminum, based on the starting product forms. Clearly, this weight distribution is dominated by non-skin plate components, followed by extrusions for structure components, followed by the plate for fuselage skin and wing components, with smaller amounts of sheet, forging, and forged block materials.

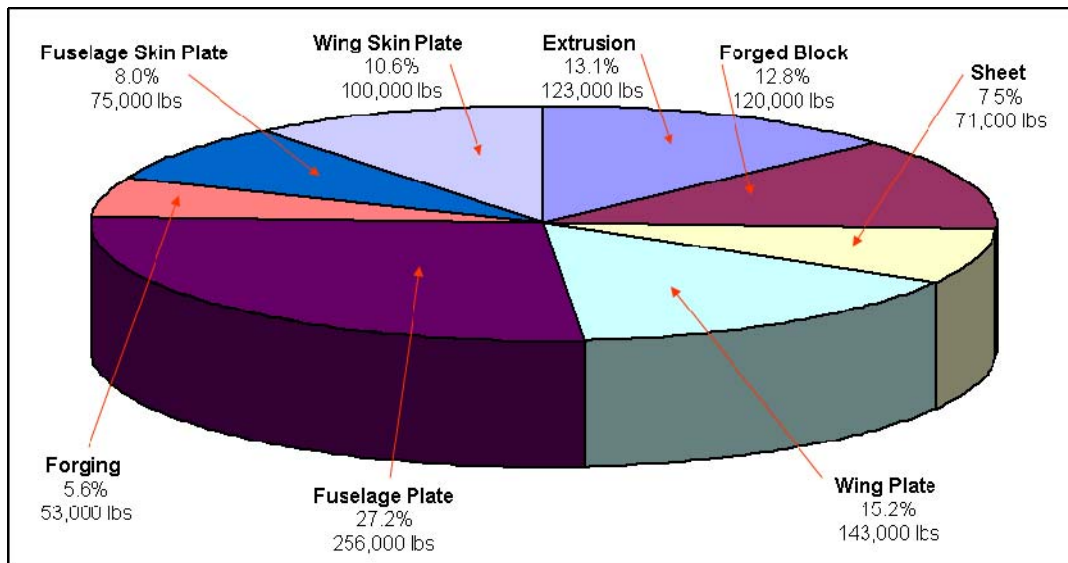


Figure 4.2.1-12. Distribution of buy weight of aluminum parts, by starting product form / application area.

The data from Figures 4.2.1-11 and 4.2.1-12 have been combined to produce the average buy-to-fly values for each of the aluminum product types / application areas. These values are provided in Table 4.2.1-4. The results are sorted by BTF value, in descending order. The data for the three largest values are then summarized as High BTF component group, and the remaining components fabricated from other product forms are summarized as a Low BTF grouping.

Table 4.2.1-4. Buy to fly values of Aluminum product forms for 777 aircraft components.

Product Form Application	Fly weight (lbs)	% of fly weight	Buy weight (lbs)	percent of buy weight	BTF
Wing Plate	3900	1.9	143000	15.2	36.67
Fuselage Plate	10200	5.1	256000	8	25.10
Forged Block	9000	4.5	120000	12.8	13.33
Sheet	14000	7	71000	7.5	5.07
Extrusion	30000	15	123000	13.1	4.10
Wing Skin Plate	40000	20	100000	10.6	2.50
Forgings	33000	16.5	53000	5.6	1.61
Fuselage Skin Plate	60000	30	75000	27.2	1.25
Totals	200100	100	941000	100	4.70
High BTF (Plate, Block)	23100	11.5	519000	55.2	22.47
Low BTF	177000	88.5	422000	44.8	2.38

Not surprisingly, the high BTF components are the non-skin plate applications, which include items such as wing ribs, bulkheads, frames, beams, and so on, as well as parts fashioned from Forged Block. These are all items with complex, 3-dimensional geometries, which have been

increasingly converted from built-up assemblies to unitized components, fabricated from thick plate or forged block, using high speed machining to hog out and finish the parts. Such components were envisioned at the start of this project to be the best candidates for applying the SSJ technologies to reduce BTF values. Extrusions and forgings have the expected much lower BTF values, consistent with these being methods to create near-shape product forms for specific part applications, where geometry features are consistent with the limitations of these fabrication methods. The low BTF values for plate applications on skin and fuselage are as expected, with the values for fuselage applications being lower than for wing skin applications. Wing skin sections often are fabricated with built-in stiffening features, while these are generally added by fasteners on fuselage sections. A surprising observation was the relatively high BTF for average usage of sheet products. It does suggest that there is a lot of material lost in the fabrication of small components from sheet stock, which perhaps should be the subject of some technical improvement approach, not covered by the processes being investigated in this project.

This analysis shows that while the overall actual average BTF for aluminum components on the 777 (4.7:1, on average) is considerably lower than the 8:1 value cited in Table 4.2.1-2, the components do breakdown into two categories of High BTF and Low BTF, with the values close to the 20:1 and 2:1 used in the initial Energy Baseline Savings projections.

After performing the above analysis of the aluminum components on a 777 aircraft by product type and application, effort turned to assessing the percentages of these high BTF components that might actually be candidates for building and using a preformed blank. The intent was also to evaluate the potential change in average buy-to-fly achievable using such additive preforms.

It was an unachievable task, with available time and budget, to take each individual model of each individual type of aluminum part stock on the 777 aircraft and compare the engineering part with the initial stock, to derive the desired assessment of possible impact across all parts. Therefore, a random sample of parts per type: Forged Block, Extrusion, Near Net Forging, Sheet and Plate were pulled from the listing of parts and studied. The sampling was approximately 13 percent of across the board of parts, with no skewing to match the process in question. After this engineering study, families of Sheet, Near Net Forging and Extrusion were eliminated from further assessment. This initial assessment verified that the Solid State Joining (SSJ) process would not be able to impact the BTF values of these product forms enough such that the energy content of the amount of material “saved” would surmount the energy and effort to create the SSJ starting stock. Plate style and Forged Block stock part families were competitive and thus the focus of further study for utilizing SSJ technology.

In the next stage, the engineering drawings of these 13 percent of the Plate and 13 percent of the Forged Block stock parts were paired first with a rendering of the starting stock for the part, based on the available summary of part by part data used in the proceeding aircraft component analysis. This was used to compute the total volume of the stock versus the total volume of the part. Next, the part was paired with a notional preform prepared by SSJ technologies. The explicit details of how this preform would be made from specific SSJ techniques were overlooked at this point, and essentially, a minimum-volume geometry was generated. Again, this approach was used to compute the total volume of the notional preform versus the total volume of the part.

Methodology for the Forged Block Study:

Each of the Forged Block (FB), engineering parts (EP) and their respective initial starting stocks (SSJ) were paired in Catia V5 (solid modeling tool) and analysis of the engineering part volume, stock volume and SSJ part volume were derived.

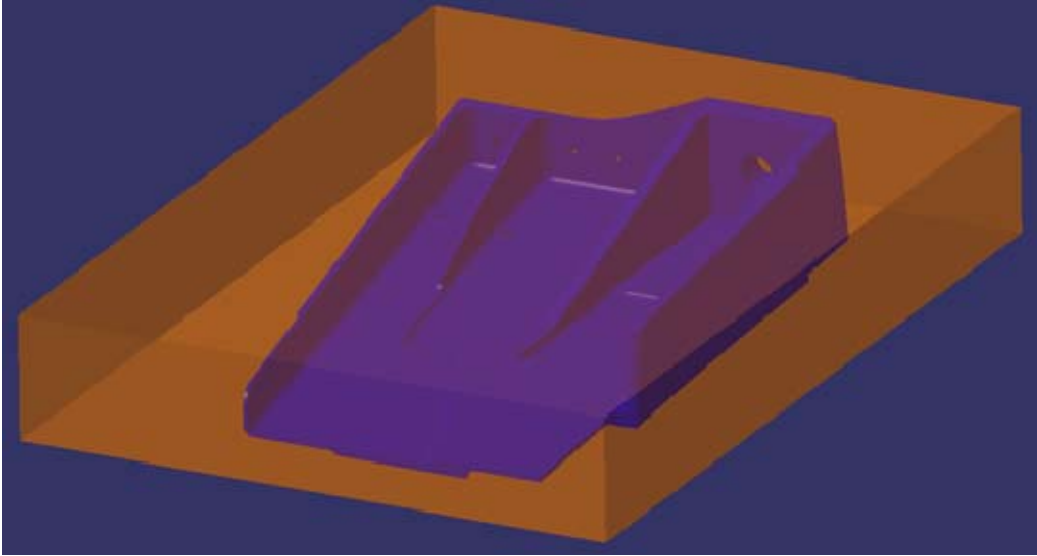


Figure 4.2.1-13. Forged Block initial stock and engineering part **514-3 paired in Catia V5.**

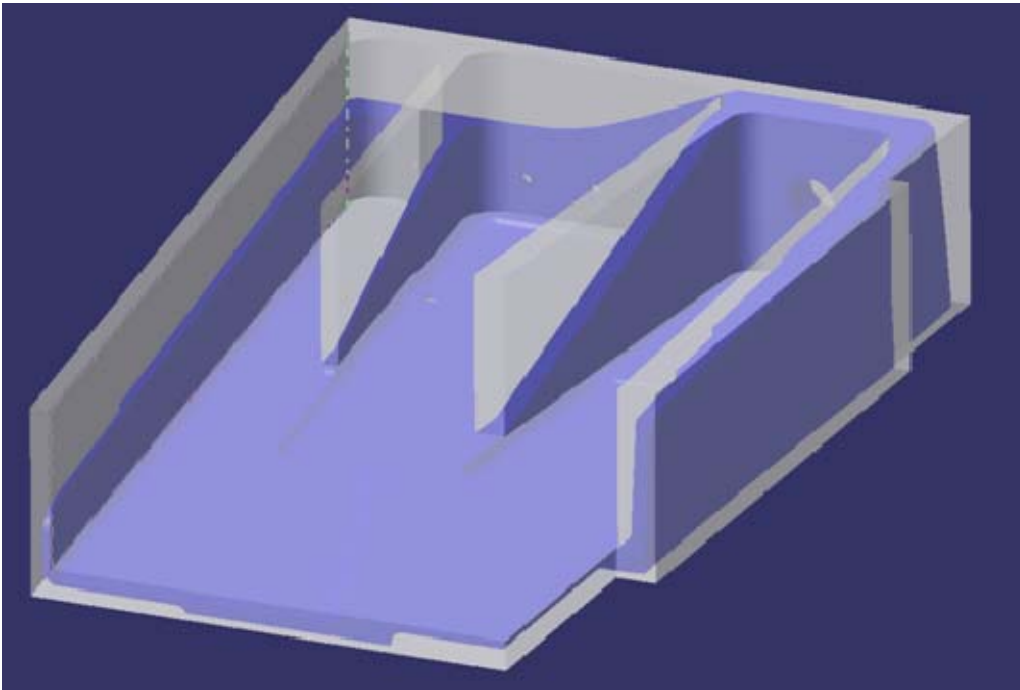


Figure 4.2.1-14. SSJ initial stock and engineering part **514-3 paired in Catia V5.**

An example of this process applied to a real 777 aircraft component currently fabricated from a forged block is illustrated in Figure 4.2.1-13, with its SSJ preform approach illustrated in Figure 4.2.1-14. (Specific part number has been hidden for competition concerns).

For this example, the volume of each of the components was: Forged Block (FB) = 1828 in³, SSJ preform = 278 in³, and the Engineering Part (EP) = 106 in³. This example yields a BTF ratio of 17:1 for the Forge Block and 2.6:1 for the SSJ starting stock respective to the same engineering part, and a $1828 - 106 = 1722$ delta in cubic inches between the FB and EP and a delta from the SSJ and EP of $278 - 106 = 172$. Therefore, if SSJ would be applied to this part, $1722 - 172 = 1550$ cubic inches (the delta of the delta) of material would not be purchased, shipped, machined away and shipped back to the material vendor as chips.

Methodology of the Plate Study:

As in the Forged Block sample study, the Plate was created around the engineering part per the planning callouts in the drawing (see Figure 4.2.1-15). The engineering part (EP) was analyzed for volume as was the Plate and the SSJ starting stocks in Catia V5 (see Figure 4.2.1-16) and analysis of the engineering part volume, stock volume and SSJ part volume were derived.

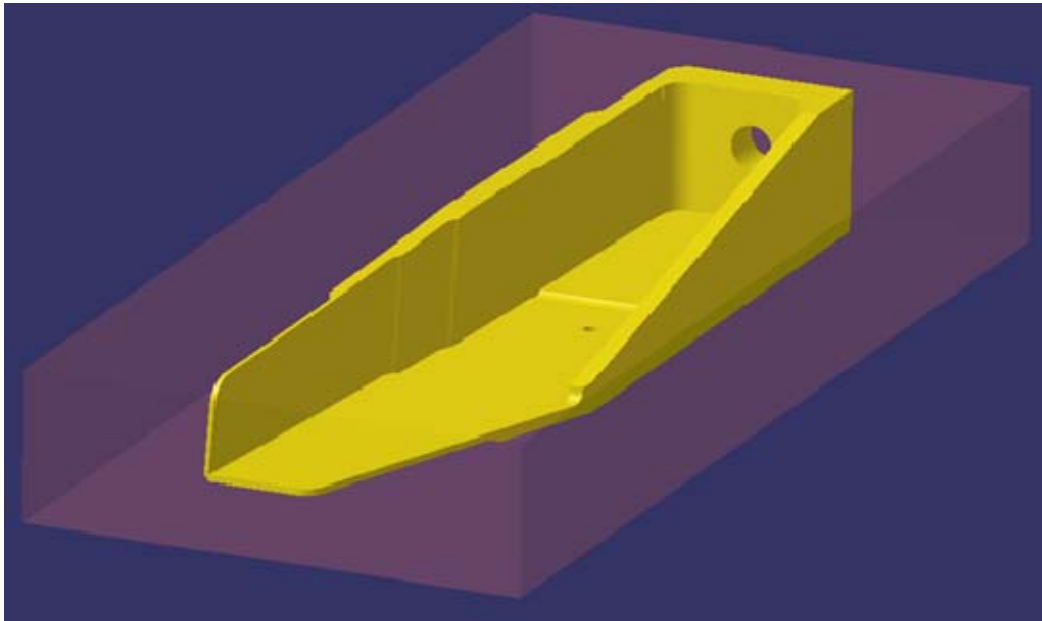


Figure 4.2.1-15. Block initial stock and engineering part ***515-3 paired in Catia V5.**

The volume of each component was: Plate = 1016 in³, SSJ = 112 in³ and EP = 62.5 in³. This example yielded a BTF ratio of 16.2:1 for the Plate and 1.7:1 for the SSJ starting stock with the same engineering part. Material removed from the plate to create the part was $1016 - 62.5 = 953.5$ cubic inches, while only $112 - 62.5 = 49.5$ cubic inches would be needed to be removed from the SSJ preform. Therefore, $953.5 - 49.5 = 904$ cubic inches of material would not have to be purchased, shipped, machined away and shipped back to the material vendor as chips if SSJ technology were applied to this part.

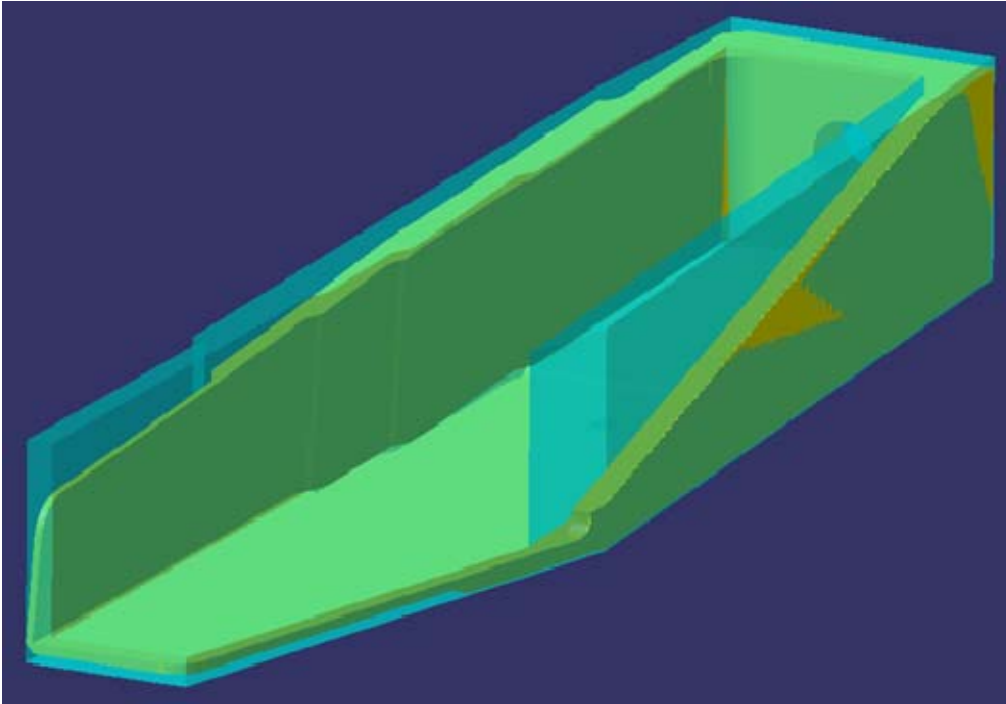


Figure 4.2.1-16. SSJ initial stock and engineering part ***515-3 paired in Catia V5.**

Results of Forged Block and Plate Studies

Table 4.2.1-5 summarizes the results of performing the full assessment of the impact of applying SSJ technologies to some of the surveyed subset of Forged Block components of the 777 aircraft. The average BTF for these selected components was 16:1, which is slightly higher than the full aircraft value from Table 4.2.1-4 of 13.3:1. The resultant BTF of producing a notional tailored block using SSJ processes are predominately in the range of 2:1 to 2.5:1. While these values derive from the taking of a very aggressive approach to making a near-net-shape with SSJ methods, these are well below the 6:1 BTF value assumed in the Baseline Energy Savings computed previously. Less conservative – and more likely to be achievable – formulations of near-net-shape performs will increase the required BTF values, but these should fall below the 6:1 value.

Due to funding limitations, the full assessments of the Plate studies were not completed, so a similar summary as shown in Table 4.2.1-5 is not available. However, individual results, such as those presented in the previous section, and for the 777 floor component used for Case Study 2 (see Section 4.2.3, below), show buy-to-fly ratio values in this same 2:1 to 6:1 value, and are again, highly dependent upon the aggressiveness in assuming very near-net-shape performs are feasible for particular geometries.

Results of Efforts in Refinement of the Global Fleet Projection of Savings of New Aluminum Requirements, based on 777 Procurement and Utilization

The in-depth review of procurement and utilization data of aluminum starting materials on the 777 aircraft, and assessment of possible implementation of SSJ processes on at least a representative subset of the 777 aircraft components fabricated from High BTF product forms, the following observations emerged.

- 1) The actual average BTF for aluminum starting product forms for the 777 are 4.7:1, considerable lower than the 8:1 value taken from other public sources. Perhaps this is not too surprising. Those public estimates are likely to have assumed that this aircraft reflected the higher BTF values observed on earlier aircraft. It is also likely that a far more aggressive use of conventional near-net-shape product forms, such as extrusions and forgings, have been utilized on this platform than previous platforms. Finally, it is possible that this utilization of lower BTF product forms has taken place on the 777 platforms in more recent models, and the higher values were indeed applicable to early models of the platform.
- 2) The product forms neatly breakdown into the two categories of High BTF and Low BTF, with average values for each grouping close to the values used in the Baseline Energy Savings calculations.
- 3) Survey studies of representative subsets of the High BTF product form components, using aggressive notional application of SSJ processes produces projected BTF values at or well below the 6:1 ratio used in the Baseline Energy Saving calculations. In addition, almost every component evaluated would benefit in realizing some reduction in BTF value, making the 60% value used for percentage of parts impacted by implementation of SSJ processes (the parameter PI in equation 4.2.1-1), seem less aggressive than previously thought.

Table 4.2.1-5. Results of Forged Block SSJ Preform Studies

Partial Part ID	Stock volume (in ³)	Part Volume (in ³)	Stock Buy to fly	Additive volume (in ³)	Delta (in ³)	Additive buy to fly
44-3	358	81	4.42	178.2	179.8	2.20
81-3	518	97	5.34	169	349.0	1.74
27-3	404	50	8.08	110	294.0	2.20
01-5	1295	135	9.59	297	998.0	2.20
61-3	222	18.5	12.00	46.3	175.7	2.50
42-3	1025	83	12.35	207.5	817.5	2.50
15-3	1545	116	13.32	255.2	1289.8	2.20
26-5	1260	89	14.16	222.5	1037.5	2.50
06-11	240	15	16.00	37.5	202.5	2.50
51-3	170	10.5	16.19	23.1	146.9	2.20
15-3	1017	62	16.40	155	862.0	2.50
29-5	1485	90	16.50	225	1260.0	2.50
14-3	1828	106	17.25	233.2	1594.8	2.20
92-7	173	9	19.22	22.5	150.5	2.50
54-7	330	17	19.41	37.4	292.6	2.20
52-7	1065	50	21.30	125	940.0	2.50
14-5	1562	72	21.69	180	1382.0	2.50
05-11	251	10	25.10	22	229.0	2.20
30-13	2280	89	25.62	222.5	2057.5	2.50
45-5	2280	89	25.62	195.8	2084.2	2.20
12-1	77	3	25.67	6.6	70.4	2.20
46-7	2736	102	26.82	255	2481.0	2.50
06-2	362	11	32.91	27.5	334.5	2.50

Should these observations drive a significant change in the Baseline Energy Savings calculation of 4.71 billion pounds of avoided aluminum starting product for full fleet replacement aircraft over 20 years? The biggest deviation in these observations from the data used in the calculations is the lower average BTF of all of the procured aluminum product forms. Similarly low values (~5:1 versus 8:1) might also be expected in other platforms which have been designed or redesigned in more recent times. Examples of this might be the A340, the A380, and the yet-to-be built A350 from Airbus, and extended-length derivatives of Boeing's 747, 737, and 767. The majority of these aircraft fall in the medium or large twin aisle categories. It can be seen from figure 4.2.1-9 that these are among the three lowest total contributors to the total amount of avoided aluminum for new aircraft production, each with a value of about 500 millions pounds of avoided aluminum in the originally calculate baseline. Even if as much as 50% of these values are eliminated from the computed total, it still leaves the total avoided aluminum starting poundage in the 4.2 billion range, corresponding to a value of avoided CO₂ of 52.4 billion pounds, about 11% lower than the previously computed baseline.

4.2.2.1 Task 2.1 - Identify Energy Input Streams for Use in SMF model:

State of Energy Consumption Model

As noted in section 4.1.2.1, the results of this task has been that the SMF model from NACFAM has been supplanted with a bottom-up approach, herein referred to as the Boeing Energy Consumption Model (ECM). The first steps in developing this model, such as reviewing available literature for the primary production processes for aluminum and specific processes for producing common aluminum stock product forms, are detailed in section 4.4 below, covering the key assumptions, current version, intended use, performance criteria, theory behind the model, hardware requirements and documentation.

Over the course of executing this project, the model has been continually updated and edited in order to best represent the full environmental impacts of the various manufacturing techniques. With further research and revisions to calculations and source data, the predictive model is now more representative of the full life cycle energy costs of primary bar stock material production, as well as green house gas emissions. These data have been combined with measured process data, obtained during the execution of Case Study 1 and Case Study 2, to expand the model's predictive capabilities. This data was obtained from Boeing's Brötje friction stir welding machine and a Cincinnati 20V milling machine, using a network-enabled power monitoring system.

Network Enabled Power Monitoring System

The Network Enable Power Monitoring System (NEPM) uses commercial-off-the-shelf (COTS) hardware and software to provide visibility and analysis of power consumption at an individual machine. The hardware is shown in Figure 4.2.2.1-2, as installed on the Brötje FSW platform; components were also installed on the Cincinnati 20V platform.

The overall architecture of the energy visibility system is shown in Figure 4.2.2.1-2. A COTS power meter is integrated into each machine to monitor power consumption and power quality. A central data logging server periodically retrieves data from each of the networked power meters and records it in a database. Typical data recorded includes measurements of power consumption, line voltage, phase, current, and harmonic distortion. Existing production schedules databases are also incorporated into the architecture to allow for the correlation of

power data to production schedules. All of this data is retrievable by the user through a web server which presents it in a human readable format



Figure 4.2.2.1-1. A. Acuvim Unit mounted on Brötje power panel. B. Close up of the front panel display of the unit.

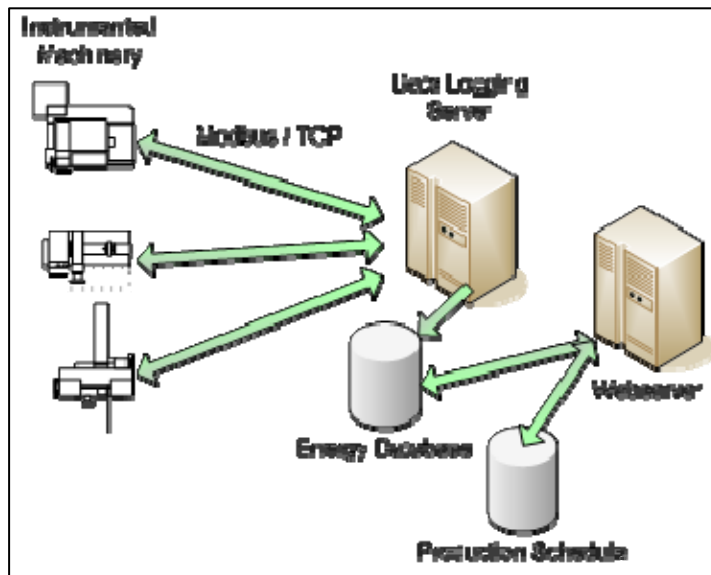


Figure 4.2.2.1-2. Energy Visibility Architecture.

Use of Case Study 1 to Advance the ECM

The completion of the Case Study #1, technically executed under Task 2.2, was so critical to providing insight into how the Energy Consumption Model needed to be modified, that it is described here, before continuing discussion on the evolution of the current state of the ECM.

As described in section 4.1.2.2, and shown in Figure 4.1.2.2-1, the pseudo bulkhead component was previously designed and developed as a demonstrator for fabrication of friction stir welded

preforms, as part of an Air Force technology transition program. For this program, the preform has been fabricated using improved clamping techniques and also an alternative welding approach involving dual-passes to ensure elimination of weld defects. This approach consisted of building up layers of material using dual-pass lap welds through 0.5 inch-thick stripes.

Overall the method consisted of:

1. procuring a 2.75" thick center plate and 0.5" thick additive plates in shapes of "U's" and strips,
2. attaching successive layers of the 0.5" thick plates to the center plate by a series of FSW lap joints. These weld paths were chosen such that the stiffeners will lie entirely within the weld nugget,
3. facing off each complete layer after welding of that layer is completed,
4. flipping the preform accordingly to maintain a near symmetric buildup, and,
5. high speed machining to the final configuration.

Figure 4.2.2.1-3a shows the improved clamping arrangement. The center plate was bolted to the welding table through holes along the perimeter. These same holes were later used to bolt the completely welded preform to the milling platform bed for final machining. Each plate was locked in place for welding by the two translatable die-spring bars which were also bolted to the welding table.

The FSW nuggets are typically asymmetric in that the material on the advancing side of the weld is extremely well mixed, while the retreating side material is considerably less dispersed such that remnants of the original interface extends a short distance into the weld nugget. This is generally of little consequence since this disbond extension acts as a crack under compression and generally does not propagate. However in view of the potentially large internal stresses generated by welding thick structures with a multiple of welds, we adopted the approach of performing a dual pass weld in which the return weld is displaced 0.125" from the initial weld, and run in the opposite direction, in order to result in a wider weld that contains two advancing sides. The metallurgical microstructure of a dual-pass weld is shown in Figure 4.2.2.1-3b.

Figure 4.2.2.1-4 is an excerpted assembly instruction drawing from the "Weld Build Plan" for the welded preform for the bulkhead and shows the start (S) locations and paths of welds designated T11, T12 and T13, which are the three welds on the 1st layer of the top surface.

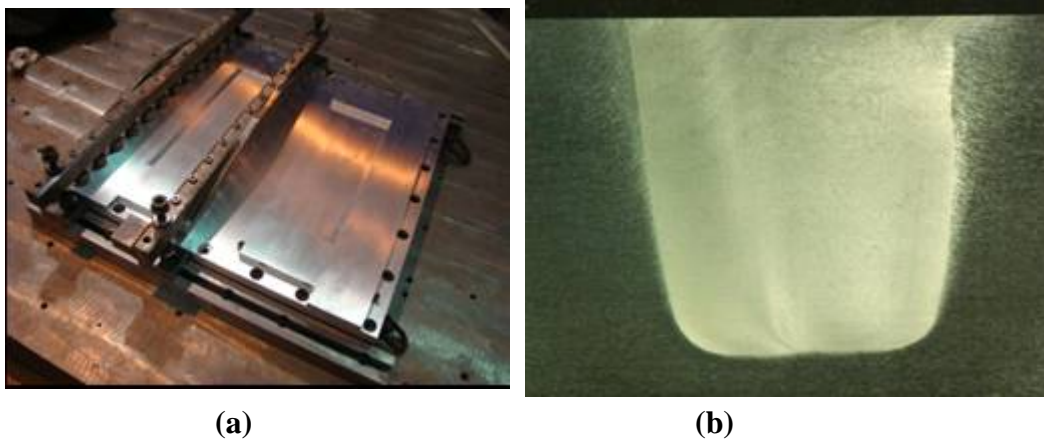


Figure 4.2.2.1-3. a) The PEEPS Pseudo Bulkhead Clamping Approach; b) a Cross-section of a dual-pass FSW Weld.

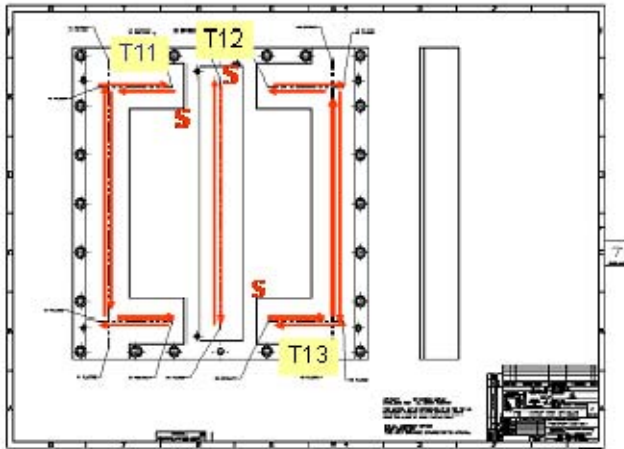


Figure 4.2.2.1-4. Schematic of the Locations of the Welds on the 1st Layer of the Top Surface.



a)



b)

Figure 4.2.2.1-5. Photographs at Two Different Stages of Weld T11.

Figure 4.2.2.1-5 contains photographs taken during the beginning (a) and near the midpoint (b) of the 1st weld (T11). When the weld reached the end of the layer of aluminum, a jog of 0.125" was made to one side, and then the weld path was reversed, to create the dual pass weld with the offset and two advancing sides of welds on the outside edges of the nugget.

Figure 4.2.2.1-6 contains photographs taken during various subsequent stages of welding the first layer (welds T11, T12 & T13). Figure 4.2.2.1-6a shows weld T11 completely welded. Figure 4.2.2.1-6b shows the preform after completion of T11, T12 and T13 welds. The photograph of Figure 4.2.2.1-6c was taken during the milling operation that removed 0.050" from the tops of all welded surfaces. This "skim-cut" milling was required to eliminate the surface roughness which occurs from the friction stir weld, so that the next layer of materials to be added could sit flush on this surface. Figure 4.2.2.1-6d shows the 1st layer in the completely finished condition, ready for subsequent layer addition of material.

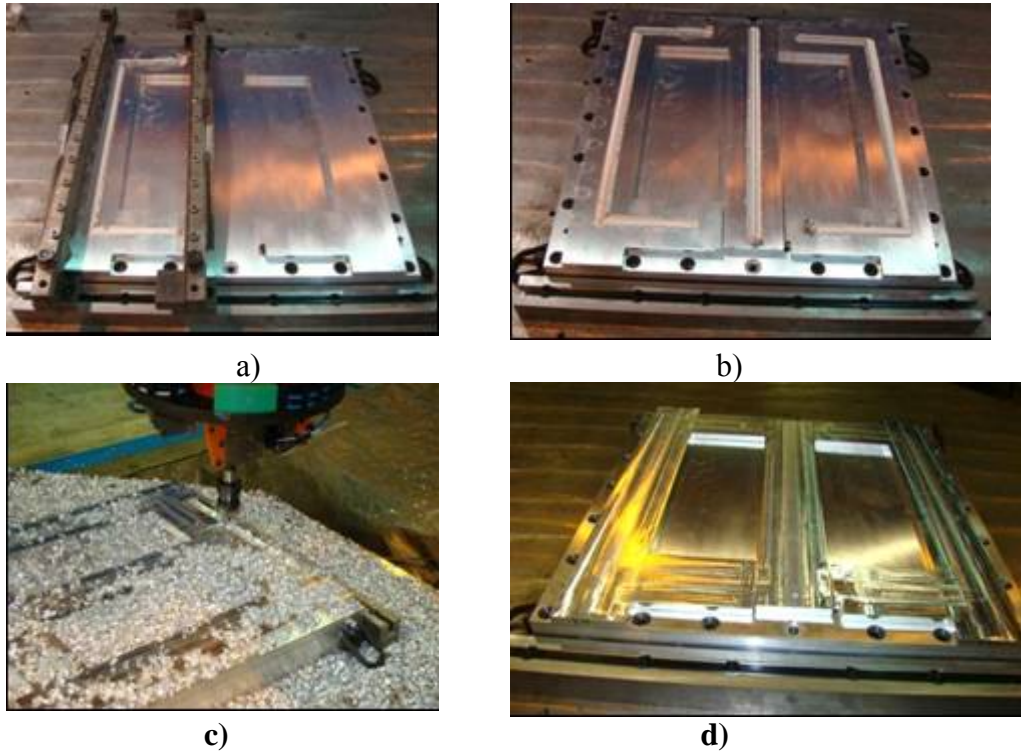


Figure 4.2.2.1-6. Various Stages of Welding of the 1st Layer of the Pseudo Bulkhead.

To reduce distortion and residual stress generation, the weldment was flipped after completion of the welding and face-off of the 1st layer. Then the 1st bottom layer of added material was welded (welds B11, B12 & B13) and faced-off. This was followed by the addition of the 2nd bottom layer (welds B21, B22 & B23) and skim-cutting of this face. The weldment was flipped back to the first surface, and the 2nd top layer was added (welds T21, T22 & T23) and then face milled yet again. A 3rd top layer was added (welds T31 & T33) and this surface finished with a smooth face-off cut. Finally, the weldment was flipped and the 3rd bottom layer added (welds B31 & B33), followed by the final skim-cut of this face. Figure 4.2.2.1-7 shows the completed bulkhead after all welding and milling stages.

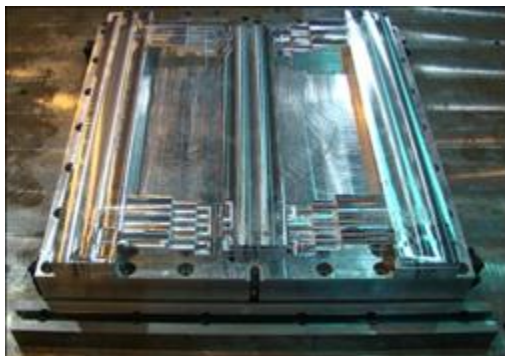


Figure 4.2.2.1-7. The Completed FSW Bulkhead Preform Ready for Final Machining.

Upon completion of all welding, this preform and a suitably sized thick 7050-T7451 block were machined to the final part configuration on a Cincinnati 20V mill platform. Figure 4.2.2.1-8 is

comprised of photographs taken during various stages of the machining operation from the thick plate.



Figure 4.2.2.1-8. Progression of the Machining Operations Reducing a Thick Plate into the Pseudo Bulkhead.

The network enable power monitoring system was used to collect and evaluate power consumption data during the fabrication processes performed on the two platforms. Figure 4.2.2.1-9 is a screen shot from the web-based user interface web-site, showing the data taken during weld operations on the Brötje FSW system. In this case, the three large groups of peaks on the left half of the figure correspond to operations during the welding of the first additive layer (welds T11, T12, and T13). The power levels during these welds ranged up to 15 KW, while in the idle time between welds, the system was observed to consume approximately 10 KW of power. When the system was put into a complete stand-down status, 2KW of power was still being consumed in operation of auxiliary components, such as compressed air supply and cooling water chiller units.

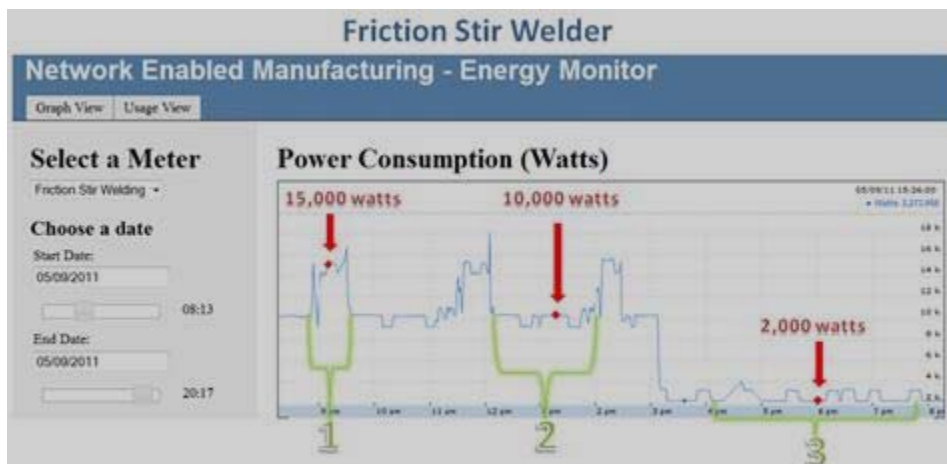


Figure 4.2.2.1-9. Web Interface of Energy Visibility Data from the Brötje FSW Platform during Welding of the Preform.

Figure 4.2.2.1-10 is a similar screenshot from the user-interface web site of the power monitoring system, showing the data collected from the Cincinnati 20V milling platform during some of the machining operations obtained during the fabrication of the final bulkhead part geometry from the FSW preform. Envelopes of power consumption above system background (idle) power levels are evident, as are more isolated peaks of consumption. The individual machining operations encountered during the production of the final part from the preform or thick plate are far more highly variable in power consumption and timing, and the system is less sophisticated in documenting these steps.

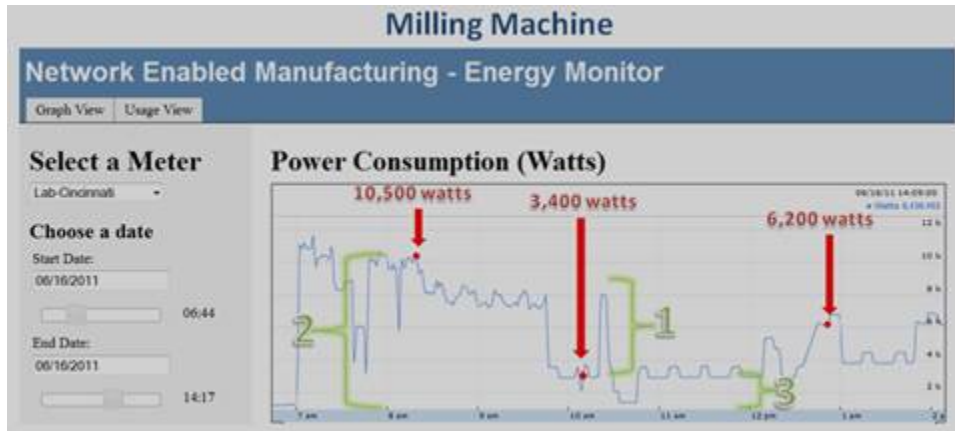


Figure 4.2.2.1-10. Web Interface of Energy Visibility from the Cincinnati 20V Milling Platform during Machining of the Preform to Final Part.

For both equipment platforms, engineering analysis of the process data was performed, in order to provide energy consumption values for populating the Energy Consumption Model. It became very clear that it would be necessary to separate the energy consumption of the individual processes (welding and machining) and the energy consumption of idle operations of the specific platforms.

Identify Energy Input Streams for Use in the Emergent Energy Consumption Model: The focus of this subtask was to develop and validate a predictive model that accepts basic part design input parameters and uses a series of calculations based on measured process data to recommend the most efficient manufacturing process. The capability goals of this model are to be able to:

- A) Consider total energy inputs from raw material processing all the way up to operational part production.
- B) Develop and utilize a method of standard evaluation of various manufacturing platforms in order to provide a fair comparison across different machines that perform the same function.
- C) Isolate process specific energy consumption independent of the machine platform.
- D) Continually assimilate process data from the SSJ/Additive techniques into the feed data calculator in order to improve the accuracy of the predictive model.
- E) Accept a set of part-specific variables and then predict the most energy efficient technique for fabrication.

Under Task 1.1., research into literature sources and revisions to calculations and source data were made, and the predictive model is now more representative of the full life cycle energy costs of primary bar stock material production, as well as green house gas emissions, meeting the intentions of goal A, above. The need to develop and utilize a standard evaluation of various manufacturing platforms, was made apparent during the Case Study 1, where the large amount of power required for simple idle functions on the Brötje FSW system became evident with the first examination of data acquired during welding operations. In order to provide a fair comparison across different machines that perform the same function, it was necessary to incorporate a feature in the model that differentiates between full machine power and process power.

Full Machine Power versus Process Power: As applied within the energy consumption model, full machine power represents the total power of a platform during processing, and includes power going to the actual process being conducted, and also platform-dependent processes, such as holding the system in an idle mode. Relative machine power represents the machine energy required to process the part above the machine's idle power consumption. It is important to make this distinction so that the impact of an energy efficient or inefficient machine can be separated from the intrinsic energy associated with a particular manufacturing process. Finally, Process Specific Power is developed from a calculation-based approach using specific processing variables to determine the energy required for the specific process. This level of detail intends to account for machine-independent factors such as tool-specific cutting efficiency, type of material being machined, welded, joined, size and geometry of weld tool, and so on.

In particular, effort was made on defining and separating full machine power and process-related power for each individual joining and machining technique on both Boeing's Brötje friction stir welding machine, and the Cincinnati 20V milling machine. With this individual investigation technique, and by setting up a framework of the necessary input variables, the predictive model's fidelity can be improved at any time in the future with the inclusion of additional process data from any specific platform executing one of the processing methods of interest. This approach achieves the goals of B and C. The whole approach to creating the internal structure and workings of the model has been made with goals D and E in mind, and it can be readily modified to incorporate ever more detailed breakdown of individual processing steps on already-imbedded processes, as well as additional processes, for ever-increasing fidelity of the model's output.

Figure 4.2.2.1-11 shows the different fabrication processes being incorporated into the energy predictive model, for comparison of Solid State Joining techniques versus conventional machining (hog-out) approaches. Full machine power, relative power, and process specific power considerations have been incorporated for all of the processes listed, except for Corner Angle welding and Linear Friction Welding.

In the case of Corner Angle Welding, the data provided by TWI (in work performed under Task 3.1) on power requirements for welding 6061, 7074, and 2024 Al alloys – which are shown summarized in Table 4.2.2.1-1, have allowed for incorporation of process specific power for this process into the model. These data are specific to the particular pin and shoulder sizing and geometry of the TWI weld tool, and are expected to be somewhat different if the latter change, but are in the same range as the weld processes performed in the pre-form fabrication done on the Case 1 study component. Because the TWI machine was not instrumented for full machine power acquisition, this and relative power concerns could not be incorporated.

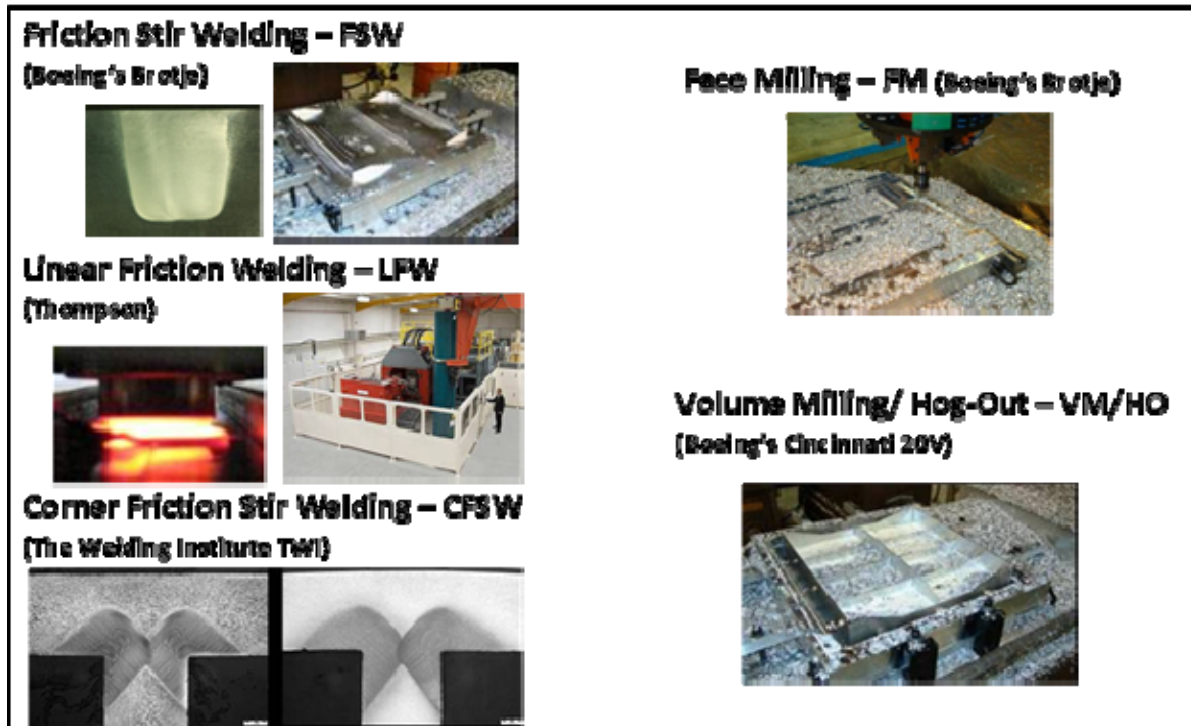


Figure 4.2.2.1-11. Current or Future Fabrication Techniques To Be Incorporated into the PEEPS Energy Consumption Model

Table 4.2.2.1-1. Weld Energy and Power data provided by TWI for Corner Angle Welding.

Matl Type	Weld ID	Derived Data		
		Heat kJ/mm	Power kJ/min	Energy kJ/in
6062-T6	102	C.39	6.14	98
	107	C.41	6.48	104
	108	C.40	6.34	102
	109	C.42	6.68	108
			6.48	8.37
7075-T6	82	L.65	2.81	142
	83	C.69	2.95	160
	84	C.80	3.02	164
	85	C.60	3.02	164
			3.98	2.98
2024-T4	91	C.88	2.78	188
	110	C.89	2.88	178
	111	C.71	2.98	160
	112	C.71	2.97	181
			3.88	2.88
7050 - T7451	T11-F	C.37	3.16	94
	T12-F	C.30	3.20	90
	B11-F	C.37	3.21	94
	B12-F	C.39	3.27	96
	T11-R	C.35	3.40	89
	T12-R	C.35	3.42	89
	B11-R	C.34	3.32	87
	B12-R	C.35	3.41	89
		3.38	3.31	82

Current version of the Energy Consumption Model:

The model is currently at version 1.2, with an effective date of August, 9, 2011. Process measurements are clearly named in the calculations section of the model with units of measure and coordinating instructions where appropriate. Table 4.2.2.1-2 shows how the process data is

assimilated in the model calculations for the multiple machining techniques. Table 4.2.2.1-3 shows the computed values of idle power, relative machine power, process power, and processing rates. These tables of measured process data and calculations provide the necessary information for the predictive model to determine the most efficient processing steps for a specific part.

Table 4.2.2.1-2. Measured process data from case studies fed into calculation table to increase predictive model's capabilities and accuracy.

Calculations Model Inputs	
Process Variable	Averages
Idle Machine Power Measurements [Machine Name]	
	Weighted Ave
Friction Stir Weld Machine [Boeing Brotje] (kW)	10.18
Face Mill Machine [Boeing Brotje] (kW)	10.18
Volume Milling Machine - Preform&Hog Out [Boeing Cincinnati 20V] (kW)	3.02
Linear Friction Welding Machine [Thompson E100] (kW)	279.00
Corner Friction Stir Welding Machine [TWI Yorkshire] (kW)	7.00
NEW MACHINE (if any other milling machine used for instance)	0.00
Full-Machine Power Measurements [Machine Name]	
	Weighted Ave
Friction Stir Weld Machine [Boeing Brotje] (kW)	14.60
Face Mill [Boeing Brotje] (kW)	13.55
Volume Milling Preform and Hog Out [Cincinnati 20V] (kW)	7.69
Linear Friction Welding [Thompson E100] (kW)	1090.25
Corner Friction Stir Welding [TWI Yorkshire] (kW)	9.95
NEW MACHINE (if any other milling machine used for instance)	0.00
Machine Independent Process Energy Calculations	
	Weighted Ave
Process Power for Friction Stir Welding (kW)	3.11
Process Power for Corner Friction Stir Welding (kW)	2.95
NEW PROCESS (new additive process?)	
Part Processing Required	
Distance of Friction Stir Weld (in)	
Area of Face Mill (in ²)	
Volume Removed for Volume Mill (in ³)	
Area of Linear Friction Weld (in ²)	
Distance of Corner Friction Stir Weld (in)	
NEW PROCESS (new additive process?)	
Part-Specific Variables	
Volume of Bar Stock Used (in ³)	
Volume of Final Part (in ³)	
If Frame Used, Volume of Frame (in ³)	
Misc Scrap Removed from Bar Stock (in ³)	

Table 4.2.2.1-3. Calculated Process Variable from case studies fed into calculation table to increase predictive model's capabilities and accuracy.

Calculations Model Outputs	
Process Variable	Feed Data
Machine-Specific Variables [Machine Name]	
Idle Power of Friction Stir Weld Machine [Brotje] (kW)	10.18
Idle Power of Face Mill Machine [Brotje] (kW)	10.18
Idle Power of Hog-Out Volume Milling Machine [Cincinnati 20V] (kW)	3.02
Idle Power of Preform Volume Milling Machine [Cincinnati 20V] (kW)	3.02
Idle Power of Linear Friction Welding Machine [Thompson E100] (kW)	279.00
Idle Power of Corner Friction Stir Welding Mach [TWI S. Yorkshire] (kW)	7.00
Machine Baseline Calculated Variables (Full-Machine Minus Idle)	
Relative Machine Power of Linear Friction Stir Weld [Boeing Brotje] (kW)	4.42
Relative Machine Power of Face Mill [Boeing Brotje] (kW)	3.37
Relative Machine Power of Volume Milling Hog Outs [Cincinnati 20V] (kW)	4.67
Relative Machine Power of Volume Milling Preforms [Cincinnati 20V] (kW)	4.67
Relative Machine Power of Linear Friction Welding [Thompson E100] (kW)	811.25
Relative Machine Power of Corner Friction Stir Welding [TWI Yorkshire] (kW)	2.95
Machine Independent Process Energy Calculations	
Process Power for Friction Stir Welding (kW)	3.11
Process Power for Corner Friction Stir Welding (kW)	2.95
Machine Processing Rates	
Linear Friction Stir Weld Rate (in/min)	2.00
Area Mill Rate for Face Mill (in ² /min)	14.72
Volume Mill Rate for Hogout (in ³ /min)	3.64
Volume Mill Rate for Preform Mill (in ³ /min)	2.35
Linear Friction Weld Rate (in ² /min)	7.50
Corner Friction Stir Weld Rate (in/min)	2.36

Table 4.2.2.1-4. The predictive model input section accepts parameters from the calculation tables shown in Table 4.2.2.1-3, user-defined part-specific variables, and processing variables cited from literature.

Predictive Model Version 1.2	
Model Inputs	
Variable Description (with Units in Parentheses)	
Machine-Specific Variables	
Idle Power of Linear Friction Stir Weld Machine (kW)	10.18
Idle Power of Face Mill Machine [Same as FSW] (kW)	10.18
Idle Power of Hog-Out Volume Milling Machine (kW)	3.02
Idle Power of Preform Volume Milling Machine (kW)	3.02
Idle Power of Linear Friction Welding Machine (kW)	279.00
Idle Power of Corner Friction Stir Welding Machine (kW)	7.00
Machine Baseline Calculated Variables (Full-Machine less Idle)	
Relative Machine Power of Linear Friction Stir Weld (kW)	4.42
Relative Machine Power of Face Mill (kW)	3.37
Relative Machine Power of Hog-Out Volume Milling (kW)	4.67
Relative Machine Power of Preform Volume Milling (kW)	4.67
Relative Machine Power of Linear Friction Welding (kW)	811.25
Relative Machine Power of Corner Friction Stir Welding (kW)	2.95
Machine Independent Process Energy Calculations	
Process Power for Friction Stir Welding (kW)	3.11
Process Power for Corner Friction Stir Welding (kW)	2.95
Processing+Machine Variables	
Linear Friction Stir Weld Rate (in/min)	2.00
Area Mill Rate for Face Mill (in ² /min)	14.72
Volume Mill Rate for Hogout (in ³ /min)	3.64
Volume Mill Rate for Preform Mill (in ³ /min)	2.35
Time Required Per Linear Friction Weld (seconds)	8.00
Corner Friction Stir Weld Rate (in/min)	2.36
Part-Specific Variables	
Volume of Bar Stock Used for Hog-Out (in ³)	1.10
Volume of Bar Stock Used for FSW Preform (in ³)	0.00
Volume of Final Part (in ³)	1.00
Inches of Linear Friction Stir Welding Required (in)	0.00
Inches of Corner Friction Stir Welding Required (in)	0.00
Number of Individual Linear Friction Welds Required (Number)	0
Area of Face Mill Required (in ²)	0.00
If Frame Used, Volume Remaining Unmachined in Frame (in ³)	0.00
Other Misc Scrap Source [Not from milling or frame] (in ³)	0.00
Material Properties	
Density of Material Used [Al 7050] (#/in ³)	0.102
Emission, Conversion and Recovery Values	
CO2 Emission per kWh of Energy [Machining STATE - MO] (#CO2/kWh)	1.84
CO2 Emission per kWh of Energy [US Base] (#CO2/kWh)	1.34
Aerospace Aluminum Scrap Recycling Recovery (%)	96%
Bar-Stock Machine Turnings Recycling Recovery (%)	90%
CO2 Equivalent Per # of Primary Al Production (#CO2/#Al)	12.476
CO2 Equivalent Per # of Secondary Al Production (#CO2/#Al)	1.78
CO2 Equivalent Per # of Bar Stock with % Recycled Assumption (#CO2/#Al)	12.36904
Primary Al Production Energy [Lifecycle Approach] (kWh/# of Al)	25.21
Secondary Al Production Energy [Lifecycle Approach] (kWh/# of Al)	3.603
Barstock Aluminum Recycled Makeup Assumption (%)	1%
Calculated Energy per # of Bar Stock [w/ 1% Secondary] (kWh/#Al)	24.994
Conversion from Pounds of Carbon to Pounds CO2	3.664

Once the available process data has been calculated in the calculation tables and input into the predictive model, all that should be required is basic part dimension data such as hog-out volumes, linear friction stir weld distances, and part framing parameters if used. Table 4.2.2.1-4 shows how the predictive model currently looks, with the part-specific input variables that are required highlighted in red. These parameters should be easily determined from a CAD file of the build part, or other production plans. Also included in the input section are all of the emission, conversion, and recovery values obtained from literature sources, as discussed in section 4.4, below. These entries are highlighted in purple in the table.

After these parameters have been added to the predictive model, energy consumption and carbon dioxide emission data should be available for the various build methods and are shown in the predictive model output section shown in Table 4.2.2.1-5.

Table 4.2.2.1-5. The predictive model output section displays energy, emissions, and fabrication data for each of the manufacturing techniques; and will have the ability to calculate the optimum construction method.

Model Outputs	
Output Variable Description (with Units in Parentheses)	
Total Machine Energy (kWh)	0.00
Linear Friction Stir Weld Energy (kWh)	0.00
Area Face Milling Energy (kWh)	0.00
Volume Milling of Hog-Out Energy (kWh)	0.00
Volume Milling of Preform Energy (kWh)	0.00
Linear Friction Weld Energy (kWh)	0.00
Corner Friction Stir Weld Energy (kWh)	0.00
Total Scrap Produced (#)	0.01
Total Volume of Bar Stock Scrapped (in³)	0.10
Total Solid Waste [Unrecoverable Scrap] (#)	0.00
Turnings Scrap (#)	0.01
Turnings Scrap Recoverable (#)	0.01
Turnings Scrap Unrecoverable (#)	0.00
Frame Scrap (#)	0.00
Frame Scrap Recoverable (#)	0.00
Frame Scrap Unrecoverable (#)	0.00
Bulk or Miscellaneous Scrap (#)	0.00
Bulk or Miscellaneous Scrap Recoverable (#)	0.00
Bulk or Miscellaneous Scrap Unrecoverable (#)	0.00
Total Machine Processing Time (min)	0.03
Linear Friction Stir Weld Machining Time (min)	0.00
Linear Face Milling Time (min)	0.00
Hog-Out Volume Machining Time (min)	0.03
Preform Volume Machining Time (min)	0.00
LFW Machining Time (min)	0.00
Corner FSW Machining Time (min)	0.00
Total Green House Gas Emissions for Part Production (# CO2)	1.30
CO2 Emissions from Primary Material Fabrication (# CO2)	1.39
CO2 Emission Savings in Recoverable Scrap Recycling (# CO2)	0.10
CO2 Emissions from Unrecoverable Scrap + Recycling Emissions (# CO2)	0.03
CO2 Emissions from Material Contained in Final Part (# CO2)	1.26
CO2 Emissions from Machining Energy (# CO2)	0.01
Buy to Fly Ratio	1.10

While refinements to the model can continue to be made as future needs arise, the current version of the model was used in all the work described in the following sections.

4.2.2.2 Task 2.2 - Produce Case Studies for Net-Shape Preforming:

4.2.2.2.1 Predictive Model Applied to Case Study #1

After the model had been updated with all the refinements cited above, the first case study was re-examined using the model, which was built, of course, using the power measurements obtained on the Brotje FSW system and the Cincinnati 20V platform while creating the pseudo-bulkhead geometry from both the hog-out fabrication process and the SSJ preform fabrication by FSW followed by machining. The first process is captured pictorially in Figure 4.2.2.1-1, while the second process is captured pictorially in Figure 4.2.2.1-2.



Figure 4.2.2.1-1. Conventional hog-out process.

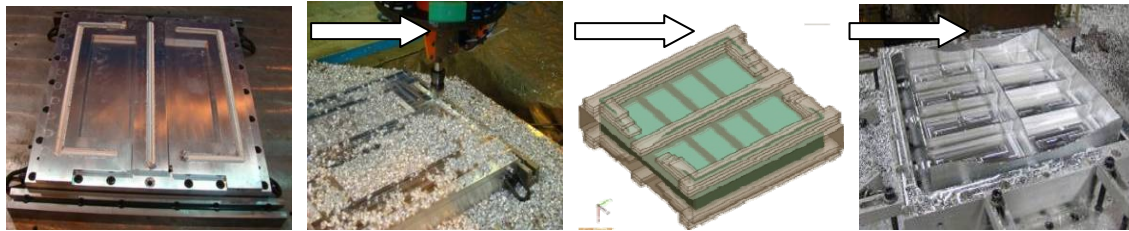


Figure 4.2.2.1-2. FSW...Face Milling....FSW/Face Milling Repeating.....Final Part.

Table 4.2.2.2.1-1. Input Table of current version of the model, for Hog-Out Machining.

Part-Specific Variables	OK
Volume of Bar Stock Used for Hog-Out (in ³)	2904.00
Volume of Bar Stock Used for FSW Preform (in ³)	0.00
Volume of Final Part (in ³)	87.52
Inches of Linear Friction Stir Welding Required (in)	0.00
Inches of Corner Friction Stir Welding Required (in)	0.00
Number of Individual Linear Friction Welds Required (Number)	0
Area of Face Mill Required (in ²)	0.00
If Frame Used, Volume Remaining Unmachined in Frame (in ³)	317.08
Other Misc Scrap Source [Not from milling or frame] (in ³)	0.00

Table 4.2.2.2.1-2. Input Table of current version of the model, for FSW preform process.

Part-Specific Variables	OK
Volume of Bar Stock Used for Hog-Out (in ³)	0.00
Volume of Bar Stock Used for FSW Preform (in ³)	2263.30
Volume of Final Part (in ³)	87.52
Inches of Linear Friction Stir Welding Required (in)	791.00
Inches of Corner Friction Stir Welding Required (in)	0.00
Number of Individual Linear Friction Welds Required (Number)	0
Area of Face Mill Required (in ²)	1648.50
If Frame Used, Volume Remaining Unmachined in Frame (in ³)	317.08
Other Misc Scrap Source [Not from milling or frame] (in ³)	0.00

The input tables for both of these cases are shown in Tables 4.2.2.2.1-1 and 4.2.2.2.1-2, respectively. With all of the process-related information and calculations imbedded in the model, the input fields are considerably reduced, requiring minimum information, such as volume of the final part, volume of the starting stock for machining or welding, inches of (linear, FS, or corner angle) welding required, number of welds, area of face milling to be done, frame material used, and so on.

The predictive model then outputs resource metrics relative to the case study geometry. These metrics include the total machine energy (kWh), the total scrap produced (lbs), total machine processing time (min), total green house gas emissions (lbs of CO₂), and buy to fly ratio. The model output for the hog-out machining scenario is shown in Table 4.2.2.2.1-3, and the output results for the FSW preform followed by machining scenario is shown in Table 4.2.2.2.1-4.

Table 4.2.2.2.1-3. Model Outputs for Hog-Out Machining Process.

	Hog Out
Total Machine Energy (kWh)	88
Total Scrap Produced (lbs)	287
Total Machine Processing Time (min)	686
Total Green House Gas Emissions per Part (lbs of CO ₂ e)	1067
Buy to Fly Ratio	33

Table 4.2.2.2.1-4. Model Outputs for FSW preform - Machining Process.

	FSW Preform Process
Total Machine Energy (kWh)	223
Total Scrap Produced (lbs)	222
Total Machine Processing Time (min)	1298
Total Green House Gas Emissions per Part (lbs of CO ₂ e)	1130
Buy to Fly Ratio	26

A comparison was made of the output metrics of the predictive model relative to the individual technologies, to provide for an easy visual comparison. This tabulation is shown in Table 4.2.2.2.1-5. As found previously, the conventional hog-out process is easily shown to be more energy efficient (60%), take less machine time to process (47%) but achieves only slightly less of a total green house gas emission burden (6%) than the FSW preform process. This reflects the balance between the energy savings due to the reduction in the amount of aluminum required to be obtained but turned into chips, and the energy differences in producing the final part using the two distinct fabrication pathways.

Table 4.2.2.2.1-5. Comparison of Processes, Case Study 1.

	Case 1 Predictive Model Results		% Decrease	
	Hog Out	FSW Preform Process	Hog Out	FSW Preform Process
Total Machine Energy (kWh)	88	223	60%	
Total Scrap Produced (lbs)	287	222		23%
Total Machine Processing Time (min)	686	1298	47%	
Total Green House Gas Emissions per Part (lbs of CO ₂ e)	1067	1130	6%	
Buy to Fly Ratio	33	26		21%

These results reflect several important facts about case study 1: a) the geometry of the pseudo bulkhead is not one that helps drive the case for fabricating a pre-form, due to the small change in buy-to-fly between the plate for hog-out and the preform, b) the existing FSW additive process is far from optimized, requiring a significant amount of aluminum “real estate” to accommodate current clamping practices required for holding parts together for the FSW process, and c) the energy consumption required for holding the FSW system in an idle mode are quite large. This latter is due in part to the size of the system, the multitude of motors driving the axes (with the “home” position being in mid-air), and multiple computers / processes in work, operating the system. At the heart of the matter, however, was a complete lack of energy efficiency being any sort of driver / consideration during the design of the equipment in the first place.

4.2.2.2.2 Surveys of High BTF Aircraft Components.

A large portion of the manpower available for this task was engaged in obtaining fleet information on aircraft to be built, current aluminum composition, and current buy-to-fly ratios under Task 1.1. When this information was in hand, effort was given to review CAD models of existing high BTF components, examine the potential for replacement of current starting aluminum product forms used to create these parts with tailored blanks, and then estimate likely BTF values for these tailored blanks. This effort was needed to validate the assumptions used in the baseline energy projection of Task 1.1.

Some first examples considered are shown in Figures 4.2.2.2.2-1 and 4.2.2.2.2-2. Both of these components fall into the high BTF category of components currently machined from stock 2124 aluminum blocks for one of the Boeing aircraft. The type of parts represented by that illustrated in Figure 4.2.2.2.2-1 will not benefit from the additive processes being evaluated in this program. The majority of removed material is from an interior pocket / cross-section, as well as reduction in exterior cross-section, while retaining a large end piece section. In contrast, the part illustrated in figure 4.2.2.2.2-2, which includes an outline of the block from which it is machined, can easily be envisioned to be fabrication of a combination of Friction Stir Welding to create the L cross-section of the part, followed by formation of the cross bracing using linear friction welding. An efficient use of FSW would be to fabricate very long sections of the L cross-section and then cut to length to obtain the lengths required for individual parts.

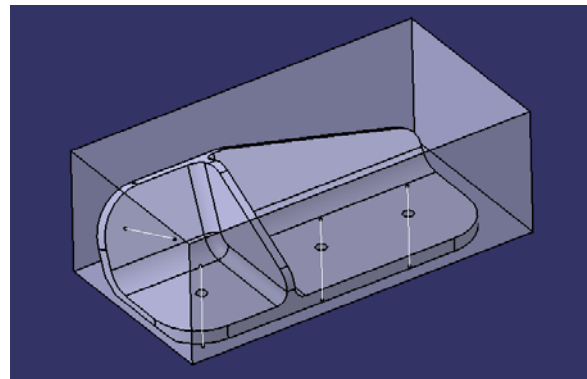
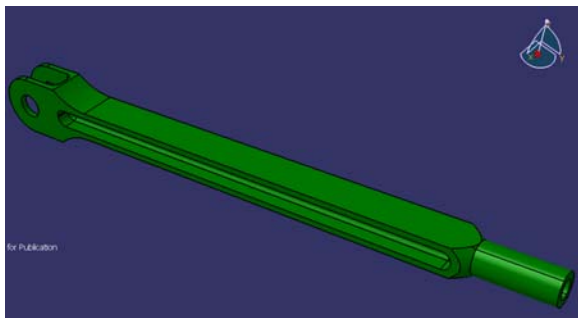


Figure 4.2.2.2.2-1. Part machined from 2124 block. Figure 4.2.2.2.2-2. Part machined from 2124 block.

As covered in Section 4.2.1, above, a sub-set survey and examination of the components of the 777 aircraft platform was performed, and then extrapolated to the rest of the aircraft fleet to provide some validation of the reduction in BTF assumed in the calculation of energy savings baseline produced in Task 1.1. Again, these results were all covered in Section 4.2.1.

4.2.2.2.3 Task 2.2 - Produce Case Study for Net-Shape Preforming, Case Study 2

During the survey work, a 777 floor article was identified as an ideal candidate high BTF part that would benefit from an additive manufacturing process. Figure 4.2.2.2.3-1 shows two views of this 777 floor article, which weighs 9.83 lbs as a fly-away final part. It consists of a thin mid-planar sheet with stiffened lightening holes, an outer angled cap along one side plus a short vertical stiffener. Presently it is machined from a 2.25" x 11" x 113" block of 7055Al, with a BTF value of 28.45:1.

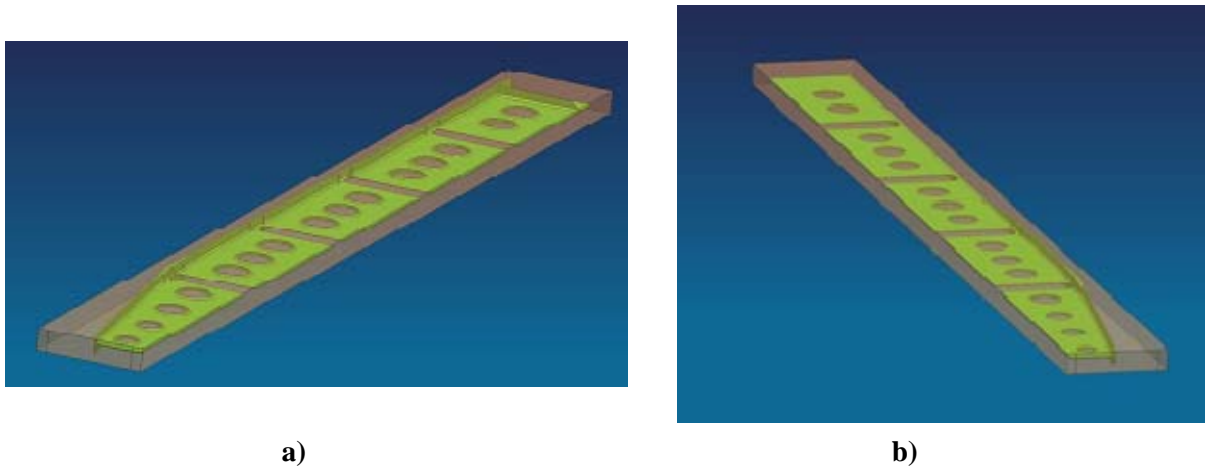


Figure 4.2.2.2.3-1. 777 Floor Component: a) Top Surface and b) Bottom Surface.

To be able to use existing tooling, we chose to eliminate two of the three inner sections and create a subtended article as the actual case study component. This part geometry is shown in Figure 4.2.2.2.3-2.

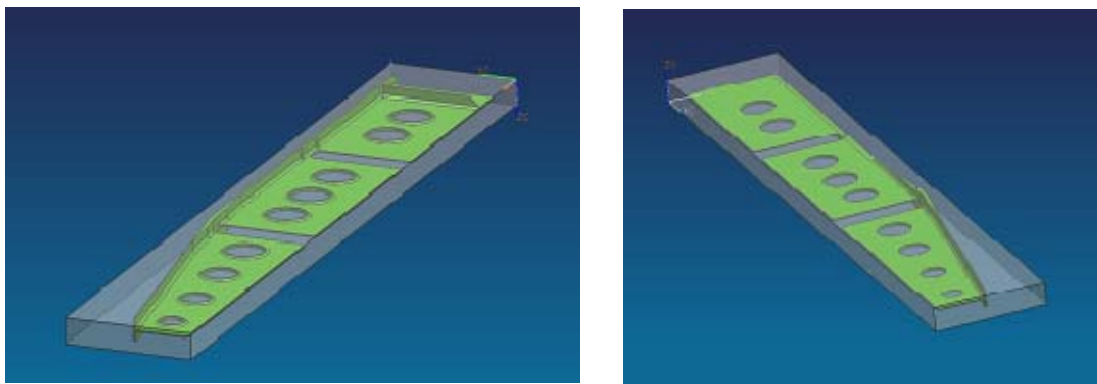


Figure 4.2.2.2.3-2. The Top (left) and Bottom (right) Surfaces of the Subtended Version of the 777 Floor Component.

This subtended version is 42” shorter but still retains the complicating features such as the angled cap and short vertical stiffener along the wider end of the part. Note that the two surfaces are not mirror images of each other. The bottom surface does not contain the short vertical stiffener nor does its cap run the entire length.

The chosen demonstration approach (#1) is represented in Figure 4.2.2.2.3-3, which shows a cross section with relevant dimensions as well as a schematic of Boeing’s layered build-up approach, using lap welding to increase the thickness in specific areas. As discussed in Section 4.2.2.3, this is not the optimum SSJ approach to building this type of component, but this was one which could actually be carried out by Boeing, given some capability limitations of the Brotje FSW platform, and current state of knowledge of fixturing systems that work sufficiently.

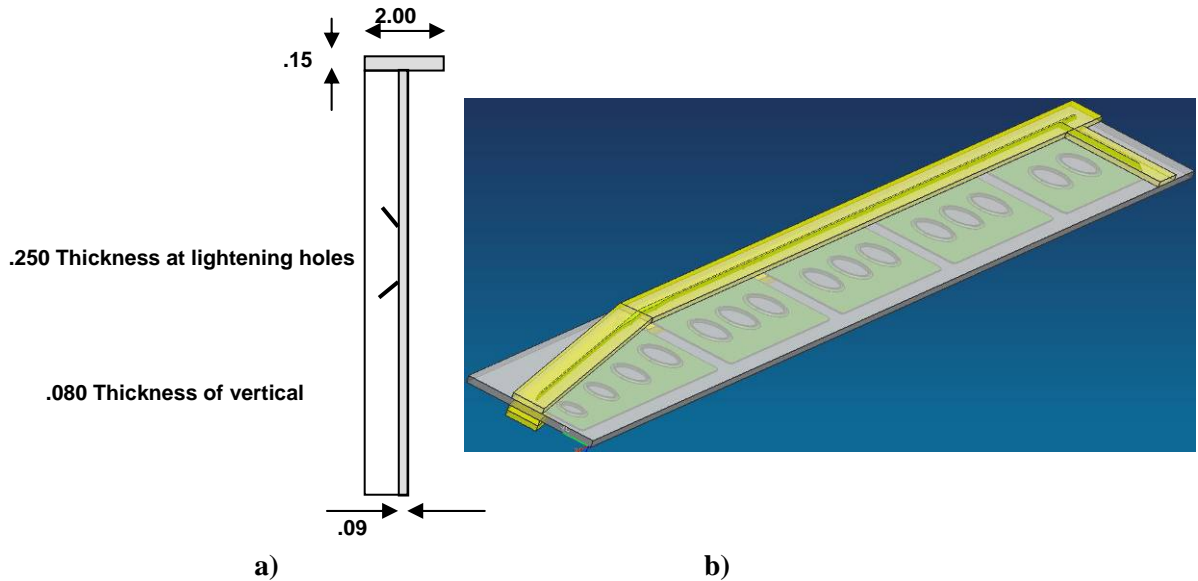


Figure 4.2.2.2.3-3 a) Cross-Section of the 777 Floor Article Showing Pertinent Dimensions and b) A Top View Showing the Plates that will be Welded onto the Top Surface.

The subtended article was essentially a 0.090 inch-thick sheet, which contains the stiffened lightening holes, a 2 inch-high, 0.150 inch-thick cap that extends along one long side, and a short 0.080 inch-thick stiffener on the top surface. Boeing's FSW layered build-up approach to produce the required preform for this subtended article was to attach 3 inch-wide by 0.5 inch-high strips by successive lap joints; similarly to the fabrication of the Pseudo Bulkhead that was described in Section 4.2.2.2.1. To achieve the final part geometry, a 0.625" center plate was used, which was thick enough such that the lightening holes could be machined out of that center plate. To accommodate the cap and rib features, two 0.5 inch-thick plates were to be added to the lower surface and one such plate to the top surface. Figure 4.2.2.2.3-3b shows the approximate length of each strip on the top surface. The green area shows the location of the final part; the heavy outline shows the perimeter of the center plate, which accommodates both the "picture frame" for part hold down during machining, as well as run-on tabs for start and stoppage of weld runs. After welding the strips (Layer 1) to the top surface, a 0.5 inch-thick block of aluminum was epoxied onto the center plate along the lower edge. The purpose of this block was to provide a stable surface when this part was flipped for attaching two layers to the lower surface. Figure 4.2.2.2.3-4 shows the plates that would be welded to the bottom surface of the preform. Note that this lower surface contained two shorter strips and no vertical stiffener. After welding (Layer 2) and facing off this layer of welds, the two strips of the next layer (Layer 3) were attached in the same manner. After this welding step, a small 1" thick 7050 block was epoxied onto the center plate, to stabilize the preform for machining. With the welded surfaces and this block faced-off, this preform was complete and ready for machining to final part geometry.

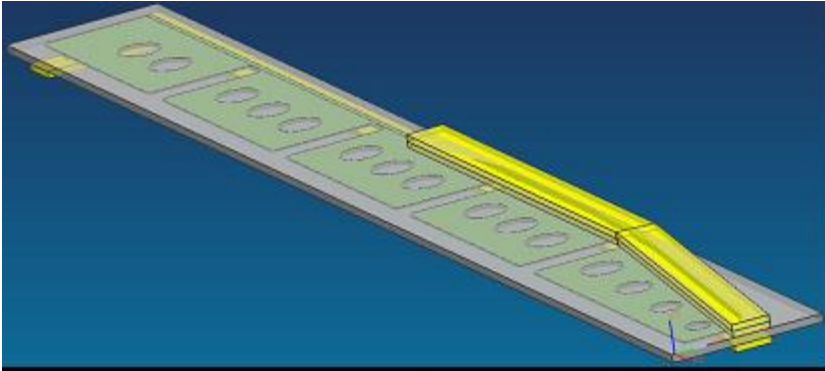


Figure 4.2.2.2.3-4. Schematic of Bottom Plate Attachment Welds.

The preform for the subtended article was welded on the fixture known as the octagon (Figure 4.2.2.2.3-5). The octagon is only 65” wide; hence the 73” long subtended article had to be welded in two steps, as shown in Figure 4.2.2.2.3-5. Locating pin holes were reamed into both the center plate and octagon. Bolt holes were drilled in the center plate and tapped into the octagon to facilitate the shifting from the A set-up to the B set-up. Usage of the pins and bolts at each step was an absolute requirement towards guaranteeing that the final machined flanges were located entirely within the weld nuggets. The welding of the strips on the bottom face of the preform could be achieved with a single set-up, shown in C.

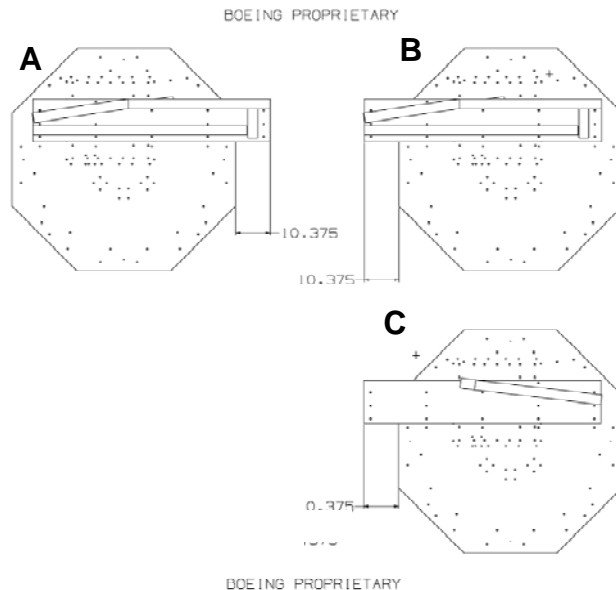


Figure 4.2.2.2.3-5. The Approach for Welding the Subtended Article.

The FSW tools that were used to produce the welds of this final subtended article carry a designation of FSW0100. The diameter of the pin tip of this set of tools is 0.223 inch-wide, which results in a nugget width at the interface of approximately 0.300”. Since the maximum flange thickness approaches this value, our approach to obtain a welded nugget wide enough to contain the rib again relied on “dual path” welding. After a first pass in one direction, the weld path was shifted a distance (between 0.100” and 0.125”) to the right at the end of a weld and then

the second weld pass was made back towards the initial starting point in a path parallel to the initial weld path. Since the torque experienced during welding shifts the tool 0.020" towards the advancing side, this results in a nugget width of approximately 0.450" as shown in Figure 4.2.2.2.3-6. This greater nugget width ensures that the machined flanges will be contained entirely within the nugget.

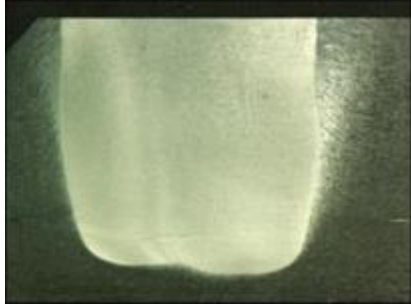


Figure 4.2.2.2.3-6. Cross-section of a Double Pass Weld.

In view of the absence of available clamping fixtures suitable for this large structure, a series of tack welds were used to attach the Layer 1 plates to the center panel. Full-length welding could then be conducted in the absence of any clamp fixturing. Figure 4.2.2.2.3-7 shows the nine (9) tack welds used in welding Layer 1.

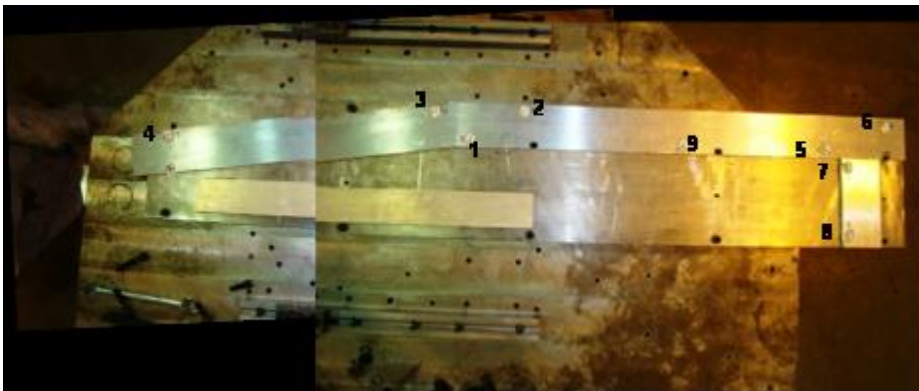


Figure 4.2.2.2.3-7. The Subtended Article After Tack Welding and in Position for Welding Weld 1 of Layer 1.

Figure 4.2.2.2.3-8 shows the weld path #1. It starts at the left end (S) and progresses to the right until it reaches the vicinity of tack weld #2 (Figure 4.2.2.2.3-7) at which point it shifts 0.100" to the right and then progresses parallel to the initial weld and exits close to the initial start (S) position.

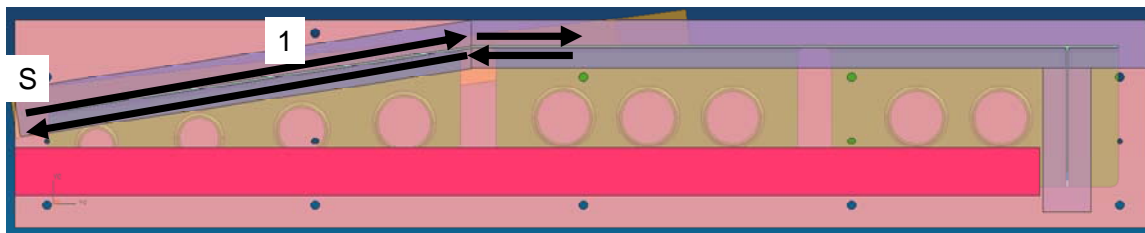


Figure 4.2.2.2.3-8. A Schematic Showing the Location of Weld #1 of Layer 1.

After completion of Weld 1 of Layer 1, the welded panel was shifted to the left (position B of Figure 4.2.2.2.3-5) in preparation for Weld 2. Figure 4.2.2.2.3-9 depicts weld 2, which starts at position S, welds the short vertical flange, and then progresses to the left to overlap Weld 1, and finally exits near the S point. This weld also shifts 0.100" to the right at each point where its path changes by 180°.

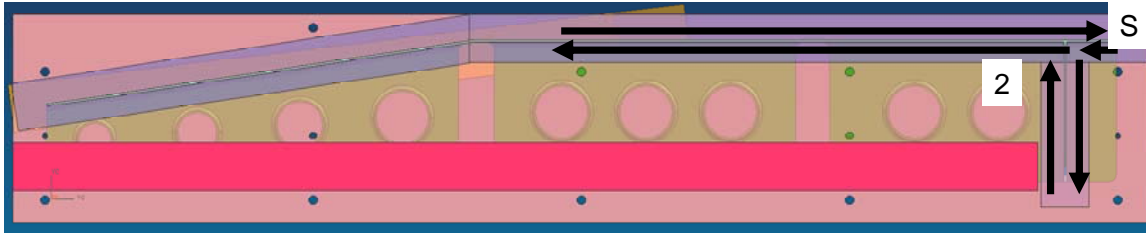


Figure 4.2.2.2.3-9. A Schematic Showing the Location of Weld #2 of Layer 1.

Figure 4.2.2.2.3-10 shows Weld 2 of Layer 1. After completion of Weld 2, both Layer 1 welds were faced-off to provide a flat supporting surface for the Layer 2 and Layer 3 welds. Figure 4.2.2.2.3-11 shows this operation on the right side of the article. Additionally a 0.5" thick aluminum plate was exposed in the lower left region as shown in Figure 4.2.2.2.3-10 to provide stable mounting for welding on the reverse side.



Figure 4.2.2.2.3-10. A Photograph Showing Weld 2 of Layer 1.



Figure 4.2.2.2.3-11. A Photograph Showing Weld 2 of Layer 1 After Removal of the Welding Flash.

At this point, the welded panel was flipped along the long axis and mounted as shown in Position C in Figure 4.2.2.2.3-5. Figure 4.2.2.2.3-12 shows the welds made on this side. Although the flange configuration is such that the second weld (Layer 3) could have been slightly shorter, two identical welds were performed for ease of programming. Welding was performed by the same procedure as the Layer 1 welds: welding started at point S and progressed leftward until the left end of the plate was reached, at which point it was shifted 0.100" to the right and then progressed parallel to the initial weld, and exited close to the initial start (S) position.

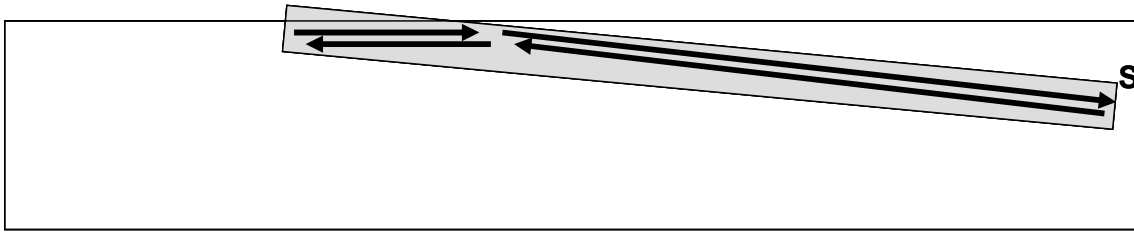


Figure 4.2.2.2.3-12. Representation of Layer 2 and Layer 3 Welds.

Since these welds were shorter than the Layer 1 welds, it was possible to clamp the 0.5” thick plates (as shown in Figure 4.2.2.2.3-13) and avoid the tack welding that was required for the Layer 1 welds. Both the Layer 2 and Layer 3 welds were successful as indicated by the photo of the Layer 3 weld in Figure 4.2.2.2.3-13.



Figure 4.2.2.2.3-13. Photograph of the Completely Welded Subtended Article Showing the Clamping Approach for the Layer 2 and Layer 3 Welds.

Upon completion of the welding, this preform for the subtended article was shipped to the Machining Development Lab where it was machined to the final part configuration on a Cincinnati 20V mill platform. The energy data were collected from both the Brötje FSW system and the Cincinnati 20V milling platform using the Network Enabled Power Monitoring system.

Figure 4.2.2.2.3-14 shows this subtended article as it was being machined from the preform, and after final machining. Visual assessment of this article concluded that weld paths were sound and correctly located. These results were confirmed with x-ray examination and dye-penetrant examination of the finished article.



Figure 4.2.2.3-14. The Subtended Article During and After Machining.

4.2.2.3 Task 2.3 - Compare Energy Consumption of FSW Preform to Baseline:

Comparison of Actual Power Usage with Predicted Model Calculations for Case Study 2.

The power usage data captured on both the Brotje and Cincinnati platforms by the NEPM system were compared with the model predictions. Table 4.2.2.3-1 lists the power usages measured for the FSW and face milling in fabricating the preform, and then the volume milling operations of taking the preform to final geometry of the subtended article.

Table 4.2.2.3-2 lists the input data which was used in the ECM for the fabrication of the subtended article. The actual preform fabrication processes used differed slightly from the specific processes whose data were originally populated the model. The original large-face milling tool used in Case Study 1 was replaced by a smaller, $\frac{3}{4}$ inch-diameter end mill during the fabrication of the preform for Case Study 2. Therefore, the model input value of $14.7 \text{ in}^2/\text{min}$ for area mill rate was replaced with a value of $5 \text{ in}^2/\text{min}$, as measured for this specific tool.

Table 4.2.2.3-1. Measured Power Usage Collected During Fabrication of the Subtended Article.

Operation	Power Usage (kWhr)
FSW Layer 1, Weld 1	8.9
FSW Layer 1, Weld 2	9.9
Face Milling of Layer 1	5.8
FSW Layer 2	11.7
Face Milling of Layer 2	27.4
FSW Layer 3	8.8
Volume Milling of Preform	35.9

Table 4.2.2.3-2. Predictive model inputs for the Subtended Article.

Processing+Machine Variables	
Linear Friction Stir Weld Rate (in/min)	2.00
Area Mill Rate for Face Mill (in ² /min)	5.00
Volume Mill Rate for Hogout (in ³ /min)	3.64
Volume Mill Rate for Preform Mill (in ³ /min)	2.35
Time Required Per Linear Friction Weld (seconds)	8.00
Corner Friction Stir Weld Rate (in/min)	2.36
Part-Specific Variables	
	OK
Volume of Bar Stock Used for Hog-Out (in ³)	0.00
Volume of Bar Stock Used for FSW Preform (in ³)	837.00
Volume of Final Part (in ³)	57.70
Inches of Linear Friction Stir Welding Required (in)	332.00
Inches of Corner Friction Stir Welding Required (in)	0.00
Number of Individual Linear Friction Welds Required (Number)	0
Area of Face Mill Required (in ²)	720.00
If Frame Used, Volume Remaining Unmachined in Frame (in ³)	20.00
Other Misc Scrap Source [Not from milling or frame] (in ³)	0.00

Table 4.2.2.3-3 lists the corresponding output power predictions of the ECM.

Table 4.2.2.3-3. Energy Consumption Model Output Results for the Subtended Article.

Total Machine Energy (kWh)	114.30
Linear Friction Stir Weld Energy (kWh)	40.34
Area Face Milling Energy (kWh)	32.52
Volume Milling of Hog-Out Energy (kWh)	0.00
Volume Milling of Preform Energy (kWh)	41.44
Linear Friction Weld Energy (kWh)	0.00
Corner Friction Stir Weld Energy (kWh)	0.00

Finally Table 4.2.2.3-4 compares the predicted and actual power usages for creating the subtended article from a preform blank created by the FSW additive process. Energy values from Table 4.2.2.3-1 for welding of each individual layer were totaled, as were the energy values for the face milling operations required to clean up each layer before moving to weld the next. Agreement between the output values of the ECM compare very closely to the values obtained by measurement during the actual operations. This is especially true for the operations on the Brotje system. The values measured during milling operations on the Cincinnati are lower than predicted values. There was insufficient scope at this point in the project to fully investigate this shortfall, but an additional round of refinement of the model for the milling operations would undoubtedly lead to an improved precision of measured to predicted values.

Table 4.2.2.3-4. Comparison of the Predicted and Actual Power Usages for fabrication of the Subtended Article.

Operation	Predicted Power Usage (kWhr)	Actual Power Usage (kWhr)
FSW	40.34	39.3
Face Milling	32.52	33.2
Volume Milling	41.44	35.9
Total	114.3	108.4

As discussed in Section 4.2.2.3, welding approach #1 is not the optimum SSJ approach to building this type of component, but was one which could actually be carried out by Boeing, given capability limitations of the Brotje FSW platform, and current state of knowledge of fixturing systems. Our model predicts a hogout energy consumption of 59.1 kWh, which is considerably less than the measured usage of 108.4 kWh for FSW fabrication of the subtended article. However relatively minor improvements in the FSW process would significantly narrow the difference. For example a larger FSW tool could weld the lower features in a single pass thus eliminating the layer 3 FSW weld as well as the face milling of Layer 2. This would lower the power usage from 108.4 kWh to 72.2 kWh.

The Brotje FSW unit is extremely versatile, however this comes at the expense of a high idle power value of 10.18 kW. A tailored FSW unit would have lower idle power values. Halving the Brotje idle power value to 5.09 kW would reduce energy usage to 82.1 kWh; an idle power value of 3.02 kW (equal to the 20V milling machine) further reduces energy usage to 71.4 kWh. Combining the advantages of thicker plate welding capability and 3.02kW idle power usage results in a predicted welding approach #1 energy usage value of 54.4 kWh, which is comparable to the predicted hogout energy consumption of 59.1 kWh. The purpose of these exercises was not to claim energy savings of the FSW approach, but merely to point out that the achieved results could be considerably improved in a production situation.

4.2.3.1 Task 3.1 – Evaluate Combinations of SSJ techniques for Optimum Energy Efficient Preforms:

Task 3.1 – Evaluate Combinations of SSJ techniques for Optimum Energy Efficient Preforms: As finally scoped, Task 3.1 included identifying a number of different fabrication pathways using combinations of additive welding techniques and using the Energy Consumption Model, now populated with appropriate energy consumption data for each SSJ process, to predict the net energy and carbon dioxide impact for each of them.

A total of five distinct fabrication pathways, utilizing different combinations of welding methods, including corner angle welding, and linear friction welding, have been identified as possible approaches to building a preform for either the original 777 floor component or the subtended version used for Case Study 2, using current capabilities and process knowledge. These pathways, along with the standard hog-out process, were evaluated using the Energy Consumption Model to ascertain which, in theory, could be projected to be the most energy efficient pathway. Only one, of course, has actually been tested against the model, as has been described in Task 2.3, above. The details of the five pathways considered in this task are presented next.

The first pathway considered for a preform for a full-size 777 floor component is the same as used for the subtended article, described in detail in Task 2.3. The second pathway is similar to the first approach except that a finished center sheet (having the desired final thickness and the lightening holes already pre-formed) would be used instead of the 0.625” thick center plate. To accommodate the now-needed added thickness in material for the vertical ribs, FS welding on of one more layer of strips would be required. There are several potential advantages to this approach, including less final machining and a lower weight of starting materials. This approach

has certain risks/disadvantages involved in welding an additional layer, such as increased likelihood of distortion issues caused by asymmetric attachment of thick plates to a thin center sheet. In addition, the formed center sheet with incorporated lightening holes would have to have its own manufacturing flow or procurement process.

The third approach involves attaching the vertical stiffeners by iterative FSW passes, milling the outside edge, and attaching the cap by welding through the cap into the plate and rib with a continuous weld. Figure 4.2.3.1-1 depicts this approach. This approach has the advantages of a significantly lower BTF of the cap pieces, a single weld for attachment of the cap, and fewer milling steps. Disadvantages include the requirement of a completely new clamping fixture and a directional change in the FSW weld at the junction of the two cap pieces. This type of cap welding has been demonstrated by Boeing on the Brötje FSW system in the past, but requires specific fixtures and tooling for the welds.

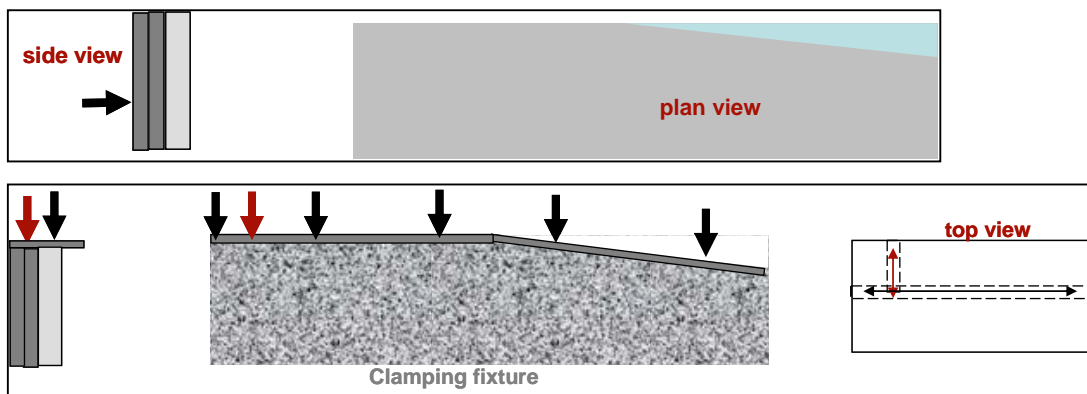


Figure 4.2.3.1-1. The Third Welding Approach for the Subtended Article, Based on Welding through the Cap.

The fourth approach is a combination of FSW with linear friction welding (LFW), which is presently not accessible for Boeing, but which has been successfully demonstrated in aluminum alloys. This combination fabrication pathway is depicted in Figure 4.2.3.1-2.

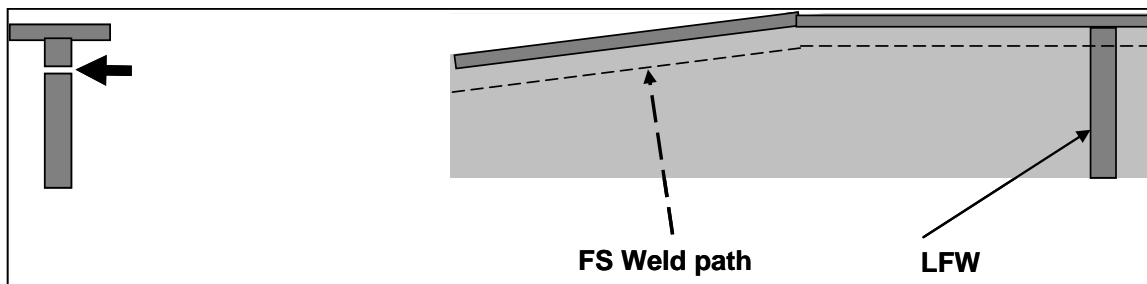


Figure 4.2.3.1-2. The FSW/LFW Welding Approach for the Subtended Article.

This approach consists of attaching the cap to a 0.25 inch-thick center plate with a butt joint weld (shown by the dotted lines) and then attaching the vertical rib by LFW. This type of attachment, which achieves full welded interfaces to two concurrent surfaces, has been demonstrated to be achievable by LFW in aluminum alloys. The amount of FSW welding is considerably reduced by this combination approach, compared to the first three options. The major disadvantage of

this path is that the cap would presently have to be machined from a thick plate (although a joggled extrusion could be possible).

The fifth and final approach considered is a combination of Friction Stir Corner Welding (FSCW) and LFW and is depicted in Figure 4.2.3.1-3. This approach consists of attaching the cap to the center plate by Friction Stir Corner Welding. This process has been further developed and demonstrated by TWI, reported under Task 3.2, below. The vertical rib would then be attached by LFW. In this program, TWI has demonstrated success of FSCW in 7075 Al and has worked with Boeing to develop a weld head/tool capable of performing FSCW on the Brötje system. This is an attractive combination of two new technologies that holds promise for a low BTF and an efficient energy consumption path. One risk is introduced by the joggle in the cap, since presently FSCW has only been demonstrated for straight surfaces.

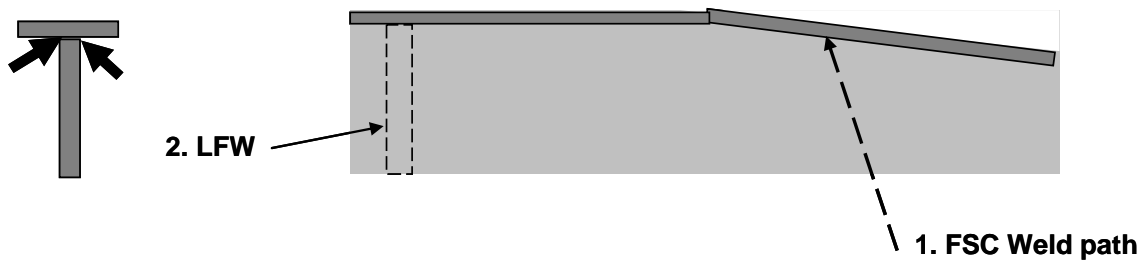


Figure 4.2.3.1-3. The FSCW/LFW Approach for the Subtended Article.

Figure 4.2.3.1-4 visually compares the five approaches. The brown-lined area represents the plate used for a hog-out approach. The red arrows indicate the location and direction of weld plunge for each approach.

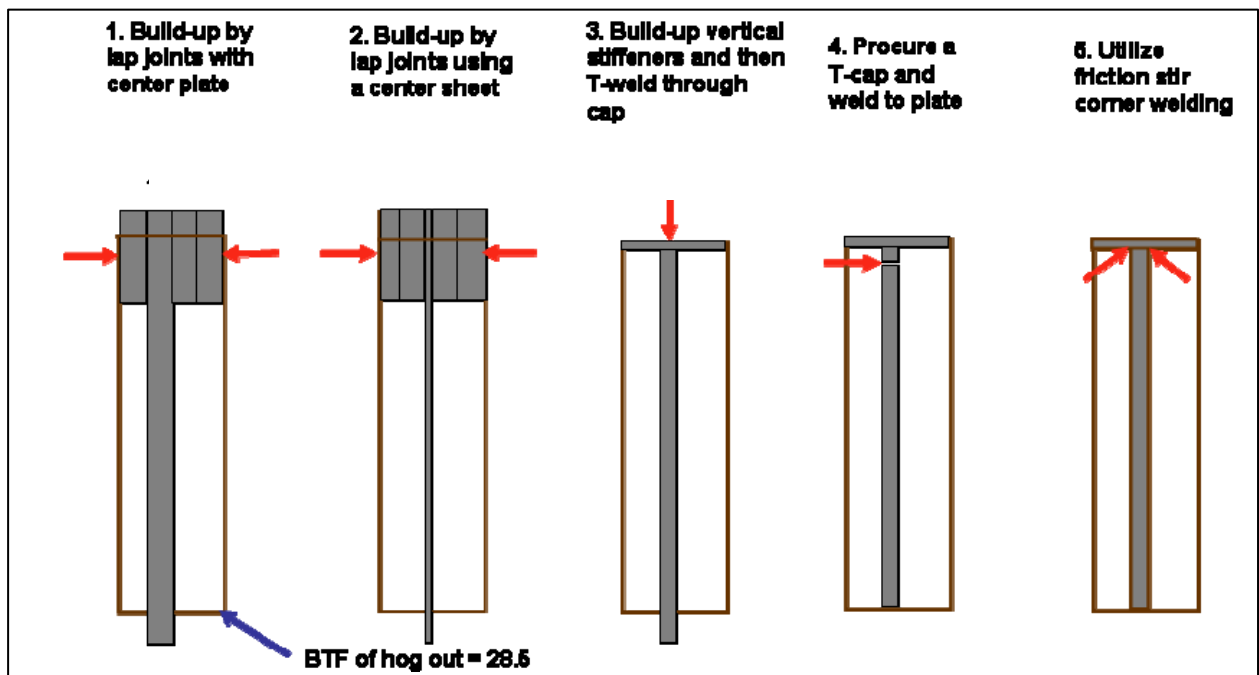


Figure 4.2.3.1-4. Cross-Sections of the Full-sized Article Depicting the Amount of Procured Material.

Note that the short vertical caps are not shown in order to simplify these sketches; the LFW approaches (#4 & #5) require slightly less material for this stiffener than the approaches using FSW. The first two approaches require a large amount of material to weld the cap angle. Presently three inch wide plates are used to provide room for clamping fixtures and the FSW tack welds. This could be improved somewhat, but their BTFs will still be higher than the other three.

We have used the ECM to compute the energy usage for the full scale part for all five approaches, as well as a standard hog-out approach, and to identify the lowest energy pathway. Entering input data into the EP model is very easy as shown in Figure 4.2.3.1-5 which is the actual input data for the full-scale 777 floor component, taken from detailed analysis of the 3-D models of each of the five performs, as generated in Catia, using the five pathways described above.

	Hogout	#1	#2	#3	#4	#5
Vol of Plate Stock for Hog-Out	2797					
Vol of Plate Stock for FSW Preform		1246	686	938	505	775
Volume of final part	98.3	98.3	98.3	98.3	98.3	98.3
Inches of FSW Required		500	748	148	113	0
Inches of Corner FSW Required						226
Number of Linear Friction Welds Required					1	1
Area of Face Mill Required		750	1136	330	0	0
Vol Remaining Unmachined in Frame	169	169	38.6	169	108	169
Other Misc Scrap						

Figure 4.2.3.1-5. Energy Consumption Model Input Data for the Five Approaches to Fabricate the 777 Floor.

It needs to be pointed out that these inputted volumes of bar stock for approaches #3 through #5 include the joggled plate or extrusion cap as shown in the sketches. The energy consumption for these processes is not presently known and thus is not captured in these predictions. Hence the predictions for approaches 3 to 5 will be slightly more favorable than actual.

Figure 4.2.3.1-6 compares the total machine energy usage predictions for the six scenarios. Approaches 3, 4 & 5 potentially offer considerable savings over the hogout approach, whereas approaches 1 & 2 consume more energy.

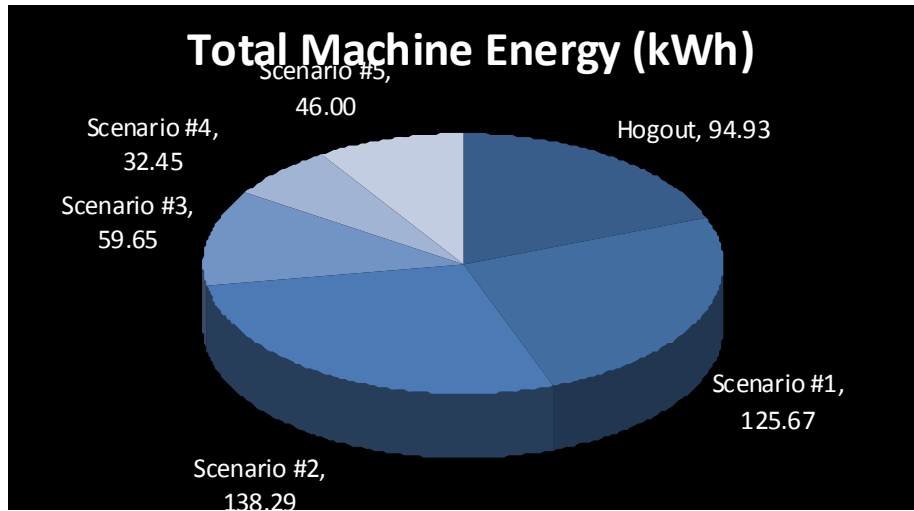


Figure 4.2.3.1-6. Total Energy Predictions for Fabricating the 777 Floor Article by each of the Six Scenarios.

All five approaches are predicted to result in significantly fewer carbon dioxide emissions than the hog out approach as shown in Figure 4.2.3.1-7. This result is expected in view of the large amount of energy required to produce aluminum from raw materials.

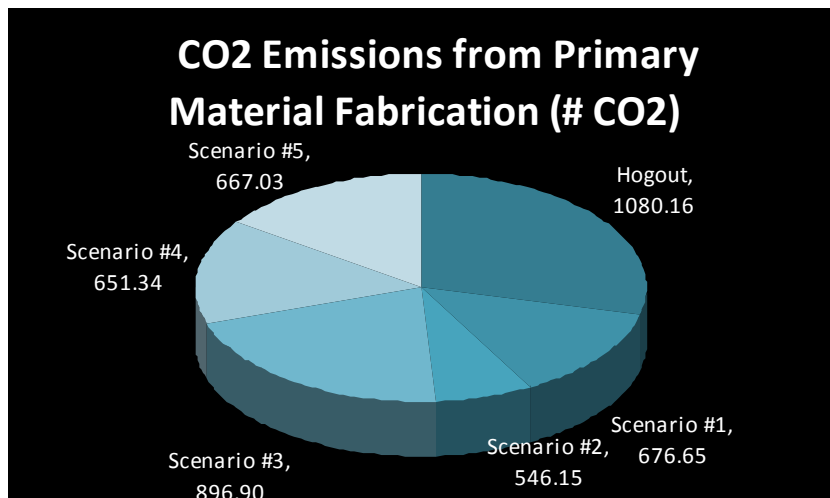


Figure 4.2.3.1-7. Carbon Dioxide Emission Predictions for Fabricating the 777 Floor Article by each of the Six Scenarios.

As expected, all approaches resulted in significantly less scrap than the hog out approach (Figure 4.2.3.1-8).

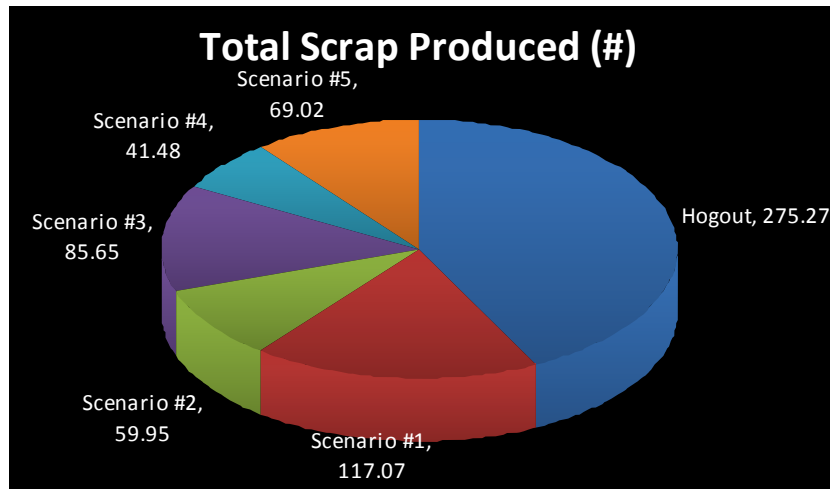


Figure 4.2.3.1-8. Total Scrap Predictions for Fabricating the 777 Floor Article by each of the Six Scenarios.

The Buy-to-Fly ratios (Figure 4.2.3.1-9) were calculated from the input data, rather than being predicted from the model. These track very closely to the Total Scrap Produced (Figure 4.2.3.1-8) as expected. Note that at least one of these pathways (#4) has a BTF of less than 6, the “target” range of reduced BTF values that achieves the baseline energy savings projections of Task 1.1.

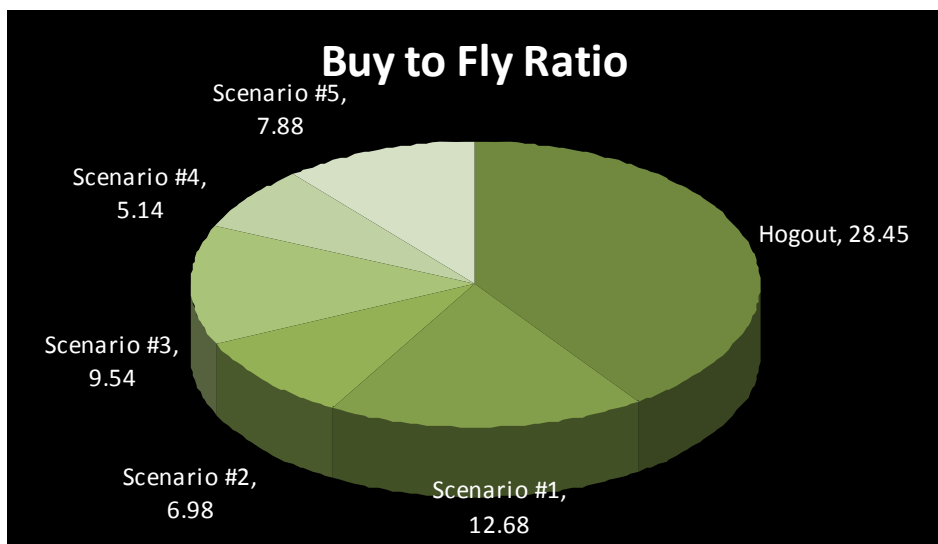


Figure 4.2.3.1-9. Buy-to-Fly Calculations for Fabricating the 777 Floor Article by each of the Six Scenarios.

Finally, the Total Machine Processing Time predictions (Figure 4.2.3.1-10) indicate that approaches 1 & 2 are comparable to the hogout approach. This result is due to the high efficiency of high speed machining. Approaches 4.2.3.1-5, which require significantly smaller amounts of FSW, result in improvements of at least 50% in processing time.

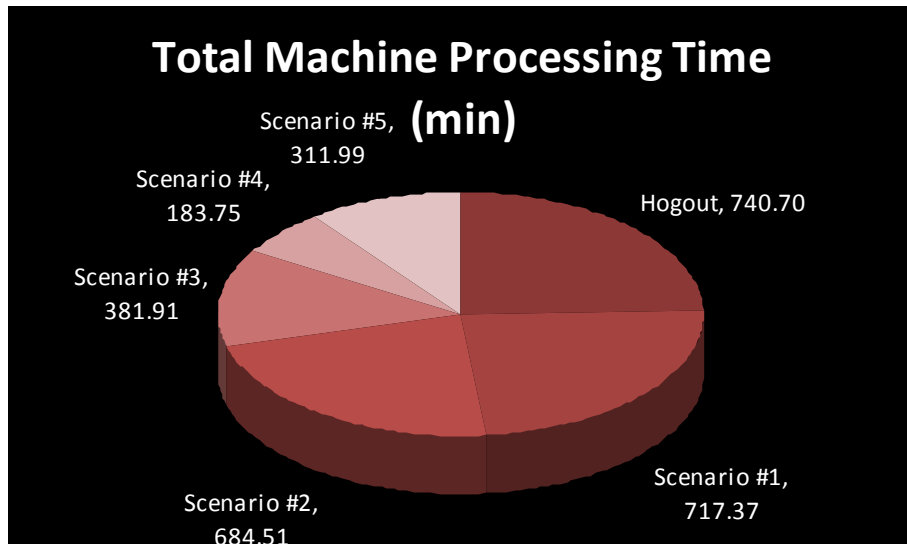


Figure 4.2.3.1-10. Total Machine Processing Time for Fabricating the 777 Floor Article by each of the Six Scenarios.

In summary, the Energy Consumption Model was applied to five fabrication pathways for the full size 777 floor article. All five approaches result in carbon dioxide emission savings of at least 60%. Certain previously described assumptions/omissions may have skewed the results for 3-5 as being more favorable than reality, but these are believed to be minor in magnitude. Finally it should be noted that the FSW data was generated using the Brötje FSW system, which clearly has not been designed with low-energy consuming idling modes. It also has limited torque capability, impacting the thickness of material that can currently be added through welding strips of material. Hence further savings could well be attained in practice with a more energy-efficient, higher torque capacity FSW unit. This analysis completed the requirements of task 3.1.

4.2.3.2 Task 3.2 - Development of Corner Angle Welding for Vertical Stiffener Joining:

TWI has completed work on all four tasks required under their sub-contract. The focus of this work was on obtaining energy consumption data while fabricating T butt joints with high quality welds in 8 mm thick high-strength aluminum alloys of interest to Boeing for aircraft components, using Stationary Shoulder Corner Angle (SSCA) Friction Stir Welding. Figure 4.2.3.2-1 illustrates the general concept of using two corner angle welds to join a vertical rib section to a web piece. The hatched areas illustrate the orientation of the stationary shoulder. Note the opposite rotations of the two pin locations, placing the interface lines to be obliterated on the advancing sides of the overlapping weld paths. Figure 4.2.3.2.-2 shows a resulting T-section sample plate produced in this study. TWI developed a set of FSW tools and process parameters capable of corner welding 8mm thickness plates in AA6082-T6, AA7075-T6 and AA2024-T4, with minimized energy consumption. They provided process parameters and weld records of best effort welds in the three aluminum alloys for calculation of energy usage data for this process. These values have been incorporated into the ECM, as covered in Section 4.2.2.1.

TWI also provided two demonstration T components in the three aluminum alloys, and a final report covering all these activities. Finally, they provided feedback on the Boeing proposed design for a weld tool for performing SSCA friction stir welding on the Brotje FSW system.

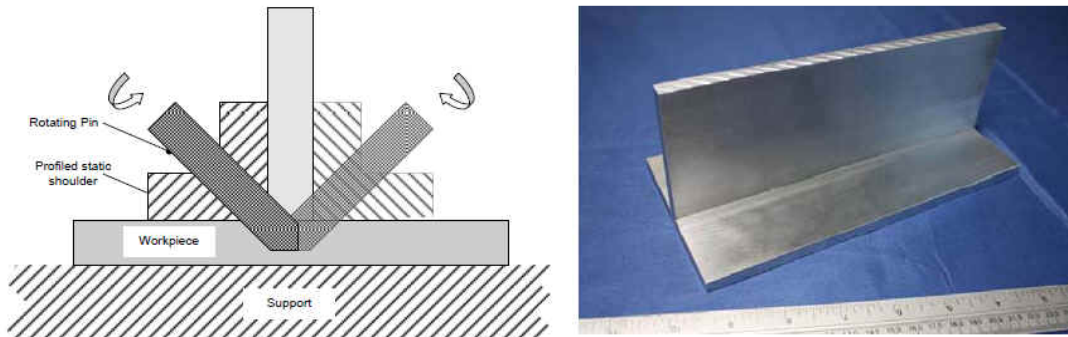


Figure 4.2.3.2-1. Two Corner Welds to create a Tee. Figure 4.2.3.2-2. Corner Welded Tee.

Figure 4.2.3.2-3 shows the successfully created, fully consolidated welds in 2024 T4 Al, for both the original and the revised tool geometry, showing both defect-free nuggets, sufficient overlap of the nuggets, and complete elimination of the interfaces along the junction between pieces. Note the wider width of the nuggets where they exit the material in the right side micrograph, illustrating the large, more robust size of this tool. Figure 4.2.3.2-4 shows photographs of both the improved pin tool, which has a larger diameter at the base of the tool to prevent fracture and larger threads for improved material movement, and a revised shoulder tool, with a larger bore to accommodate the larger pin diameter.

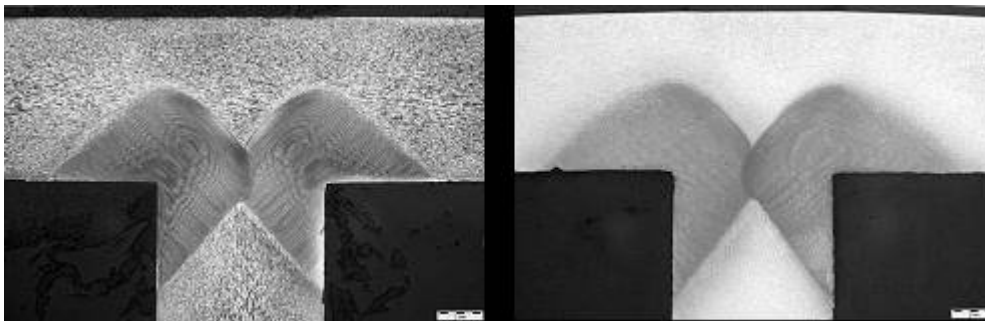


Figure 4.2.3.2-3. Cross Sections of welds obtained in 2024 T4 with original (left) and revised tool design (right).

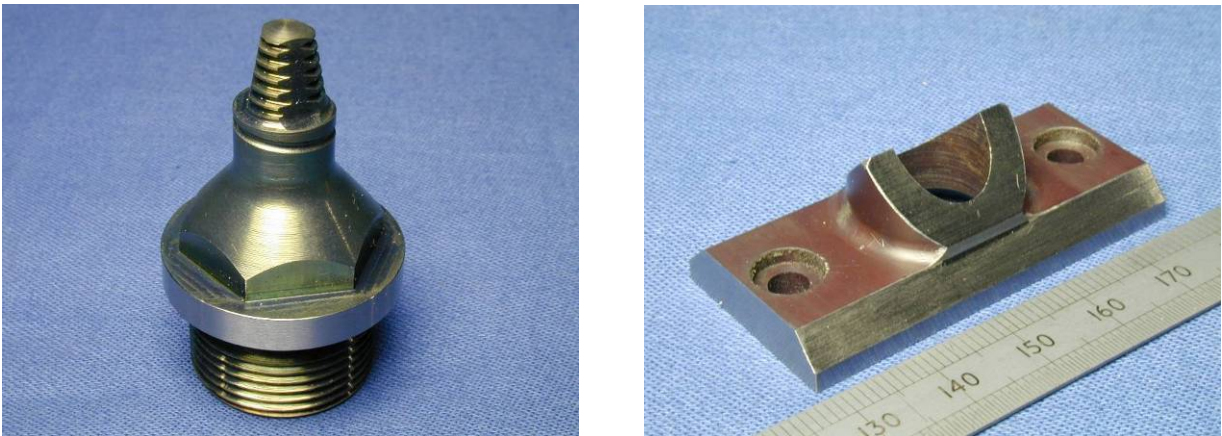


Figure 4.2.3.2-4. Stronger Tool and Shoulder, as designed by TWI under this CRAD.

Similarly to the Brötje FSW system, the TWI FSW system was instrumented to gather process related forces and torque. This data, which are illustrated in Figure 4.2.3.2-5 for one of the process runs, are used to extract heat input for each weld, using the formula in equation 4.2.3.2-1:

$$E = 2 \pi r T / 1000 v \quad (\text{egn 4.2.3.2-1}),$$

where ‘E’ is the heat input in kJ/mm, ‘r’ is the spindle speed in rev /min, ‘T’ is the steady state torque in Nm, and ‘v’ is the traverse speed in mm/min (or comparable units in the English system). The steady state torque was taken from the average value that could be determined from weld records, as in Figure 4.2.3.2-5.

Examination of these records, for instance for the two welds shown in figure 4.2.3.2-3, was used to calculate that the energy input for the welding in 2024 T4, with the new tool design, was about 0.60 kJ/mm, which was less than half of that to produce the welds on the left with the original tool. This observation was complicated by the fact that the torque values for the welding with the original tool were erratic over the course of the welding, and a true steady state value was not achieved. Summaries of energy input data for all three alloys was provided by TWI, and these values as well as data from the welding of the Pseudo Bulkhead welds, have been listed in Table 4.2.2.1-1, in the corresponding results section, above. These data show that the energy input values required for different aluminum alloys are all in the same range, but do vary by alloy to some extent. This table of data was provided to the Boeing engineers who worked on the Energy Consumption Model, for inclusion in that model, to bring better fidelity to the model by being able to adjust for alloy identity.

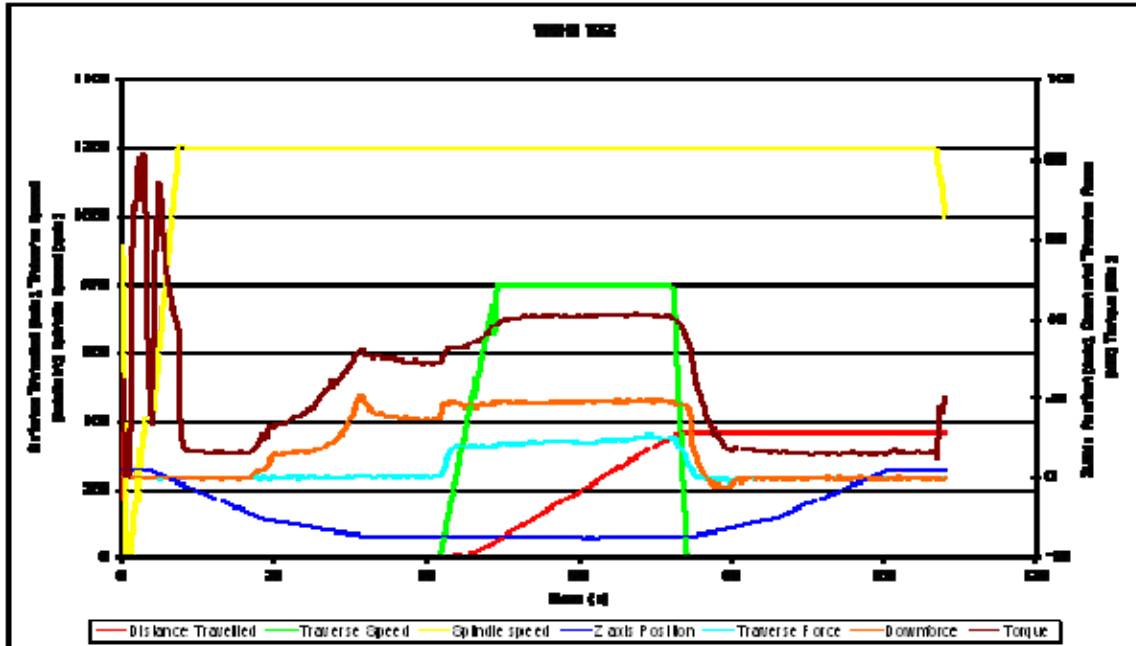


Figure 4.2.3.2-5. Force, Torque, and other Data Collected from the TWI FSW System during a Weld Operation.

Boeing design and TWI review: Jonathan Martin, TWI lead engineer, visited the Boeing FSW facilities in Saint Louis, on March 9 and 10, 2011. This visit provided an opportunity for Boeing engineers to share details of the Brötje machine operation, tool mounting mechanism, and other critical details of system, in order to enable TWI to provide engineering insight into possible means of creating a corner angle weld tool / head fit for use on the Brötje machine. TWI had earlier provided Boeing with drawings of their mechanical fabrication of a FSW tool, with details of internal construction required for stationary operation of the confining shoulder, while the pin rotates in the material to provide the energy source for plasticizing and moving the material to be welded. A photograph of the TWI design, which fits their in-house FSW system, is shown in Figure 4.2.3.2-6. Later, Boeing engineers completed a draft design of a tool for use on the Brotje FSW system, and a rendering of this tool is shown in Figure 4.2.3.2-7. Detailed drawings along with a 3-D electronic model of the part were submitted to TWI engineering personnel for their review and consideration. TWI provided written comments and suggestions for modifications back to Boeing. These comments have been reviewed and incorporated into final revisions of the design. Boeing intends to use this design to fabricate a first article tool and then test the performance. This will take place at some future time using Boeing's own internally-funded FSW development work.



Figure 4.2.3.2-6. TWI Stationary Shoulder Corner Angle Friction Stir Weld Tool.

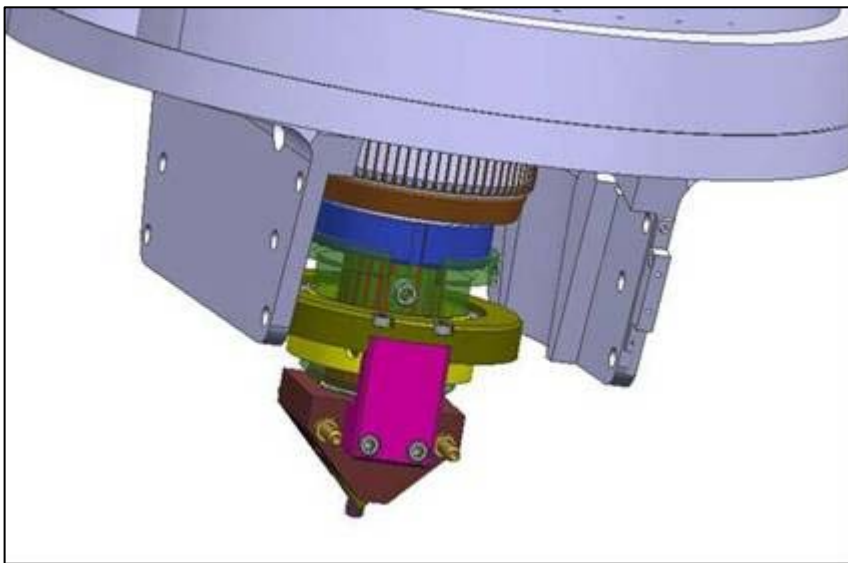


Figure 4.2.3.2-7. Boeing Preliminary Design of SSCA FSW tool for use on the Brotje FSW System.

4.3 Project Milestones:

Milestone #1: Completion of a simulation and energy prediction, using the SFM software, for selected 3-D test geometry, comparing 100% machining from billet versus a friction joined preform of the same test geometry.

The objectives of this milestone have been met and completed, but the usage of the Sustainable Manufacturing Framework software from NACFAM has been replaced by a Boeing-generated model – the Energy Consumption Model (ECM), built upon Excel spreadsheets. The demonstration of its ability to compare machining from billets versus machining from a fabricated tailored preform fabricated using Friction Stir Welding have been accomplished in both the Case Study 1 and Case Study 2 efforts, as covered in the results sections for Task 2.

Milestone #2: Completion of shop trials on corner angle Friction Stir Welding and incorporation of the energy consumption measurements into the SFM software.

The objectives of this milestone have been met and completed, but again, the usage of the SFM software from NACFAM has been replaced by the Boeing-generated ECM. Performing under subcontract to Boeing, TWI completed the development of new tools for quality, low-energy corner angle welding in 6061, 2024, and 7075 Al alloys, as covered in the results section for Task 3.2. Energy consumption data for welding of all three alloys has been incorporated in the ECM, as covered in the results section for Task 2.1, and utilized in comparison studies of multiple preform fabrication pathways for tailored preform for the 777 floor component, as covered in the results section for Task 3.1.

4.4 Computer Modeling: The Boeing Energy Consumption Model

4.4.1 Model Description: The PEEPS Energy Consumption Model is a Microsoft Excel spreadsheet model that outputs key ‘energy based’ performance metrics associated with pre-form based solid state joining technologies for Aluminum. These metrics include Total Machine Energy (kWh), Total Material Scrap Produced (lbs), Total Machine Processing Time (min), and Total Green House Gas Emissions for Part Production (lbs of CO₂) and Buy to Fly Ratio. These outputs are achieved by inputting key process information such as material density, emission, conversion and recovery values, machine specific variables, processing variables, and process power requirement information.

4.4.2 Key Assumptions:

- This model assume that miscellaneous scrap is recycled with a 90% melt efficiency
- Assumes every Linear Friction Weld takes 8 seconds of processing time
- By default, for CO₂ Emissions from material contained in final part the model assumes part is not recycled. Estimate based on low/no secondary material typically used in aerospace Al production If part is recycled at bulk scrap rates, this value is reduced 82%
- Lifecycle CO₂ Emissions based on 51% recycled material contained in barstock
- The area mill rate for face milling assumes .050” of surface removal

4.4.3 Version: Final Name = ‘FINAL PEEPS Energy Consumption Model 09AUG11.xlsx’

4.4.4 Intended Use: The intent of the model design was to create a model framework that could easily be modified or expanded upon in future studies and with additional feed/process data. At a minimum, it was intended to be capable of providing a meaningful comparison between fabricating an aluminum component using a hog-out approach using plate as the starting material from an approach based on fabricating a friction stir welded tailored blank.

4.4.5 Goals of the Model: Three goals of the model, which influenced the way it was set-up to operate, were a) create a tool which could help down select between alternative manufacturing pathways of producing an aluminum component, based on the best balance of energy consumption and environmental impact; b) create the tool such that it would be capable of accounting for the detailed impact of utilizing one type of aluminum product form (plate, extrusion, forging) over another; and c) create the tool such that it could be readily modified by

the user to account for improved input values for all of the underlying parameters in the computations, based on improved sources of literature or empirical measurements.

In creating the tool, such that it was able to accept a set of part-specific variables and then predict the most energy efficient technique for fabrication, the authors needed to:

- Consider total energy inputs from raw material processing all the way up to operational part production.
- Develop and utilize a standard evaluation of various manufacturing platforms in order to provide a fair comparison across different machines that perform the same function.
- Isolate process specific energy consumption independent of the machine platform.
- Continually assimilate process data from the solid state joining techniques into the feed data calculator in order to improve the accuracy of the predictive model.

4.4.6 Performance criteria for the model related to the intended use: The model was evaluated by using a case study approach of different representative geometries. This approach applies specific energy burdens to producing a single representative part, such as the bulkhead geometry identified in the previously submitted quarterly report. This type of approach allows for a more accurate prediction of energy savings when applied to large scale production environments.

In order to be able to predict the energy consumption and green house gas emissions of a complete part manufacturing process, it was necessary to separate each individual machining technique into its own part and interpret independently. With this individual investigation technique, and by setting up a framework of the necessary input variables, the predictive model's fidelity can be improved in the future with the inclusion of additional process data. These process measurements are clearly named in the calculations section of the model with units of measure and coordinating instructions where appropriate.

4.4.7 Theory behind the model, expressed in non-mathematical terms:

4.4.7.1 Determination of Energy Consumed in Bar Stock Aluminum Production

An important factor in determining the true energy costs between different manufacturing techniques such as hog-out machining and friction stir weld preform fabrication is determining the energy costs of the raw material inputs. It is clear that from a manufacturing standpoint, the preform buildup process consumes more electrical energy, time, and man power than a simple hog-out milling process. However, when considering the energy intensive processes of turning bauxite into alumina through the Bayer process, and subsequent aluminum ingot production with the Hall-Heroult process, the analysis becomes more complex. Ultimately the energy consumption model will take all of these considerations into account, and with respect to bar stock energy consumption costs, the life-cycle energy approach is utilized most often in literature, and is detailed further in the section below. In literature the energy consumed is represented as mega joules of energy per ton of aluminum produced. For instance, an Energy and Environmental Profile of the U.S. Aluminum Industry report prepared for the Department of Energy by Energetics Inc. in 1997 cites the values of 167,750 MJ per ton of primary aluminum ingot produced and 7,500 MJ per ton of secondary aluminum ingot^[3]. It is important to notice that the energy required to create secondary, or recycled, aluminum is approximately 5% of the

energy required to make primary aluminum. This raises another question with respect to raw material input selection for various applications, such as how much recycled material is used in a typical aluminum alloy. For aluminum can production, the EPA's Solid Waste Management and Greenhouse Gases report states that 51% secondary aluminum is utilized^[4]. Aerospace aluminum grades typically have significantly higher restrictions on elemental residuals that may preclude utilization of secondary materials and increase the overall energy costs of the bar stock. It is for this reason, that a "Percent Secondary material used" variable is adjustable in the model. Currently the recycled material content is assumed to be only 1% barring the discovery of a more significant value in literature; this value can be easily modified by the end-user if significant secondary material is known to be used in the aluminum bar stock material.

An ASM International publication on Aluminum Recycling and Processing Energy goes one step further than the Energetics Inc. report by taking into account energy costs with turning ingot into bar stock material. When rolling operations are included, a value of 200,882 MJ for total energy per ton of primary rolled aluminum is determined, as shown in Figure 4.4.7.-1, while secondary rolled aluminum is cited as 28,590 MJ or 3.603 kWh per pound^[5].

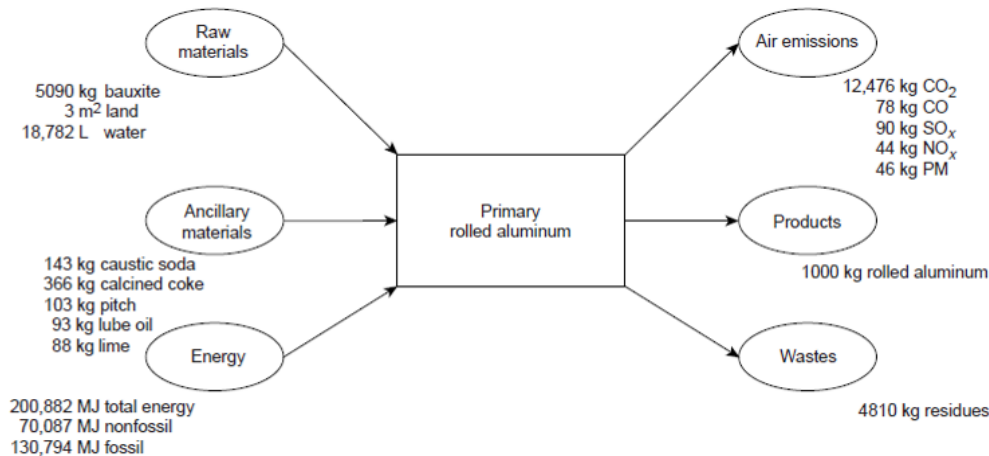


Figure 4.4.7-1. Inputs and outputs of production for 1000 kg of primary rolled aluminum, utilizing the Life-Cycle Analysis (LCA) method.

This value of 200,882 MJ converts to 25.21 kWh, and with the assumption of 1% secondary aluminum used, the model uses a value of 24.99 kWh per pound bar-stock for all applicable calculations. In the model this value is labeled as "Calculated (Life-Cycle) Energy in a Pound of Bar Stock [w/ 1% Secondary] (kWh/#Al)". This value is consistent with the value reported by T.E. Norgate which cites 26.6 kWh per pound of primary aluminum production^[6].

4.4.7.2 Reason for Life-Cycle Analysis Method Selection

The Life-Cycle Analysis (LCA) method of characterizing the energy consumption of aluminum bar stock material was used for the predictive model. The purpose of the LCA approach is to consider all of the energy costs involved with primary aluminum production and are shown in Figures 4.4.7-2 through 4.4.7-6, selected from an ASM International publication^[5]. Energy inputs are considered from the Bauxite mining, alumina refining, carbon anode production, aluminum smelting and finally the aluminum casting processes. While Figure 4.4.7-7 summarizes the energy costs associated with secondary aluminum ingot production.

The Life-Cycle Analysis also breaks the energy inputs out into various categories such as process electric, process non-electric, transportation and feedstock energy costs; for both primary and secondary ingot production as seen in Figure 4.4.7-8 below [5]. It is only through this complete evaluation of all of the processing energy and material inputs, that a competent energy consumption model can be based. Without such considerations, green house gas emissions and total part production energy cost estimates would significantly underestimate the real values.

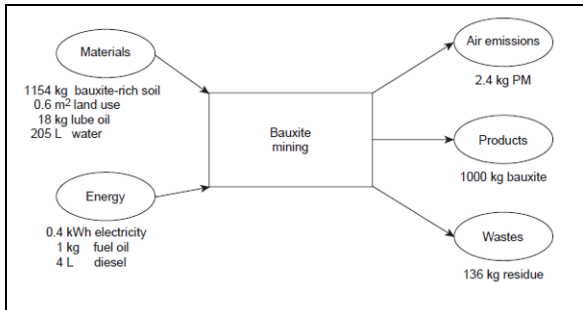


Figure 4.4.7-2. Bauxite mining constituent of the primary aluminum life-cycle analysis.

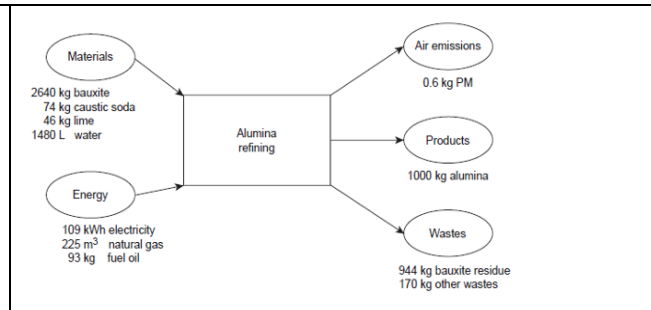


Figure 4.4.7-3. Alumina refining constituent of the primary aluminum life-cycle analysis.

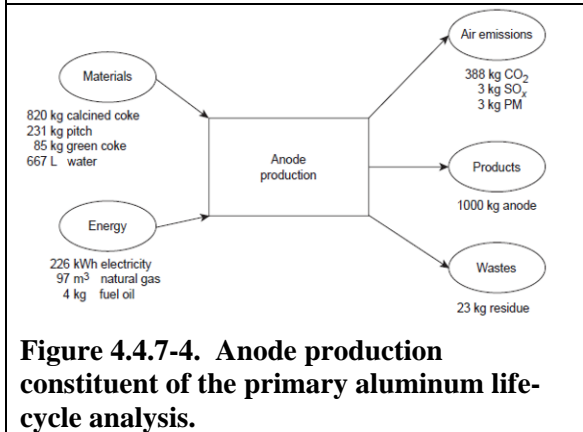


Figure 4.4.7-4. Anode production constituent of the primary aluminum life-cycle analysis.

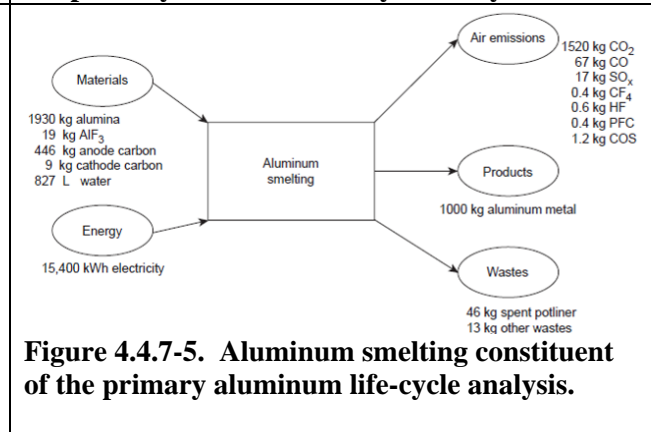


Figure 4.4.7-5. Aluminum smelting constituent of the primary aluminum life-cycle analysis.

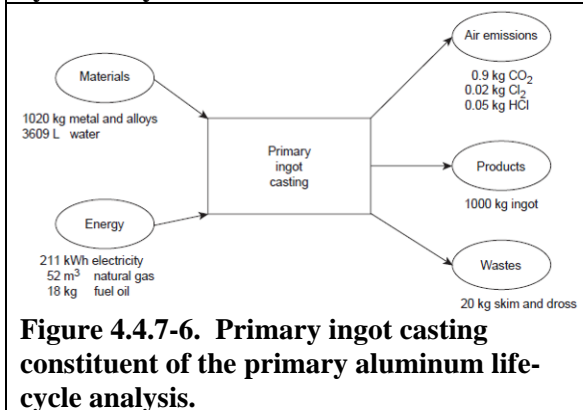


Figure 4.4.7-6. Primary ingot casting constituent of the primary aluminum life-cycle analysis.

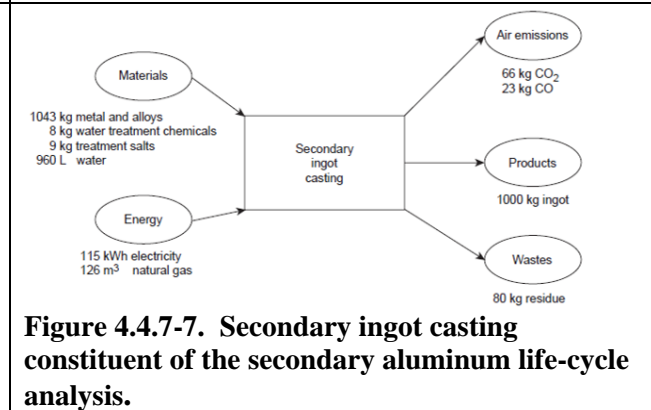


Figure 4.4.7-7. Secondary ingot casting constituent of the secondary aluminum life-cycle analysis.

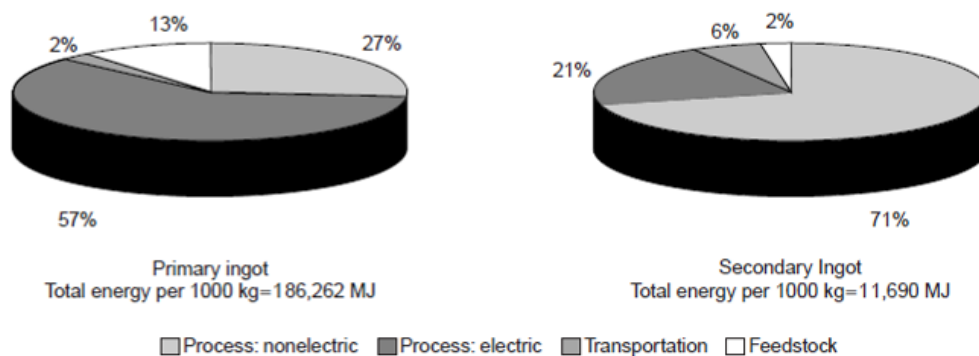


Figure 4.4.7-8. Primary and secondary ingot energy inputs broken down into, process non-electric; process electric, transportation and feedstock categories.

4.4.7.3 The Determination of a Carbon Dioxide Emission Per Pound of Primary Aluminum Production

Much consideration and research has gone into the idea of finding a single value to describe the amount of green house gas emissions in terms of pounds of carbon dioxide per pound of bar stock aluminum production. A 1997 Energetic Inc. report cites data from Nolan Richards in 1994 as “Total CO₂ releases (combustion-related and from manufacturing) for the unit processes of bauxite mining through the production of molten aluminum in a crucible, representing a blend of technologies in North America, have been estimated at 11.7 kg CO₂/kg of aluminum”^[3]. This is equivalent to 11.7 pounds of CO₂ emissions per pound of aluminum produced, however this value does not take into account ingot casting and rolling to bar stock energy costs, nor is it defined as a life-cycle analysis value which would mean that this value likely underestimates the green house gas emissions according to the metrics used in the rest of the model. While the EPA’s says that 4.27 MTCE or metric tons of carbon equivalent are produced in the manufacturing and transportation of a ton of aluminum cans from primary materials^[4]. This value converts to 17.25 pounds of CO₂ emissions per pound of aluminum, and is equivalent to a Life-Cycle Analysis that assumes no secondary material use. However, this value is for aluminum cans which likely have greater energy costs involved with rolling to aluminum sheet thicknesses, and associated fabrication costs. The final value referenced from literature is from an ASM International publication that reports 12,476 kg of CO₂ emissions per ton of primary rolled aluminum^[5], which is equivalent to 12.476 pounds of CO₂ emissions per pound of aluminum. This value is a LCA, and considers the energy costs of ingot to bar stock processing. It does not however explicitly detail a carbon dioxide equivalent emission value, which could underestimate the real green house gas emissions impact. With all of the above information considered and without a standardized method to interpolate a more representative value between 12.476 and 17.25, it was decided that the model would use the 12.476 pounds of CO₂ emissions per pound of aluminum value from the ASM International source. However, as with all other constants and assumptions used in the model, this value is open for user redefinition at a later date.

4.4.8 Mathematics to be used, including formulas and calculation methods: The ‘FINAL PEEPS Energy Consumption Model 09AUG11.xlsx’ file is completely open and provides

comprehensive cell reference data that is straightforward, easy to understand. All formulas used are simple math calculations.

4.4.9 Whether or not the theory and mathematical algorithms were peer reviewed: The mathematical algorithms were peer reviewed by Boeing technical experts but were not, in the sense, academically peer reviewed. All formulas used are simple math calculations, easily checked and simple to understand.

4.4.10 Hardware requirements: No special computing hardware requirements are necessary for this model. If the computer is capable of running Microsoft Excel 2003 or 2007, it is capable of reading the 'FINAL PEEPS Energy Consumption Model 09AUG11.xlsx' file. (Excel 2003 will need a converter function available to convert from an xlsx format to an xls format.)

4.4.11 Documentation: All documentation in terms of users guide information is embedded within the 'FINAL PEEPS Energy Consumption Model 09AUG11.xlsx' file. The model inputs and outputs are clearly identified by color. In addition, there are 'self-check' boxes identified in dark green that indicates if data was entered correctly by the user of the model. The value description boxes clearly provide direction for model input and assumptions made within the model.

5.0 Benefits Assessment

Widespread and aggressive implementation of advanced solid state joining process in the fabrication of near-net-shape tailored blanks (preforms), for subsequent final machining into fly-away aircraft components, has been shown to have the potential to avoid the consumption of 4 to 5 billion pounds of high-strength aluminum, in starting product forms (plate, sheet, extrusions, forgings), summed over the next 20 years of commercial aircraft production. With each pound of aluminum in such product forms requiring 16.71 kWh of energy to produce, resulting in 12.476 pounds of CO₂ emissions for each pound of aluminum, the potential energy savings for implementing these technologies could range from 66.9 to 83.6 billion kWh, resulting in reduced CO₂ emissions ranging from 49.9 to 62.4 billion pounds.

These numbers have been generated only by considering the potential to reduce buy-to-fly ratios for starting aluminum materials obtained for production of commercial airliners. These same methodologies are applicable to military aircraft, roto-craft, and space and space-launch vehicles. In addition, they are already making their way into other portions of the transport industry (trucks, automobiles, coach – rail and motor).

In addition to impacting energy consumption and environmental emissions due to avoidance of vast amounts of aluminum production, the reduction in buy-to-fly values should also have impact due to reduction in the weight of product forms being shipped and transported throughout the aircraft-component fabrication system, from foundries to forming centers to fabrication centers and on to the aircraft assembly centers. Similarly, with reduced chips being generated, there should be significant reduction / avoidance of energy consumption and environmental consequences encountered in moving, sorting, and preparing the volume/weight of this scrap material through the recycling systems.

Although not necessarily of a direct impact on energy or environmental concerns, the fabrication of tailored preforms using SSJ technologies should offer significantly faster production cycle times, particularly with respect to forgings. The latter requires production and retention of geometry-specific tooling die and fixtures. For new parts, there are very long lead times in development and fabrication of acceptable final die geometries. The cycle time reduction of SSJ technologies with respect to traditional forging approaches may tip the selection of the production route of a new component towards SSJ technologies, where the BTF ratios for the two approaches might be very similar. If some portion of the current or future components that are currently produced using near-shape forgings are replaced with SSJ technologies, there will be a measurable energy and environmental benefit via the reduction in the production and use of matching dies, furnaces used for soaking forging billets, forging presses, climate controlled tooling storage, tool tracking, transportation, and facility operations.

6.0 Commercialization

The pathway to commercialization of solid state joining processes is very complex and murky. Significant barriers to implementation remain; some are technical and some are related to industry infrastructure and segmentation.

The commercial aircraft fabricators, such as Boeing, Airbus, Embraer, Bombardier, etc., increasingly function as only system integrators, farming out component fabrication to a broadening supply chain of so-called Tier 1 suppliers. Certainly, there is some remaining fabrication within the internal capacity of the system integrators, but only for highly value-added, critical components. While these system integrators still do significant amounts of process technology development, to ensure that advanced manufacturing technologies, critical to reduce weight, improve performance, lower both manufacturing and product operating costs, are being identified and pushed to implementation-ready levels, they increasingly expect these technologies to be implemented by the Tier 1 suppliers, or their suppliers – the Tier II suppliers, from the integrators perspective. The system integrators increasingly are focused on developing those technologies that impact their principal manufacturing challenge, assembling and delivering an operational platform. Nevertheless, they retain the critical function of ensuring / certifying that all components going into that platform will perform as required / expected over the lifetime of the platform. Ultimately, the fabrication of preforms for aircraft components will be carried out in the supply chain somewhere between primary aluminum product form fabricators and aircraft part fabricators, with requirements for acceptable means, methods, and performance flowing down from the integrators. Along this chain, the costs and benefits of the implementation of new technologies must be shared – both risks and rewards. It is unclear how both economic and regulatory pressures will drive – or hinder – this implementation.

Among the principal technical barriers, all of the SSJ technologies require the accumulation of large amounts of performance data for certification of usage in aircraft applications. Measurement and implications of static strength values are pretty straightforward to obtain and apply. Where values of joined materials are approximately equal to or better than parent materials, direct substitution is reasonably straightforward in applications where only static properties drive acceptability. Where there is a loss of strength due to the SSJ processes, designs can be modified to accommodate this loss, although this usually carries a weight penalty, and this penalty must be overcome by some other benefit of utilizing the process in a particular

application. One issue here is that performance data often has to be accumulated for any significant change in material thickness, joint configuration, and alloy and temper combination. There remain insufficient compendia of “accepted / qualified” performance data to avoid “point-design” certification for each newly attempted application. All of the above comments grow in geometric intensity with respect to flight critical applications, where performance factors relating to fracture, fatigue, durability, and damage tolerance come into play. And these are precisely the application areas where typical aircraft components fabricated from high BTF product forms or near-shape extrusions are being used. The usage of unitized, highly-integrated structural components over the last decades has been greatly accelerated by extensive and diligent measurement of performance properties of bulk product forms, particularly with respect to the uniformity of these properties throughout the bulk. Certification of these unitized structures has been greatly aided by the advances in computer modeling of the behavior of these complex structures under flight loading conditions, with respect to crack initiation, crack propagation, and so on, reducing the time and cost of component testing. Presumably, these tools will be similarly useful in certifying complex structures unitized via joining processes. However, significant work remains in both gathering the appropriate material performance properties of what are potentially very-inhomogeneous materials in and around the joints, and validating that the models are capable of predicting the in-service performance of the structures.

As for the FSW process itself, it is clear that for this process to achieve the benefits of energy and environmental emission avoidances, the joining process must be much more energy efficient in order to prevent the process-required energy from consuming the energy savings associated with the reduced BTF over a thick plate hog-out or machining of an extrusion. This energy efficiency can come in two forms – a more efficient platform, and a more efficient process than encountered with the multi-axis Brotje FSW platform. The latter platform was designed for welding over large area of complex counter geometries, and is quite spectacularly capable of doing so. It was also designed to weld to a depth of only around 0.5 inches. This is the wrong design of a platform for creating tailored blanks. First, a much simpler machine geometry is all that is required, as weld paths in combinations of only two dimensions (a plane) are required. This means an FSW platform for making preforms can have fewer drive axes and few motors, and other constraints, all of which would enable a low-energy idle mode. Secondly, the platform should have a higher-torque weld spindle, to enable much thicker weld depths, and wider weld nuggets. This would enable the use of many fewer welds than required by the Brotje, as encountered in the case studies performed here. It is expected that torque requirements (and energy consumption) will scale with depth and width – meaning a more energy efficient platform will consume the same process energy to make the same total weld volume – but compared to the case study methods explored here, the multiple passes will be eliminated, as will the inter-layer face-milling steps will be eliminated / reduced when doing deeper and wider weld passes with a more torque-robust system. When data consumption values and reduction in milling requirements, consistent with these assumptions, were used with the ECM, the SSJ approaches appear to be essentially energy neutral with respect to the traditional hog-out approach, and all the energy benefits of reduced BTF values may be achievable.

7.0 Accomplishments

This project had five major accomplishments.

The first achievement was in completing the evaluation of the potential impact of implementing solid state joining technologies to reduce the buy-to-fly of aluminum product forms required to produce components for the next twenty years of production of the world's commercial airline fleet (the baseline energy usage impact computation). This required gathering information to create a model of year-by-year, type-by-type production of aircraft. It required gathering information to understand the current picture of both average buy-to-fly utilization of aluminum products and a distribution of that average BTF between high BTF and low BTF component families, again on a type-by-type basis. Then, a basis of impact of implementation of SSJ processes on the high BTF components had to be assumed, and applied to the year-by-year, and type-by-type projections with both a delay-to-implementation period and a ramped implementation period. All of this effort allowed a summing over all years and all aircraft types of the amount of new aluminum product which may be avoided with the implementation of SSJ technologies. This quantity of "avoided" aluminum production has been equated with the energy consumption required to produce the aluminum starting product, and the CO₂ emissions level associated with producing that energy.

The second achievement was the creation of the Boeing Energy Consumption Model. In building this model, revised, more defensible energy / CO₂ emission values for the production of a pound of aluminum were identified, and used in the baseline energy usage impact calculation above. The model was then constructed so that the energy requirements for both producing starting product forms, and then tailored preforms, could be computed for multiple pathways to generating those preforms. The ECM was also constructed so that users could populate the model with user-determined energy consumption values for specific platforms and specific processes. These user-defined inputs include values for machining processes, which are needed to produce final component geometries, whether from current starting product forms, or from existing or to be developed SSJ processes. The ECM has been demonstrated to be able to compare multiple pathways to obtain a final component, enabling its use as a pathway selector tool based on energy consumption and environmental impact.

The third accomplishment was completing a survey of aluminum components used in the 777 aircraft. This effort yielded: a revision of the current total usage aluminum usage (fly weight), the total buy weight, and a resultant average BTF value for this modern design aircraft. Analysis of the aluminum components used on this aircraft, by application area and type, confirmed that the actual BTF values for all parts do break down into two distinguishable categories of high BTF and low BTF. Random surveys of the high BTF components showed that, with aggressive reduction of part footprints in notional tailored blanks would indeed take these high BTF starting materials into the 6 to 1 or less range targeted for implementation of SSJ technologies. Completion of this survey provides an archetype of analysis which could be applied to other major aircraft types, such as the Next-Generation 737, currently the highest production rate aircraft in the Boeing-produced fleet, to provide the "energy-case" base argument for implementing the SSJ technologies on those platforms.

The fourth accomplishment was the fabrication of actual tailored preforms using FSW as the SSJ process, and then the fabrication of actual components via machining from the preforms. While the fabrication of the Case Study 1 pseudo bulkhead was not expected to be found to bolster the energy case for using a preform, given the minor reduction in BTF value over a thick plate, it was instrumental in both guiding the development of the ECM and populating it with actual

energy consumption process data for both the FSW process and the machining processes. The completion of the fabrication of the Case Study 2 preform and final component yielded a clear demonstration of the practical state of FSW as a preform building process, even though the component produced was subtended from the geometry of the full-scale 777 component from which it was derived (to avoid the cost and time of having to make a larger welding fixture). It again highlighted the shortfalls of this particular welding platform with respect to process and energy efficiency and points to the need to utilize a purpose-built platform for FS welding of preforms. The distortion encountered in the machining of the final component is a reminder that these forming / joining processes do leave residual stresses in the blanks, which need to be properly understood. Boeing is working independently on methods by which knowledge of the state of stress in a preform can be coupled with knowledge of machining-induced stresses to produce final machined components with zero net distortion.

The final accomplishment was the advancement of Stationary Shoulder Corner Angle (SSCA) Friction Stir Welding. Under this project, TWI developed improved tools for welding 2024 and 7075 Al alloys. They obtained energy consumption data which Boeing incorporated into the ECM, and then used in a comparison of multiple pathways to produce a preform for a 777 floor component, demonstrating the value of the ECM in predicting the most energy efficient pathway for this component, given current SSJ process capabilities.

8.0 Conclusions

Solid State Joining processes, such as Rotary Friction Welding, Linear Friction Welding, Friction Stir Welding, and Stationary Shoulder Corner Angle welding, could have a significant impact on energy consumption and greenhouse gas emission by the aircraft fabrication industry, if they become widely and aggressively implemented. Based on a projected implementation, starting within three years, and ramped up to full implementation within another three years, the potential energy savings over the next twenty years of new, worldwide aircraft production could range from 66.9 to 83.6 billion kWh, resulting in reduced CO₂ emissions ranging from 49.9 to 62.4 billion pounds. This would principally be due to the reduction in the buy-to-fly ratio of the extensive number of aircraft components that already have been converted from being built-up assemblies of thin, formed aluminum sheet or extruded product forms into large, complex structures machined either from large aluminum forgings or from thick aluminum plate stock. Using the SSJ processes allows the fabrication of tailored preforms which retain the ability of obtaining the large, complex structural form but with starting from a lower buy-to-fly product form.

The successful demonstration articles produced in this project show that these technologies are approaching the practical stage of implementation, but that to achieve this promise of energy savings and environmental impact reduction, some improvements of the joining processes are still required, especially with respect to the energy efficiency of FSW. A properly energy efficient FSW platform would have low energy consumption during idle times, minimal axes and drive motors, to reduce energy of platform motion, and high torque capacity to enable maximum depth and width of welding to produce the necessary volume of added material in single weld passes. Technical barriers to implementation still exist, which relate principally with the accumulation of sufficient performance data and analytical modeling capability to enable facile

certification of performance, especially in flight-critical applications where fitness for application includes consideration of durability and damage tolerance performance.

Commercialization of these processes will depend upon a complex relationship and risk/benefits sharing between members of the aircraft component supply chain, including the systems integrators, component fabricators, and the material suppliers. The system integrators will lead this commercialization through pathfinder projects such as this and internally-funded ones, but it is unclear how these initiatives will eventually flow down into the supply chain. Today, there seems little incentive for the material suppliers to move from their baseline business model of selling more and more poundage of product at market-driven pricing, regardless of how energy efficient its consumption may be or the environmental impact of its production.

9.0 Recommendations

First, and most obvious, among possible follow-up R&D work would be the gathering of energy consumption data on a purpose-built machine, one optimized for platform energy efficiency, and instrumented to gather processes consumption data. The impact of scaling the width and depth of welding needs to be confirmed, and charted for several high strength aluminum alloys.

A second subject area would be to undertake additional case studies, with added focus on acquisition of performance characteristics, including pathfinder data in such areas as crack initiation, crack growth, stress corrosion cracking, and so on, in some key high strength alloys, such as 7050 and 7055 aluminum. Demonstrating how these data would be used in qualifying the utilization of a welded preform to meet the performance criteria for some particular flight-critical aircraft application would go a long way towards breaking the “logjam” confining implementation. Although this would rely on establishing point-design allowable data, such a demonstration would clearly define an acceptable implementation pathway which could be followed with others, building momentum for the acceptability of the processes, and forming the basis of wider applicability.

Another area which has not been addressed in this project is the need for additional 3-D joining capabilities. The SSCA welding can only be used to add a standing rib in one direction. If another rib is added at an angle to this rib, the junction between the two cannot be accommodated today by a friction stir process. It can be achieved with a “keystone” linear friction welding process. This is a specific variant of Linear Friction Welding, and was the process assumed to be available for usage in the preform pathways #2 and #3, of Section 4.2.3.1, above. In the keystone process, joints are made against both horizontal and vertical adjacent surfaces and the added piece, to create a complex, 3-D corner. There is another emerging technique, known as friction hydro pillar processing (see www.twi.co.uk) which can also fill the junction between two ribs created by corner angle welds. Much work needs to be done to bring this technique from emerging laboratory status to a more practical state for implementation.

Finally, all of the assessments on the impact of the implementation of SSJ technology have been made at the technical level, with respect to BTF reduction and the energy savings and environmental impact associated with the avoided consumption of starting aluminum product form. The overwhelming driver for implementation, however, will be a business case argument, and any follow-on work funded by the Department of Energy would be well served if the

development of a business case model for SSJ would be a major component of that work. All of the factors associated with the ECM have costs associated with them, and this would be a good starting point for a model, with provisions for users to add/modify cost data and computational formulations specific to their organizations and supply chain. Because the underlying costs data are so commercially sensitive, having a generic model whose underlying data can be modified by specific users is a key to acceptance and utilization.

On a non-technology-driven note, one clear insight raised by this project has been the recognition that, in light of increasing urgency to control growth of energy consumption and reduce greenhouse gas emission footprints, process-platform designers need to be made aware of the potential impact of poor energy efficiency of these systems. This was particularly evident for the FSW platform at Boeing, which is a multi-axis system, to accommodate welding of complex curvature structure, is massive in size, with counter-acting drive motors for low back-lash operation. Because the system designers never even considered the energy implications, all these motor drives remain in active mode while the rest of the system is idle, consuming around 8 kW of power. Even when these drives shut down, the baseline components – computers, displays, cabinet climate controls, etc., consume 2 kW of power. Surely, if energy efficiency of the platform had been a design requirement, alternative operating modes would have been built into the system. Multiply the potential impact on this one machine across the thousands of process platforms in industry, and the impact of improved standards for platform efficiencies is enormous.

10.0 References

1. Das, S., Yin, Weimin, “*Trends in the Global Aluminum Fabrication Industry.*” *Journal of Metals* (Feb. 2007) 83-87, 2007.
2. “*Report: Global Aluminum Market to Cross 51 Million Tons by 2012*”. (San Jose, CO: PR Newswire, November 12, 2008)
3. “*Energetics Inc., Energy and Environmental Profile of the U.S. Aluminum Industry: a Report Prepared for the U.S. Department of Energy Office of Industrial Technologies.*” Columbia, Maryland: Energetics Inc., 1997.
4. United States Environmental Protection Agency. “*Solid Waste management and Green House Gases Report: Third Edition*”, 2006.
<http://epa.gov/climatechange/wycd/waste/downloads/metals-chapter10-28-10.pdf>.
5. J. Green, “*Life-Cycle Inventory Analysis of the North American Aluminum Industry,*” in *Aluminum Recycling and processing for Energy Conservation and Sustainability*, ASM International, 2007, pp. 33-66.
6. T. Norgate, S. Jahanshahi, W. Rankin, “*Assessing the environmental impact of metal production processes,*” *Journal of Cleaner Production*, 15, pp. 838-848, 2007.